Meteorologiska Institutionen
Uppsala Universitet
Meddelande Nr 121

Lars Dahlgren

SOLAR RADIATION CLIMATE NEAR SEA LEVEL IN THE CANADIAN ARCTIC ARCHIPELAGO

Arctic Institute of North America Devon Island Expedition
1961–1962

1975

Uppsala 1974

SOLAR RADIATION CLIMATE NEAR SEA LEVEL IN THE CANADIAN ARCTIC ARCHIPELAGO

Arctic Institute of North America Devon Island Expedition
1961 - 1962

Doctoral dissertation

Lars Dahlgren
Fil.kand. Kalmar

to be publicly discussed in the lecture room of the Meteorological Department, Uppsala University, on January 17, 1975, at 10 a.m. for the Degree of Doctor of Philosophy (according to Royal proclamation No. 327, 1969).

Uppsala 1974

Digitized by the Internet Archive
in 2026

https://archive.org/details/IA41548926_0035

Meteorologiska Institutionen
Uppsala Universitet
Meddelande Nr 121

Lars Dahlgren

SOLAR RADIATION CLIMATE NEAR SEA LEVEL IN THE CANADIAN ARCTIC ARCHIPELAGO

Arctic Institute of North America Devon Island Expedition
1961–1962

Uppsala 1974

Doctoral dissertation at Uppsala University 1974

ISBN 91-506-0001-X

© Lars Dahlgren
Printed in Sweden 1974
LiberTryck

Contents

Abstract

Introduction

1. Direct solar radiation
   - 1.1. Theory
   - 1.1.1. Ångström's turbidity coefficient
   - 1.1.2. Linke's turbidity factor
   - 1.1.3. The absorption of solar radiation by the water vapor of the atmosphere
   - 1.2. Calibration of the pyrheliometer
   - 1.3. Results and discussion
   - 1.3.1. Direct solar radiation
   - 1.3.2. Ångström's turbidity coefficient
   - 1.3.3. Linke's turbidity factor
   - 1.3.4. Comparison between the radiation regimes of the two stations on Devon Island
   - 1.4. The duration of sunshine and the cloudiness

2. Calibration of the Eppley pyranometer
   - 2.1. Calibration with the Ångström pyrheliometer
   - 2.2. Investigation of some characteristics of the Eppley pyranometer
   - 2.2.1. The instrument error with the Eppley in an upright position
   - 2.2.2. The instrument error with the Eppley in an inverted position
   - 2.2.3. The response time of the Eppley as regards the radiation from the back side

3. Albedo

4. The diffuse radiation from a clear sky

5. Global radiation
   - 5.1. Global radiation with a clear sky as a function of the solar altitude
   - 5.2. Daily totals of global radiation with a clear sky G_0
   - 5.3. Global radiation with a dense overcast
   - 5.4. The relation between solar altitude h and g_{10}/g_0 with differents cloud types
   - 5.5. Relative insolation G/G_0 with actual cloud cover

Appendix

Abstract

Measurements of direct solar radiation, global radiation and duration of sunshine were performed together with observations of cloudiness in 1961 and 1962 on a coastal plain in northern Devon Island in the Canadian Arctic Archipelago at lat. 75°40'N, long. 84°32'W. From filter measurements, made in 1962 with the Ångström pyrheliometer the turbidity coefficient β was derived at which the influence of filter constants and of the spectral distribution of energy upon the derivation was discussed. The turbidity showed a minimum at midsummer which is opposite to the expected annual variation of β. The amount of precipitable water in the atmosphere was derived from the pyrheliometric measurements. In doing so, suggestions made by A. Ångström in 1961 and 1964 were taken up, and a method was tried which takes into consideration the combined effect of scattering by dust and absorption by water vapor.

The relation between the relative duration of sunshine and the cloudiness was studied.

Unacceptable instrument errors were encountered when evaluating the measurements with the Eppley pyranometer. Thus, the error could reach 30 % of the real value when the instrument was used over a snow surface to measure the diffuse clear sky radiation. After returning home, corrections were determined by comparisons with a pyranometer of a different construction. The relation between the diffuse clear sky radiation and the altitude of the sun with the turbidity of the air as a parameter was determined. Also the influence of the albedo of the underlying surface upon the diffuse clear sky radiation was studied though it should be pointed out that no measurements of the regional albedo were made.

Normal values of the global radiation with a clear sky were calculated for every month during the light season. Knowing these values, the relative insolation with an overcast sky and with actual cloudiness could be computed. The relative insolation with an overcast sky as a function of the altitude of the sun was studied for different cloud types. The relation between the relative insolation with actual cloudiness and the relative duration of sunshine was determined. The annual total of global radiation calculated with different methods from simple observations of cloudiness or relative duration of sunshine were compared with actually measured values in order to investigate the usefulness of these methods in climatological work.

Introduction

Devon Island is situated in the midst of the archipelago of the Queen Elisabeth Islands of arctic Canada. The interior of the eastern part of the island is covered with an ice cap which has an area of 13000 km^2 and reaches an altitude of 1885 m above m.s.l.

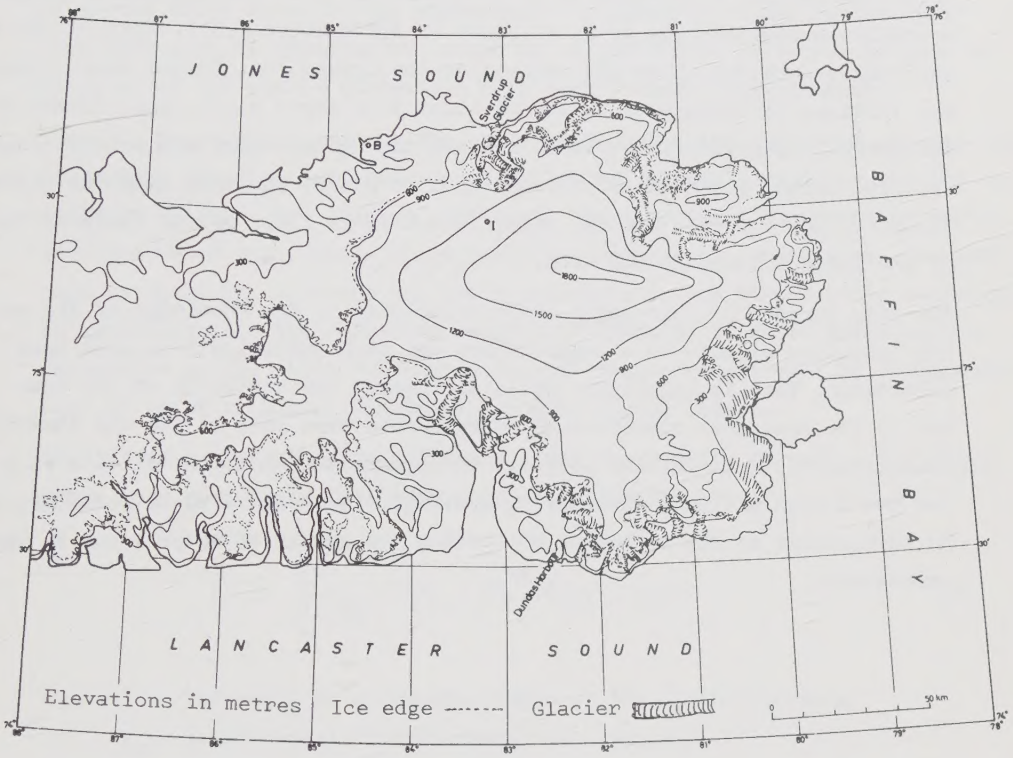

Map showing the eastern part of Devon Island and the position of the meteorological stations during the Devon Island Expedition 1961-1962.
B: Devon Base Station
I: Devon Ice Cap Station

In May, 1961 the Arctic Institute of North America started a long term field program on Devon Island which has continued to the present time. The original object of the Devon Island Expedition was to investigate interrelationships between the ice cap with its outlet glaciers, the ocean in Jones Sound and the atmosphere. To that end a multi-disciplinary program was designed which involved meteorology, glaciology, oceanography, marine biology and geology. The meteorological program during 1961-1962 included climatological and micro-meteorological measurements at two stations. Devon Ice Cap Station

(lat. 75°30'N, long. 83°10'W) was established on the north-western slope of the ice cap at an altitude of 1320 m above m.s.l. and the result of the measurements made there was published by B. Holmgren (1971).

Devon Base Station (lat. 75°40'N, long. 84°32'W) is located on a coastal plane at an altitude of 15 m above m.s.l. and 3 km from the sea. The distance between the two stations is 50 km. The surface in the station area is nearly horizontal within a distance of 5–10 km from the sea. Further inland plateau mountains ascend steeply to an altitude of 300 m above m.s.l. Most of the lowland was sea bottom after the retreat of the inland ice. Raised beach ridges and terraces reaching an altitude of about 50 m above m.s.l. were formed by the gradual upheaval of the land. Between the ridges there are several lakes and also marshy ground with numerous shallow ponds. The base camp was established on the top of a smooth, raised beach ridge close to the shore of one of the largest lakes in the area.

The main purpose of this paper is to contribute to the knowledge of the solar radiation climate in a region where few such investigations have been undertaken. This is especially valid as regards the turbidity of the air. Due to the fact that simultaneous measurements were made at Ice Cap Station (Holmgren, 1971) it is also possible to compare the radiation climate of a low and a high altitude station. In addition, it appeared to be worth while to look closer at the method of evaluating the amount of water vapor in the atmosphere.

1. Direct solar radiation

1.1. Theory

The purpose of the direct solar radiation measurements at Devon Base Station was to determine the transmission properties of the air as described by Ångström's turbidity coefficient, Linke's turbidity factor and the amount of precipitable water in the atmosphere. In addition, other radiation instruments such as pyranometers could be calibrated at different heights and azimuths of the sun in connection with pyrheliometer measurements.

The main factors determining the transmission of solar radiation through the atmosphere are the scattering by molecules and aerosol particles and the absorption by gases and aerosol particles. The atmosphere's content of particles and water vapor shows short periodic and seasonal variations. Information on these fluctuations and their influence on the direct solar radiation is important when the radiation climate of the area is to be investigated. Variations in the ozone and carbon dioxide concentration will be disregarded here as being of minor importance compared to the others.

The intensity of the solar radiation after the passage through a dry atmosphere is given by the following simplified equation

$$I' = \int_0^\infty I_{0\lambda} e^{-(b_\lambda + \beta\lambda^{-\alpha})m} d\lambda - C(m) \qquad (1)$$

where I' = intensity in a dry atmosphere at the earth's surface
$I_{0\lambda}$ = monochromatic extraterrestrial intensity
b_λ = Rayleigh extinction coefficient
β = Ångström's turbidity coefficient
m = optical air mass
λ = wavelength
α = wavelength exponent

$C(m)$ is a correction for the absorption by ozone, oxygen and other gases, except water vapor. As can be seen from formula (1) differences in the optical masses of the Rayleigh and the dust atmospheres as functions of the solar altitude have been ignored. The attenuation of radiation caused by

Rayleigh scattering takes place along the entire path of the solar beam in the atmosphere while the attenuation caused by aerosol particles is usually confined to a rather shallow layer. Such differences are significant only when the sun is close to the horizon or when the air pressure differs much from normal sea level pressure.

1.1.1. Ångström's turbidity coefficient

When the turbidity of a humid atmosphere is to be determined it is advantageous to measure the radiation energy in a part of the solar spectrum where the water vapor with its highly variable concentration has no absorption bands, i.e. below 700 mμ. Thus the energy within the intervals 0 - 525 mμ, 0 - 630 mμ and 525 - 630 mμ, corresponding to the lower cutoffs of the OG 1 and RG 2 filters, was determined with the pyrheliometer.

The energy within the intervals mentioned can be calculated from the integrals

$$I_g = \int_0^{525} I_{0\lambda} e^{-(b_\lambda + \beta\lambda^{-\alpha})m} \, d\lambda - C_1(m) \qquad (2)$$

$$I_r = \int_0^{630} I_{0\lambda} e^{-(b_\lambda + \beta\lambda^{-\alpha})m} \, d\lambda - C_2(m) \qquad (3)$$

$$I_{rg} = \int_{525}^{630} I_{0\lambda} e^{-(b_\lambda + \beta\lambda^{-\alpha})m} \, d\lambda - C_3(m) \qquad (4)$$

Within the wavelength intervals mentioned the solar radiation intensities obtained from pyrheliometric measurements and reduced to mean solar distance are compared with the energies calculated from Eqs. (2-4) for different turbidity and air mass values. In this way it is possible to determine the actual turbidity with a moderate amount of effort. Such energy calculations can be given in the form of tables or diagrams.

The accuracy of the determination of the turbidity depends, besides on the quality of the pyrheliometric measurements, on how exact Eqs. (2-4) with the

extinction coefficients applied describes the process of radiation attenuation in the actual atmosphere.

The outcome of the calculations of the integrals Eqs. (2-4) depends on the following factors used in the formulas

1) The solar constant and the spectral distribution of extraterrestrial solar radiation energy.

2) The extinction coefficient for Rayleigh scattering.

3) The extinction coefficient $\beta\lambda^{-\alpha}$ for the aerosol scattering and absorption.

4) The correction C(m) due to absorption by gases, mainly ozone, oxygen and carbon dioxide.

With the support of spectral investigations showing that under average atmospheric conditions the attenuation by the aerosol is a continuous function of wavelength, A. Ångström (1929 and 1964) expressed the aerosol extinction coefficient by

$$\beta_\lambda = \beta\lambda^{-\alpha} \qquad (5)$$

where λ is given in μ and β corresponds to the extinction coefficient at 1 μ.

Ångström also found that the wavelength exponent α could be given a standard value 1.3 corresponding to an average size distribution of the aerosol particles in the atmosphere. The exponent α can vary widely, but is generally, according to Ångström (1961), found to vary between 0.5 and 1.6. Ångström (1964) has derived a method which facilitates the calculation of α by using the ratios β_{rg}/β_g where β_{rg} and β_g refer to the turbidity coefficients derived from the measured intensities within the wavelength intervals 525-630 mμ and 0-525 mμ, respectively. Here β_{rg} and β_g have been derived from standard tables made under the assumption that α = 1.3. The true β-value can then be found from the actual α-value with Ångström's method. Unfortunately, this method does not apply well to very low turbidity values such as those generally found in the polar regions. Under such conditions a small absolute measuring error in β would cause large deviations in the ratio β_{rg}/β_g and so in α.

It is quite clear from the present investigation that no conclusions can be drawn from single absolute values of α and the same applies to the mean absolute values for the whole measuring period. As will be discussed explicitly

later on in this paper, two different tables showing the calculated values of the integrals Eqs. (2-4) were used for the derivation at β. Two filter factors were used. One was the so called Davos filter factor obtained from the manufacturer. The other was determined with a method given by Ångström and Drummond (1961) based upon determination of the wavelengths of the filter cutoffs. In the four cases arising from combinations of the two integral calculations and the two filter factors mentioned the mean values of α turned out to be 1.2, 1.7, 2.4 and 3.0. The conclusion must be that neither the calculations of the integrals nor the pyrheliometer measurements are accurate enough to permit derivations of the absolute value of α at such low turbidity values as in the present case. However, without any reference to the absolute α-values the variation of ten-day means of the ratio β_{rg}/β_g during the measuring season will be discussed later on in this paper in a comparison between Devon Base Station and Devon Ice Cap Station regarding the parameters obtained from pyrheliometric measurements (see Section 1.3.4).

The turbidity values have been derived from the measured intensities by means of two different tables. Hoelper's tables (Hoelper, 1939) have been employed frequently in pyrheliometric work and their use should consequently facilitate a comparison with turbidity values from other places. The Rayleigh scattering coefficients used for the calculation of these tables are purely empirical. Because Hoelper's table for derivation of β_r, i.e. from the RG 2 filter measurement, was calculated with 625 $m\mu$ as the upper limit instead of the proper value 630 $m\mu$, a correction has been added and the corrected values, reduced to International Pyrheliometric Scale (IPS) 1956, can be found in Table 4 of the Appendix.

As will be discussed in more detail later on in the present paper, discrepancies were found between the β-values derived from intensities measured within the wavelength intervals 0-525 $m\mu$, 0-630 $m\mu$ and 525-630 $m\mu$. Also the amount of precipitable water derived by methods which have proved to give good results in other investigations turned out with too high values. Although the filter factors must, in the first instance, be suspected as a cause for the conditions mentioned, it appeared to be interesting to investigate the influence of the choice of energy integral calculation. See Section 1.1.3.

Therefore, in addition to Hoelper's tables, new ones were calculated from data computed by Sivkov (1968). These data give the spectral distribution of

radiation energy in an ideal atmosphere, i.e. an atmosphere without water vapor and aerosol particles. Sivkov used the extraterrestrial energy distribution given by Johnson and adjusted to agree with the value of the solar constant, 1.98 cal $cm^{-2}min^{-1}$, adopted by the International Radiation Commission 1957. Vigroux's values on the absorption coefficients of ozone valid for a temperature of + 44°C was used and the total ozone content was taken to be 0.3 mm NTP. The Rayleigh scattering coefficient computed by Penndorf was employed and allowance for the anisotropy of air molecules was made by the factor 1.061.

In order to obtain the intensities in a dry and turbid atmosphere Sivkov's values have been multiplied with $e^{-\beta_\lambda m}$ where β_λ is given by Ångström's relation Eq. (5) which has been assumed valid throughout the whole spectrum. The intensities have been calculated for the wavelength intervals 0 - ∞ , 0 - 525 mμ, 525 - 630 mμ and 0 - 630 mμ with β (referred to the wavelength 1 μ) as a parameter. The results can be seen in Tables 5-8 of the Appendix.

The measured intensities have been reduced to mean solar distance by the factor R^2/R_m^2 where R is the actual sun-earth distance and R_m is the mean distance. This has to be done because the tables used for the computation of β refer to mean solar distance.

The relative air mass m_h is a function of the apparent solar elevation or, which is equivalent, the measured altitude of the sun. Knowing the true solar time t, the declination of the sun δ and the latitude φ, the true solar elevation h can be determined from the wellknown formula

$$\sin h = \sin \varphi \sin \delta + \cos \varphi \cos \delta \cos t \qquad (6)$$

By adding a correction for the atmospheric refraction the apparent solar altitude is obtained. The refraction values have been taken from Table 5 in the Appendix of IGY Instruction Manual (1958). Though these values are not supposed to be valid for polar regions, they were nevertheless used because proper data were missing. Since the measurements were made in late spring and summer when occasions with inversion conditions of the air are rather few, the error caused by this inconsistency is probably small because it is not necessary to determine the solar altitude with an accuracy better than 0°.1. Preferably, the local refraction conditions should have been investigated by measuring the solar altitude with a theodolite at frequent occasions.

With the apparent solar altitude as an argument the relative air mass m_h determined from Bemporad's function was obtained from Table 4 in the Appendix of IGY Instruction Manual (1958). Because the mass of the Rayleigh atmosphere varies with the air pressure p, a reduction factor p/p_o must be applied to m_h which is referred to normal sea level pressure p_o. The parameter $m = m_h\, p/p_o$ is usually referred to as the optical air mass or the absolute air mass. However, at the same time the reduction (see formula) is erroneously applied to the mass of the dust atmosphere, giving as a result a too high turbidity value. Therefore, β should be multiplied with p/p_o, but due to the small deviation from p_o at Devon Base Station, the pressure ranging from 997 to 1028 mb, this reduction was considered superfluous.

1.1.2. Linke's turbidity factor

The turbidity factor is a measure of how many times the air mass of an ideal atmosphere has to be increased in order to make this hypothetical atmosphere transmit the same amount of energy as does the actual turbid and humid atmosphere. The turbidity factor T is given by

$$T = \frac{\log I_0 - \log I_m}{\log I_0 - \log I_{m,\,\text{ideal}}} = P(m) \log \frac{I_0}{I_m} \qquad (7)$$

where

$$P(m) = \frac{1}{\log I_0 - \log I_{m,\,\text{ideal}}}$$

Here I_0 = the intensity of extraterrestrial solar radiation
I_m = the measured intensity at the optical air mass m
$I_{m,\,\text{ideal}}$ = the intensity in an ideal atmosphere at the optical air mass m.

Values on P(m) revised after Feussner and Dubois and valid for $I_0 = 1.98$ cal $cm^{-2} min^{-1}$ have been taken from Table 6 in the Appendix of IGY Instruction Manual. These values, being based on empirically derived Rayleigh scattering coefficients, differ from more recent values, as for instance those

computed from Sivkov-Penndorf-Johnson's radiation intensities in an ideal atmosphere (Sivkov, 1968). Table 1 shows values on P(m) obtained by the two methods and the difference between them as a percentage of P(m) according to Feussner and Dubois. The difference is considerable at low air mass values, 18.5 % at m = 1, and decreases with increasing m. Nevertheless, in order to facilitate comparisons with other investigations, there are good reasons to adhere to Feussner's and Dubois's calculations, which have been widely used since the nineteenthirties.

Table 1. The factor P(m) as a function of air mass m.

$P(m)_S$ is calculated from Sivkov's radiation values for an ideal atmosphere. $P(m)_{F,D}$ is revised after Feussner and Dubois (1930). $I_0 = 1.98$ cal $cm^{-2} min^{-1}$.

m	$P(m)_S$	$P(m)_{F,D}$	$\frac{P(m)}{P(m)_{F,D}} \cdot 100$
1	18.88	23.2	18.5
2	11.35	12.86	11.7
3	8.55	9.35	8.6
4	7.05	7.55	6.6
5	6.10	6.46	5.6
6	5.45	5.72	4.7
8	4.59	4.77	3.8
10	3.89	4.19	7.2

The turbidity factor has the disadvantage of not distinguishing between attenuation by water vapor and attenuation by dust. In addition, due to different behaviour of the Rayleigh, dust and water vapor extinction coefficients with a changing air mass, a virtual diurnal variation in T will appear. For the sake of comparison it is recommended that the T-values should be reduced to the air mass value 2.0.

Provided that there is no real, systematic diurnal variation in T and with a large number of measurements available within a fairly small range of T,

reduction terms can be obtained by plotting group means of T for suitable m-intervals in a diagram and connecting the points. However, in the present investigation the number of measurements was too small to permit such a procedure. Instead, by a graphical method, the increment or decrement ΔT within the air mass intervals 1.5 - 2.0, 2.0 - 2.5 etc. was derived for days with more than one pyrheliometric measurement or for groups of consecutive days. In each case the condition was that β and w should have remained constant during the period. The mean value of ΔT for each such m-interval was determined. The reductions arrived at are entered in Table 2.

Table 2. Reduction to optical air mass m = 2 of Linke's turbidity factor T and of the extrapolated turbidity factor T_p.

	m =	1.0	1.5	2.0	2.5	3.0	3.5	4.0	4.5	5.0	5.5
Devon Base Station	ΔT =		-0.11	$\pm$ 0	+0.09	+0.16	+0.22	+0.26	+0.29	+0.31	+0.32
Devon Ice Cap Station	ΔT_p =	-0.22	-0.09	$\pm$ 0	+0.06	+0.10	+0.13	+0.15	+0.17	+0.18	+0.19

	m =	6.0	6.5	7.0	7.5	8.0	8.5	9.0
Devon Base Station	ΔT =	+0.33	+0.33	+0.33	+0.33	+0.33	+0.33	+0.33
Devon Ice Cap Station	ΔT_p =	+0.19	+0.19	+0.19	+0.19	+0.19	+0.19	+0.19

The turbidity factor was also derived by the present author from pyrheliometer measurements made at the same time by B. Holmgren (Holmgren, 1971) at Devon Ice Cap Station 50 km to the south-east at an altitude of 1320 m above m.s.l. Because of the great deviation from standard sea level pressure, the station pressure being about 850 mb, an additional computation had to be done in order to make the values comparable with those from Devon Base Station at an altitude of 15 m above sea level. According to IGY Instruction Manual, Part VI (1958) the so-called extrapolated turbidity factor T_p is given by

$$T_p = 1 + (T - 1) \frac{P(m_h)}{P(m)} \qquad (8)$$

where m_h denotes the relative air mass and m denotes the optical (absolute) air mass. In the way just mentioned the reductions to m = 2 were determined also for the turbidity factors from Devon Ice Cap Station. The ΔT_p-values are entered in Table 2.

It can be seen from Table 2 that ΔT and ΔT_p are both increasing in the same manner with increasing m up to about m = 6 where they attain constant values. Part of the difference between ΔT and ΔT_p is explained by the extrapolation procedure. Sivkov (1968) has computed values on Linke's turbidity factor founded upon 13 000 individual measurements of radiation intensity and divided into six groups according to the atmospheric transparency. The virtual variation with m of the turbidity factor as emerging from Sivkov's data is, however, considerably smaller than that found at Devon Base Station and the minimum turbidity factor according to Sivkov's data is found at m = 3.

Kondratyev (1969) has described a method derived by Tverskoy which gives the reduction of T to m = 2. According to this method the reduction ΔT would be about half the size of that obtained here (Table 2). From Table 1 it is, however, clear that the choice of the parameter P(m) must have an influence on the virtual diurnal variation of T, thus causing differences in ΔT, which are of the same order of magnitude as those arising from the methods just mentioned.

1.1.3. The absorption of solar radiation by the water vapor of the atmosphere

Knowing the amount the precipitable water in a vertical column, determined by, for instance, a radiosounding, one can calculate the absorption of the direct solar radiation caused by the water vapor. On the other hand, by measuring the direct solar radiation and determining the turbidity coefficient at the same time, one can compute the amount of precipitable water. The intention here is to determine the amount of precipitable water and use it, together with the turbidity coefficient, to calculate the direct solar radiation from a cloudless sky at any time of the day. For that purpose one can use either monthly means of the parameters mentioned, or one can interpolate between existing values derived from measurements of the direct radiation.

Various authors have determined the absorbed energy as a function of the amount precipitable water in the path of the sun's rays. Their absorption values differ conspicuously as can be seen from Fig. 1 where the absorbed energy is plotted versus the product $m \cdot w$, which is equivalent to the amount of precipitable water along the path of the sun's rays. Here w is the amount of precipitable water in a vertical column and m is the optical air mass. The discrepancies are to some extent due to the fact that some authors consider the absorption as taking place before the extinction due to

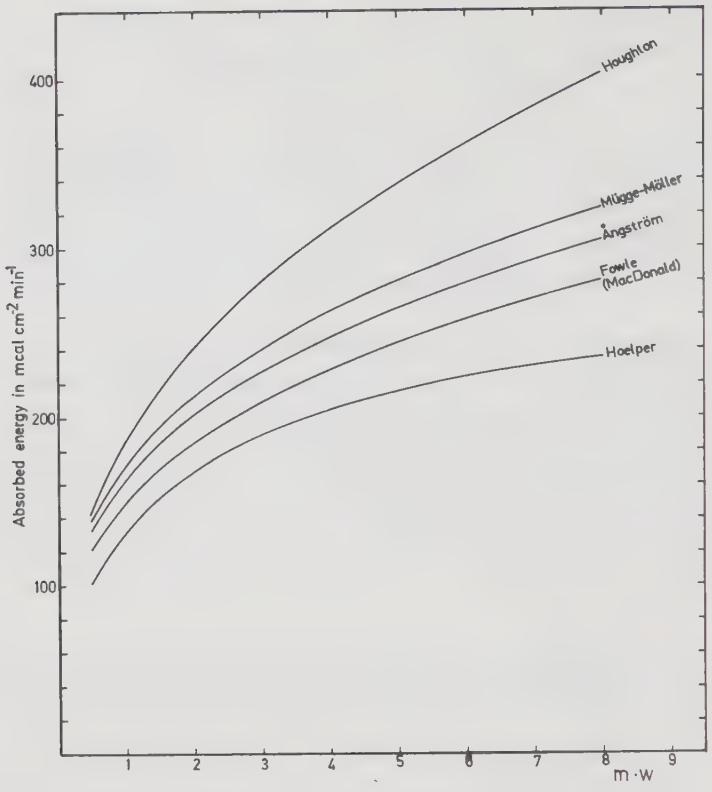

Fig. 1. Radiation energy absorbed by water vapor as a function of the amount of precipitable water m · w in the path of the rays of the sun according to various authors.

dust scattering, while others assume the opposite order. Every curve but Houghton's is derived with Fowle's investigations as the basis. Fowle's absorption data (Fowle 1912 and 1915) were derived from laboratory measurements and bolometric measurements of the solar radiation. Houghton, however, analysed an extensive body of data which had been collected at the Smithsonian Astrophysical Observatory and which were originally intended for the solar constant studies there. He arrived at absorptivities much higher than those obtained by any author mentioned in Fig. 1.

J.E. McDonald (1960) has treated several works on the absorption of solar radiation by the water vapor of the atmosphere. Using Fowle's values on the limits of the six main absorption bands and the values on the band absorptivities, reproduced in Smithsonian Meteorological Tables (List, 1951), McDonald arrived at the following formula for the insolation absorptivity,

i.e. the relative absorption

$$a = 0.077\ (w\ m)^{0.30} \tag{9}$$

Multiplication with the solar constant 1.98 cal $cm^{-2}min^{-1}$ gives the total energy absorbed by the water vapor of the atmosphere expressed in cal $cm^{-2}min^{-1}$

$$A = 0.152\ (w\ m)^{0.30} \tag{10}$$

This formula, referred to as the McDonald formula, gives the water vapor absorption when this is assumed to take place before any depletion of the solar radiation due to scattering by molecules or aerosol particles. If the Rayleigh scattering within the water vapor absorption bands is ignored, the formula also describes the real case of absorption in a humid and clean atmosphere, i.e. with the turbidity coefficient $\beta = 0$.

The absorption curves of McDonald, Ångström, Mügge-Möller and Houghton (Fig. 1) correspond to $\beta = 0$, while the Hoelper curve is derived from a large number of pyrheliometric measurements obtained during actual turbidity conditions.

When Hoelper's water vapor absorption values (see Foitzik and Hinzpeter, 1958, p. 224) were applied to the pyrheliometric measurements from Devon Base Station far too high values on the amount of precipitable water w were obtained, some values even exceeding 4 cm. The monthly means of w thus obtained were twice as high as those computed from radiosonde ascents at Resolute, 300 km to the west of the station. There might be several factors causing this inconsistency, but a very important one is the low turbidity at our station, the mean value for the summer season 1962 being only 0.024. This should be compared with the relatively high turbidity in Germany where Hoelper's pyrheliometric measurements, which formed the basis of his computation of the water vapor absorption, were performed (Hoelper, 1939). In fact, Liljequist (1956) obtained quite reasonable values on w when he used Hoelper's absorption values to compute w from his pyrheliometric measurements at Maudheim in the Antarctic in spite of the very low turbidity in that region.

It must, however, be stressed that the problem of the absorption of solar radiation by water vapor in the atmosphere is complicated. Moreover, some authors have given very few details of their derivation of the absorptivities, which makes it difficult to decide which one should be used. A. Ångström (1961 and 1964) has drawn attention to this problem and derived a for-

mula which takes into account the combined effect of the absorbing and scattering processes. According to Ångström the absorbed part of the total extinction of the monochromatic radiation is given by

$$A = \frac{\alpha_\lambda}{\alpha_\lambda + \beta_\lambda} \cdot I_{0\lambda} \left[1 - e^{-(\alpha_\lambda + \beta_\lambda) L} \right] \qquad (11)$$

Here α_λ and β_λ denote the absorption and scattering coefficients, $I_{0\lambda}$, the incident radiation and L, the distance which the radiation has traversed in the medium. The formula shows that the absorption is influenced by the scattering process. Using Fowles absorption data, as reported by McDonald (1960), Ångström arrives at a formula for practical use

$$A = 0.163 \ (w \ m)^{0.30} \cdot 0.81^{\beta \cdot m} \qquad (12)$$

It gives a higher absorption than the McDonald formula because Ångström has given attention to the strong absorption bands at 2.69 and 2.77 μ also, while Fowle only investigated the bands in the region 0.7 - 2.10 μ. The pressure influence is also compensated for in Ångström's formula, which tends to decrease the absorption.

When used to compute the amount of precipitable water from our pyeheliometric data the Ångström formula gave w = 1.35 cm as a mean for the whole period of 1962 (see Table 12 of the Appendix and Table 3). This should be compared with a mean value of w = 1.01 cm, computed from radiosoundings at Resolute, 300 km to the west of the station. The Resolute values were calculated for the same days as the pyrheliometric measurements according to the following formula

$$w = \frac{1}{g} \int_{p}^{p_0} s \, dp \qquad (13)$$

where s is the specific moisture expressed in grams of water vapor per kilogram of air, p the air pressure in mb and g the acceleration of gravity. In most cases g can be approximated to 1000 cm s^{-2}. The specific humidity is obtained from

$$s = 0.622 \cdot \frac{e}{p} \cdot 1000 \qquad (14)$$

where e is the vapor pressure in millibars.

Usually the radiosondes do not give information on the humidity in the upper part of the troposphere and in the stratosphere. Therefore a correction has been added to compensate for the missing part. It was then assumed that the amount of water vapor in the stratosphere was negligible in this connection. It should, however, be kept in mind that determination of the amount of precipitable water from radiosonde ascents generally has a fairly low accuracy. On individual days, of course, considerable differences in atmospheric water vapor content at Devon Base Station and Resolute may occur due to the rather great distance between the two stations.

The above mentioned absorption formulas are adapted to determination of the absorption when w is known. Due regard should then, of course, be given to Ångström's indication about the turbidity influence on the absorption.

But when it comes to calculating the amount of precipitable water from pyrheliometric measurements, matters are more complicated. A method often used is to identify A obtained from an absorption formula with F, which is the difference between the total solar radiation energy in a dry atmosphere having actual turbidity and the measured total energy. Expressed in mathematical terms we have

$$F = \int_0^\infty I_{O\lambda} e^{-(b_\lambda + \beta_\lambda) m} \cdot d\lambda - I - C(m) \qquad (15)$$

Here $I_{O\lambda}$ = the extraterrestrial solar intensity
b_λ = the Rayleigh scattering coefficient
$\beta_\lambda = \beta \cdot \lambda^{-1.3}$ where β is the turbidity coefficient assigned to the wavelength 1 μ
m = the optical air mass
I = the measured total intensity
C(m) = correction term due the absorption in gases like ozone.

The solar energy passing through a dry atmosphere can for instance be obtained from Hoelper's calculations of the integral (Table 1 of the Appendix) or from the calculations (Table 5 of the Appendix) based on data for an ideal atmosphere given by Sivkov (1968).

The measured energy is, however, the result of the combined effect of the scattering and absorption processes.

$$I = \int_0^\infty I_{0\lambda} e^{-(b_\lambda + \beta_\lambda + wk_\lambda) m} d\lambda - C(m) \qquad (16)$$

where w is the amount of precipitable water and k_λ is the absorption coefficient. Consequently, using arguments similar to those given by Holmgren (1971), it is not quite correct to put F equal to A. Therefore the difference

$$F = \int_0^\infty I_{0\lambda} e^{-(b_\lambda + \beta_\lambda) m} d\lambda - \cdot \int_0^\infty I_{0\lambda} e^{-(b_\lambda + \beta_\lambda + wk_\lambda) m} d\lambda \qquad (17)$$

has been computed for different values on $m \cdot \beta$ and $m \cdot w$. Because the two integrands differ only at those wavelengths where the water vapor absorbs it is sufficient to calculate F within the main absorption bands. Neglecting further the Rayleigh scattering which is small at those relatively large wavelengths, i.e. $\lambda > 1\ \mu$, and using effective β_λ- and k_λ-values referred to the centre of each band we get

$$F = \sum_1^n I_{0n} e^{-\beta_n \cdot m} (1 - e^{-k_n \cdot w \cdot m}) \qquad (18)$$

where $n = 1.2 \ldots\ldots 6$ refers to the main absorption bands usually denoted a, 0.8 μ, ρ, Φ, ψ and Ω. Here $e^{-\beta_n \cdot m}$ is the integral transmission function due to dust scattering and $(1 - e^{-k_n \cdot w \cdot m})$ is the integral absorption function due to water vapor absorption. Fowle's values on the wavelengths of the band-limits (Fowle, 1912 and 1915) together with the band absorptivities as specified by List (1951) have been used for the calculation of F from Eq. (18). The extraterrestrial solar energy I_{0n} within the absorption bands given by McDonald (1960) have been employed also. F has been computed for different values on $\beta \cdot m$ and $w \cdot m$ and the result is shown in Table 9 of the Appendix.

The ratio R between F for different values on $\beta \cdot m$ and F for $\beta = 0$ has been formed, viz.

$$R = \frac{\sum_1^n I_{0n} e^{-\beta_n \cdot m} (1 - e^{-k_n \cdot w \cdot m})}{\sum_1^n I_{0n} (1 - e^{-k_n \cdot w \cdot m})} \qquad (19)$$

R may be interpreted as the weighted mean transmission function due to dust scattering and is valid for all six absorption bands. In Eq. (19) the transmission functions valid for the different bands have been given weights corresponding to the water vapor absorption

$$I_{On} (1 - e^{- k_n \cdot w \cdot m})$$

within each band. The result of the calculations is shown in Table 10 of the Appendix.

The aim of the forming of the ratio R is to make use of the calculation of Eq. (18) (Table 9 of the Appendix) when applying any other absorption curve (Fig. 1) with due regard to the combined effect of the scattering and absorption processes. A necessary condition is that the absorption curve in question is constructed under the assumption that absorption takes place before scattering by dust. By multiplying R for different values on the parameter $\beta \cdot m$ (Table 10 of the Appendix) with the absorption values given by a suitable absorption curve, it is possible to determine w from a given F-value. Such a step ought to be justified provided that the relative absorption of each band does not differ too much from that within the corresponding band used at the calculation of R. A diagram based upon Houghton's absorption values and showing F as a function of $w \cdot m$ and with $\beta \cdot m$ as a parameter was constructed and can be seen in Fig. 2. The corresponding values are listed in Table 11 of the Appendix. The amount of precipitable water w has been determined from the pyrheliometric measurements by means of the diagram in Fig. 2.

A comparison with w obtained from the radiosoundings at Resolute (Fig. 3 a-d) indicates that the best result is obtained with Houghton's absorption values (see Fig. 2), particularly when F is computed from Table 5 of the Appendix. w is based on data calculated by Sivkov (1968). Monthly means and mean values for the whole measuring period of w are entered in Table 3 and show again that Houghton's absorption values give the best result. A comparison shows that the turbidity influence on the absorption obtained with the methods outlined here (Eq. 18) is about three times as large as the same influence according to Ångström's formula (Eq. 12).

The results shown in Table 3 and Fig. 3 are placed in this section in order to illustrate the influence of the derivation method upon the outcome of w. The rest of the parameters obtained from the pyrheliometric measurements will be discussed in Section 1.3.

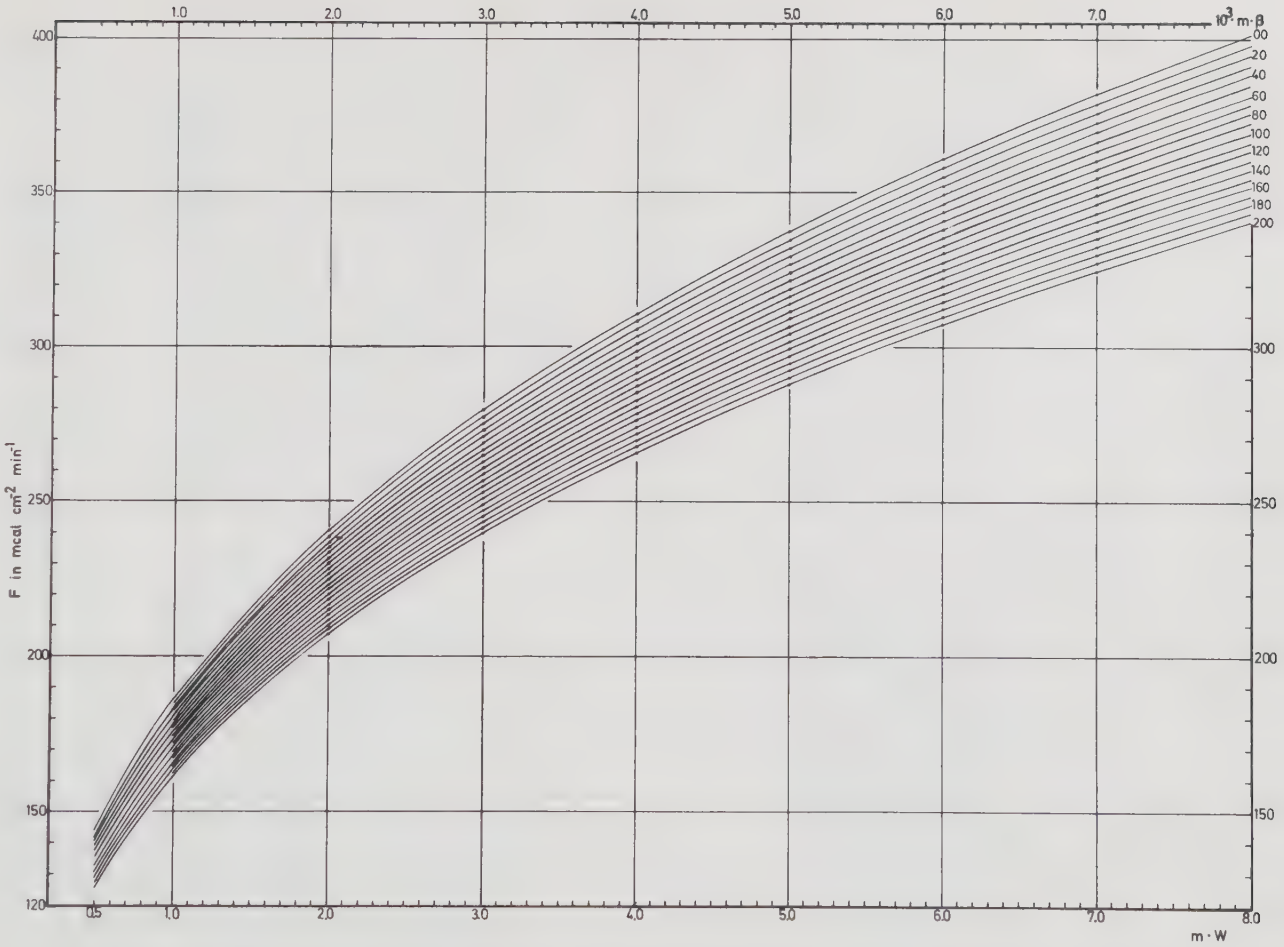

Fig. 2. Water vapor absorption F in mcal cm^{-2}min^{-1}, with $\beta \cdot m$ as a parameter as a function of the amount of precipitable water $m \cdot w$ in cm in the direction of the rays of the sun. The calculations have been based upon Houghton's absorption values corresponding to the curve $\beta \cdot m = 0$.

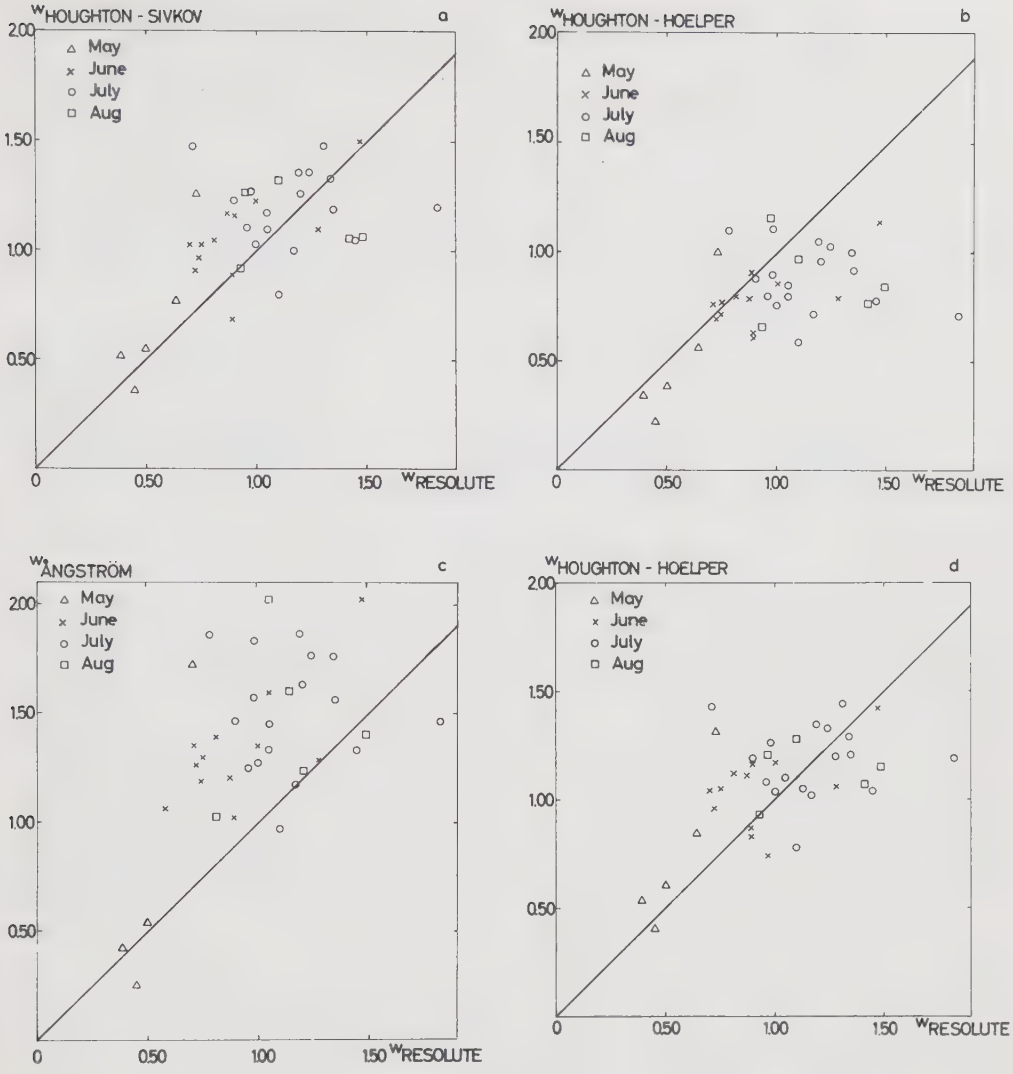

Fig. 3 a–d. Comparison between daily means of the amount of precipitable water w in cm obtained from pyrheliometric measurements and w obtained from radiosoundings at Resolute. The figure illustrates the strong influence of the choice of method of calculation upon the value of w.

a) With Sivkov's energy values in a dry an turbid atmosphere and with Houghton's water vapor absorption values.

b) With Hoelper's energy values in a dry and turbid atmosphere and with Houghton's absorption values.

c) With Hoelper's energy values and with the combined effect of dust scattering and water vapor absorption according to Ångström (1961 and 1962).

d) Same as b) but with filter constants according to Ångström and Drummond (1961).

Table 3. Monthly means of the amount of precipitable water w compared with w obtained from radiosoundings at Resolute.

Ångström's and Houghton's water vapor absorption values have been employed in the calculation of w. For the determination of the intensity of direct solar radiation in a dry and turbid atmosphere Hoelper's tables have been used together with tables based upon the intensity in an ideal atmosphere calculated by Sivkov. Davos filter constants have been used unless something else is stated.

	w Ångström, Hoelper	w Houghton, Hoelper	w Houghton, Hoelper Filter const: Ångström-Drummond	w Houghton, Sivkov	w Radiosonde
	cm	cm	cm	cm	cm
May	0.75	0.50	0.74	0.69	0.54
June	1.33	0.79	1.06	1.06	0.92
July	1.50	0.88	1.19	1.20	1.17
August	1.31	0.88	1.13	1.13	1.18
Mean	1.35	0.80	1.08	1.08	1.01

1.2. Calibration of the pyrheliometer

The measurements of direct solar radiation were made with an Ångström compensation pyrheliometer, (SMHI, Stockholm, Nr 555), supplied with the colour-filters OG 1 and OG 2, both 3 mm thick. The heating current was measured with a Siemens MV-meter L 56, R 11-48 supplied with a shunt giving a range of 0 - 0.75 amps. Temperature differences between the two blackened strips were detected with a light-spot galvanometer type GVM 11 nr. 4969 manufactured by Radiometer, Copenhagen.

Before our departure for Devon Island the milliammeter, which was claimed by the manufacturer to have an accuracy of 0.2 %, was compared with a Hartmann and Braun milliammeter having an accuracy of 0.1 %. This calibration gave a correction of -0.7 %. After the expedition a new comparison was made and the correction was then found to be -1.3 %. Assuming that these corrections represent the lowest and highest values during the time elapsed between the two occasions, a correction of -1.0 % was chosen to be applied to the measurements of heating current. If this assumption holds the maximum error of the current measurements is $\pm$ 0.3 % , other sources of error being disregarded.

The intensity of the measured solar radiation is given by $I = ki^2$ where k is the instrument constant and i is the compensation current expressed in amperes. An error of 0.3 % in current i would give an error of 0.6 % in solar radiation intensity I.

The pyrheliometer was calibrated by the Swedish Meteorological and Hydrological Institute (SMHI), Stockholm shortly before and shortly after the expedition. The calibration constant k was found to be 8.27 and 8.32, respectively. Upon our arrival on Devon Island in April 1962 the blackened strips were inspected and some minute cracks in the soot-layer were found. Assuming that the change in the calibration constant occured during the transport to Devon, possibly due to the low temperatures in the spring, 8.32 was chosen as the relevant instrument constant. This is supported by a third calibration made by SMHI, Stockholm in July, 1973 with the standard pyrheliometer nr 158 as reference at a turbidity parameter $m \cdot \beta = 0.055$ giving as a result $k = 8.32$.

On the other hand, as shown by Ångström and Rodhe (1966), such a difference or even greater may occur when the pyrheliometer is calibrated against a standard instrument with a different aperture angle. In such a case the exposed blackened surface will not receive the same amount of radiation from the circumsolar sky. Since the intensity of the aureole fluctuates with the turbidity of the air, comparisons between two instruments may give different results on different occasions. However, later findings by Rodhe (personal communication) indicate that the magnitude of the error has been overestimated, for which reason no correction of this error will be applied to the present measurements.

As already mentioned, by measuring the intensity of the solar radiation behind the filters OG 1 and RG 2 and subracting these intensities from those

obtained without filters, it is possible to get the radiant energy within intervals where the water vapor absorption is negligible.

Ideal OG 1 and RG 2 filters would transmit all radiation of wavelengths higher than 525 mμ and 630 mμ, respectively. A real filter may have a short-wave cutoff that differs from the standard limit and the transmissivity is always less than 100 % in the main transmission band. There is also an upper limit, in this case 2800 mμ, above which the glass filters for practical purposes can be regarded as non-transparent.

Each filter is tested by the Davos observatory and a reduction factor is given which takes into account deviations from the lower limit of the ideal filter and which also makes allowance for the radiation losses in the main transmission band. Thus the filter factors given by Davos observatory were 1.147 for RG 2 and to 1.121 for OG 1.

However, Ångström and Drummond (1959, 1960 and 1961) have pointed out that the filter factor would vary with air mass, turbidity and water vapor content of the air if the filter cutoff differs from the standard filter limit. They have shown experimentally that the extinction in the main transmission band, which is mainly due to reflections between the glass surfaces, can be accounted for by a filter factor 1.100 ± 0.005. This factor seems to be the same for different melts and varies only slightly with the glass thickness.

In case of a deviation of the shortwave cutoff from the standard limits 525 mμ and 630 mμ, respectively, the measured radiation energy must be reduced to the value which would have been measured behind a standard filter. This can be done by the application of an additive correction which is a function of the relative air mass and the turbidity. Consequently, it is important to determine the position of the cutoff centre. In our case this was done with a Beckman Mod. DU Spectrophotometer giving as a result that the OG 1 cutoff centre was at 529 mμ and the RG 2 cutoff centre at 637 mμ (instead of the standard values 525 mμ and 630 mμ).

Ångström and Drummond (1961) have computed the energy in the intervals 525-535 mμ and 630-640 mμ for different air mass values and with β as a parameter. By multiplying the energy values, which are valid for a 10 mμ wavelength interval, with 0.4 and 0.7, respectively, additive corrections for the actual OG 1 and RG 2 measurements have been obtained. Thus the energy value measured behind a filter has been multiplied with a factor 1.103, and a correction valid for the actual air mass and turbidity has been added.

The position of the lower cutoff shows a small shift towards higher wavelengths with increasing temperature (IGY Instruction Manual, 1958). According to the IGY Manual this effect can be eliminated by applying a correction to the measured intensity of + 0.2 per cent per ^{o}C for OG 1 and + 0.3 per cent per ^{o}C for RG 2. The mean temperature on the occasions when the pyrheliometric measurement were made at Devon Base Station in 1962 was + 5.4^{o}C and the reference temperature for the filter factors was + 22.5^{o}C. Hence, the correction turned out to be -0.3 % for OG 1 and -0.5 % for RG 2. This correction has not only been added to the Davos filter factor but also to the filter factor 1.103 of the Ångström-Drummond method, at which the turbidity influence was neglected.

The glass filters OG 1 and RG 2 has a long-wave cutoff at 2800 mμ. There is, however, a small amount of solar energy above that limit, the magnitude depending on the amount of precipitable water along the path of the sun's rays. A correction for that missing energy which decreases with increasing humidity is given in Table 1 of IGY Instruction Manual. The correction has to be added to the intensity values measured behind the filters. In this investigation the correction amounts to 4 - 16 m cal $cm^{-2}min^{-1}$.

1.3. Results and discussion

The results from each series of pyrheliometric measurements are shown in Table 12 of the Appendix. These data comprise:

Optical air mass m
Turbidity coefficient β
Turbidity factor T and $T_{m = 2}$
Product β · m
Amount of precipitable water w
Absorption F caused by water vapor.

The turbidity coefficient β is the mean value of β_r and β_g derived from measurements with RG 2 and OG 1 filter, respectively. The turbidity factor denoted by T is valid at the actual optical air mass value while $T_{m = 2}$ is reduced to the optical air mass 2.0. F has been obtained as the difference between the actually measured total intensity and the intensity in a dry atmosphere with the same turbidity. β and F have been determined both with Hoelper's tables and tables based upon Sivkov's calculations, though only one of the β-determinations is

listed in Appendix 12 because the mean values show a close coincidence. The amount of precipitable water has been derived through the use of both Ångström's and Houghton's absorption values (see Section 1.1.3.).

1.3.1. Direct solar radiation

The measured solar radiation intensities reduced to mean solar distance are plotted versus the solar altitude corrected for refraction in Fig. 4. Group means are computed and a smoothed curve is drawn. Intensities calculated with mean values of β and w for the whole measuring period are also entered

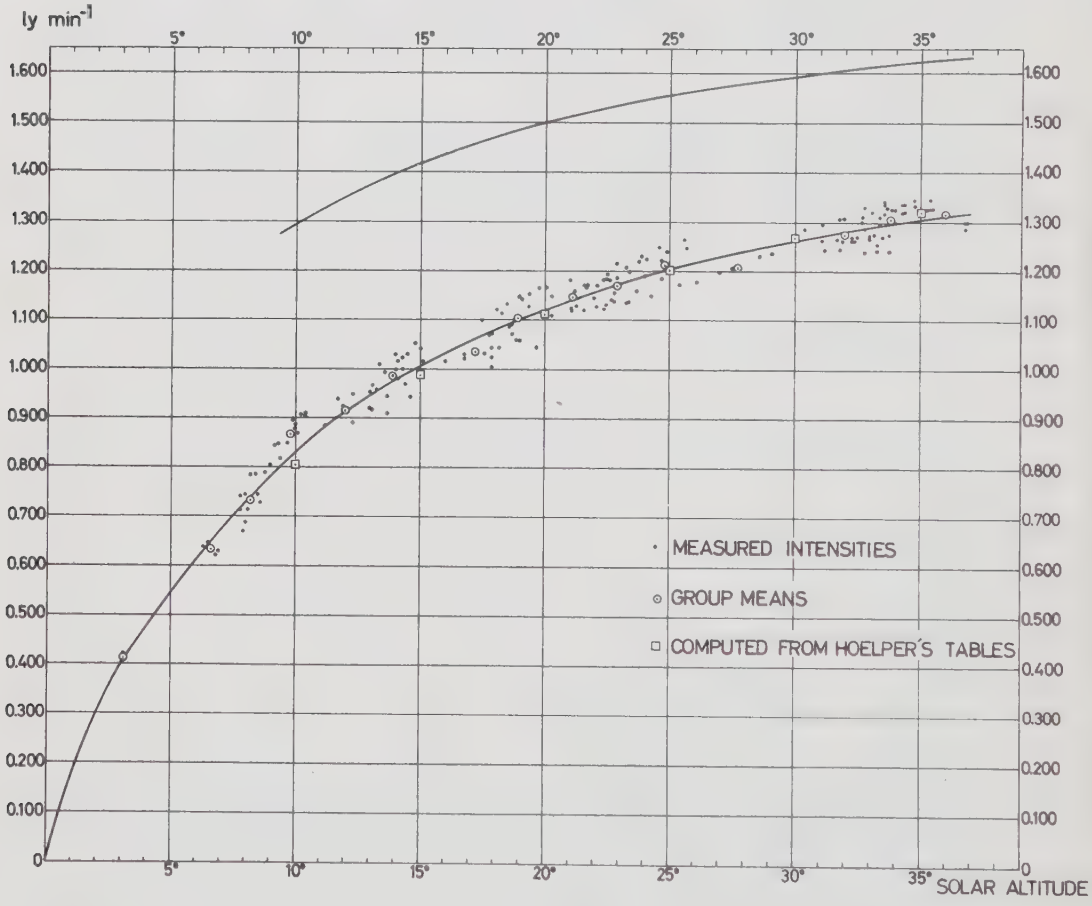

Fig. 4. Intensity of the direct solar radiation as a function of the solar altitude. The intensities are reduced to middle solar distance and the solar altitudes are corrected for refraction. Computed values are obtained from Hoelper's tables reduced to IPS 1956 (Appendix 1) with β = 0.024 and from Houghton's absorption curve (Fig. 2) with w = 0.80 cm. The upper curve shows the intensity in an ideal atmosphere according to Hoelper's computations.

in the diagram for every five degrees solar altitude. The upper curve of Fig. 4 shows the radiation energy in an ideal atmosphere, i.e. an atmosphere without water vapor and aerosol particles. These latter values have been taken from Hoelper's tables adapted to agree with the International Pyrheliometric Scale 1956 by multiplying with 0.98. The measuring points show a maximum deviation of $\pm$ 0.070 cal $cm^{-2}min^{-1}$ from the mean curve and the standard deviation amounts to 0.032 cal $cm^{-2}min^{-1}$ obtained with the latter curve as base.

Measured and also calculated values of direct solar radiation intensities can be studied in Table 4 where, as a comparison, also intensities obtained from the Devon and Greenland ice caps are entered. Table 5 shows the intensities at the relative air mass m_h = 2.00, corresponding to a solar altitude of 30° for some selected station. At South Pole, with its high elevation (2800 m above m.s.l.) m = 2.0 corresponds to a solar altitude of 20° while the same optical air mass is attained at a solar altitude of 30° at sea

Table 4. Direct solar radiation intensity in cal $cm^{-2}min^{-1}$.

All radiation intensities are reduced to mean solar distance. (IPS 1956).

Relative air mass, m_h	10.40	5.60	3.82	2.90	2.36	2.00	1.74	1.55
Solar altitude, h	5°	10°	15°	20°	25°	30°	35°	40°
Ideal atmosphere		1.30	1.42	1.50	1.55	1.59	1.62	1.65
Devon Base 1962, calculated, β = 0.024, w = 0.80 cm, 15 above m.s.l.		0.80	0.99	1.11	1.20	1.27	1.32	1.36
Devon Base 1962, measured (from smoothed curve of Fig. 4),15 above m.s.l.	0.55	0.83	1.01	1.12	1.20	1.26	1.31	
Devon Ice Cap 1962, 1963, 1320 above m.s.l. Holmgren (1971)		0.97	1.14	1.24	1.31	1.37	1.42	
Greenland 1959, 1013 above m.s.l. Ambach (1963)	0.68	0.97	1.11	1.22	1.30	1.34	1.38	1.42

level. The intensities at the arctic stations seem to be in agreement with each other with due regard to altitude differences. They are generally lower than intensities found in the Antarctic, possibly due to a smaller water vapor content of the atmosphere there. It can also be seen in Table 5 that the intensity at the same optical air mass increases with the elevation of the station.

Table 5. Intensity of direct solar radiation at a relative air mass $m_h = 2.00$ ($h = 30^\circ$) and at an optical air mass $m = 2.00$. Mean solar distance. IPS 1956. $\beta_p = \beta \cdot p/1000$ and $m = m_h \cdot p/1000$ where p is the air pressure.

	Height above sea level in m	Intensity cal $cm^{-2} min^{-1}$		β_p
		$m_h = 2.00$	$m = 2.00$	
Devon Base Station 1962	15	1.26	1.26	0.024
Devon Ice Cap Station 1962, 1963, Holmgren (1971)	1320	1.37	1.31	0.016
Greenland Ice Cap 1959, Ambach (1963)	1013	1.34	1.31	0.015
Little America 1957, 1958, Fritz and MacDonald (1960)	44		1.35	
Little America, 1957, 1958, Hoinkes (1960)	44		1.38	
South Pole, Fritz and MacDonald (1960)	2800		1.46	
Maudheim Antarctica, 1949-52 November-February, calculated. Liljequist (1956)	37	1.37	1.37	0.020

1.3.2. Ångström's turbidity coefficient

Monthly means of β_g, β_r, β_{rg} and β are shown in Table 6. Here β_r, β_g and β_{rg} are derived from the radiation intensities in the wavelength intervals 0 - 630 mμ, 0 - 525 mμ and 525 - 630 mμ, respectively. β is the mean value of β_r and β_g. According to Table 6 it is evident that Hoelper's tables and the calculations, based upon Sivkov-Johnson's energy distribution in an ideal

Table 6. Monthly means of Ångström's turbidity coefficient at Devon Base Station.

β_g and β_r are obtained from measurements with OG 1 and RG 2 filters, respectively. β_{rg} is obtained from the difference between OG 1 and RG 2 measurements. β is the mean value of β_g and β_r.

Number of days	Energy calculations according to Hoelper							
	Davos filter factors				Filter factors according to Ångström-Drummond			
	β_g	β_r	β_{rg}	β	β_g	β_r	β_{rg}	β
May 5	0.033	0.031	0.030	0.032	0.027	0.023	0.020	0.025
June 12	0.020	0.019	0.014	0.019	0.015	0.012	0.007	0.014
July 17	0.024	0.021	0.017	0.023	0.019	0.015	0.009	0.017
Aug. 5	0.029	0.028	0.027	0.028	0.024	0.021	0.016	0.022
Mean 39	0.025	0.022	0.019	0.024	0.020	0.016	0.014	0.018

Number of days	Energy calculations according to Sivkov-Penndorf-Johnson							
	Davos filter factors				Filter factors according to Ångström-Drummond			
	β_g	β_r	β_{rg}	β	β_g	β_r	β_{rg}	β
May 5	0.033	0.032	0.036	0.033	0.027	0.025	0.026	0.026
June 12	0.019	0.020	0.021	0.020	0.014	0.014	0.013	0.014
July 17	0.023	0.023	0.022	0.023	0.018	0.016	0.015	0.017
Aug. 5	0.028	0.029	0.032	0.029	0.023	0.022	0.022	0.022
Mean 39	0.024	0.024	0.025	0.024	0.018	0.017	0.017	0.018

atmosphere, give almost coinciding values for β_g, β_r and β while the β_{rg}-values determined with Davos filter factors are lower by about 0.006. All turbidity values derived by employing Davos filter factors are higher by about 0.006 than values derived with filter factors according to Ångström and Drummond (1961). However, such divergencies in the turbidity values are of significance only at a very low turbidity. In fact, on 12 occasions in June and July, the measured intensities in the interval 525-630 mμ determined with filter factors according to Ångström and Drummond, turned out to exceed the intensities in an ideal atmosphere as given by Hoelper for the same interval.

Until the question about the radiation energy in an ideal atmosphere has been quite settled, there seem to be good reasons to adhere to Hoelper's tables when deriving turbidity values because these tables have found frequent application in pyrheliometric work. In the continued discussion, unless otherwise stated, the turbidity values determined with Hoelper's tables will be used. The amount of precipitable water which is determined with Hoelper's tables together with Houghton's absorption values will also be employed (see Section 1.1.3.).

The variation of the monthly means of β, β_r, β_g and β_{rg} during the measuring season 1962 for Devon Base Station and for Devon Ice Cap Station (Holmgren, 1971, p. 19) is shown in Fig. 5. The annual variation of β (i.e. the mean

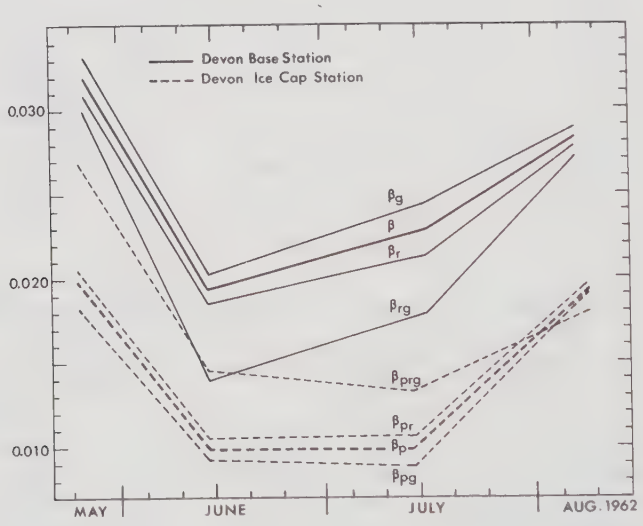

Fig. 5. Variation of monthly means of the turbidity coefficients β, β_r, β_g and β_{rg} at Devon Base Station (15 m above m.s.l.) and Devon Ice Cap Station (1320 m above m.s.l.). Note the low values in June and July. For the derivation of β Hoelper's tables and Davos filter factors have been used.

value of β_g and β_r) for the two stations show the same features, with a fairly constant difference of about 0.010 between the monthly means (Fig. 5 and Table 6). A peculiarity is the summer minimum which is contrary to the annual variation generally found. Thus Liljequist (1956) at Maudheim, Antarctica found a maximum at midsummer, which he ascribed to the hygroscopic particles becoming more effective in an optical sense with increasing water vapor content of the atmosphere. If such a process is active on Devon Island, its influence must have been concealed by other processes. Ångström (1961) suggests that the turbidity maximum, which is often found in early summer, is due to the increasing instability of the atmosphere at that season, causing dust from the heated ground to be carried to higher levels by convection. Obviously, this latter explanation is not applicable to the conditions on Devon Island. Holmgren (1971) suggests that the summer minimum on Devon Island may be a consequence of an increased wash-out of aerosol particles in June and July due to the greater precipitation during that period. In May, according to Holmgren, the stable stratification of the atmosphere may restrain the sedimentation of aerosol particles advected from lower latitudes, thus causing a higher turbidity.

1.3.3. Linke's turbidity factor

Table 7 shows the variation of Linke's turbidity factor (reduced to m = 2.0) according to measurements made in 1962 at Devon Base Station (15 m above m.s.l.). As a comparison, the turbidity factor is also given for Devon Ice Cap Station (1320 m above m.s.l.) and for North Pole 6 according to Kondratyev (1969, p. 295). The turbidity factor at the two stations on Devon Island varies in 1962 in the same way with a maximum in August and a minimum in June, while North Pole 6 in 1957 shows quite a different variation with a maximum in June and minimum in September. However, variations from one year to another may occur making the North Pole measurements incomparable with those from Devon Island. The daily means from Devon Base Station fall within the interval 2.35-2.76, those from Devon Ice Cap Station within the interval 1.94-2.45.

From 9 measuring days in June and July 1959 on the Greenland Ice Cap (1013 m above m.s.l.) Ambach (1963) found for T_p at the relative air mass m_h = 2.0 a mean value 2.27, a maximum value 2.52 and a minimum value 2.13. Further, at the level of this station, the optical air mass 2.0 corresponds approximately to m_h = 2.25. Ambach's values should therefore be somewhat reduced in order to be comparable with the Devon Island measurements. Depending on which value

Table 7. Annual variation of the Linke turbidity factor T reduced to optical air mass m = 2.00.

T = turbidity factor
T_p = extrapolated turbidity factor
n = number of days

		May	June	July	Aug.	Sept.	Mean
North Pole 6, 1957 Kondratyev (1969) (after Sivkov and Zvereva)	T =	2.40	2.54	2.29		2.08	
Devon Base Station, 1962	T =	2.52	2.46	2.55	2.66		2.54
	n =	5	12	17	6		40
Devon Ice Cap Station, 1962	T_p =	2.16	2.07	2.14	2.20		2.12
	n =	13	23	17	7		60

is used on the virtual diurnal variation, that from Table 2 or that appearing from Ambach's values, the reduction would be -0.03 or -0.06, respectively. Similarly, the values in Table 7 from Devon Ice Cap Station situated at the 850 mb - level should be increased by 0.05 in order to be valid at $m_h = 2.0$.

1.3.4. Comparison between the radiation regimes of the two stations on Devon Island

In order to compare the radiation regimes at a low and at a high level station more closely, ten-day means of all parameters evaluated from pyrheliometric measurements made in 1962 at Devon Base Station (15 m above m.s.l.) and Devon Ice Cap Station (1320 m above m.s.l.) are put together in Fig. 6. A number of parameters which may be assumed to influence the radiation conditions are also entered in the diagram. The water vapor pressure e at the two stations and the temperature difference ΔT obtained from screen measurements at the two places have been chosen as being of interest in this connec-

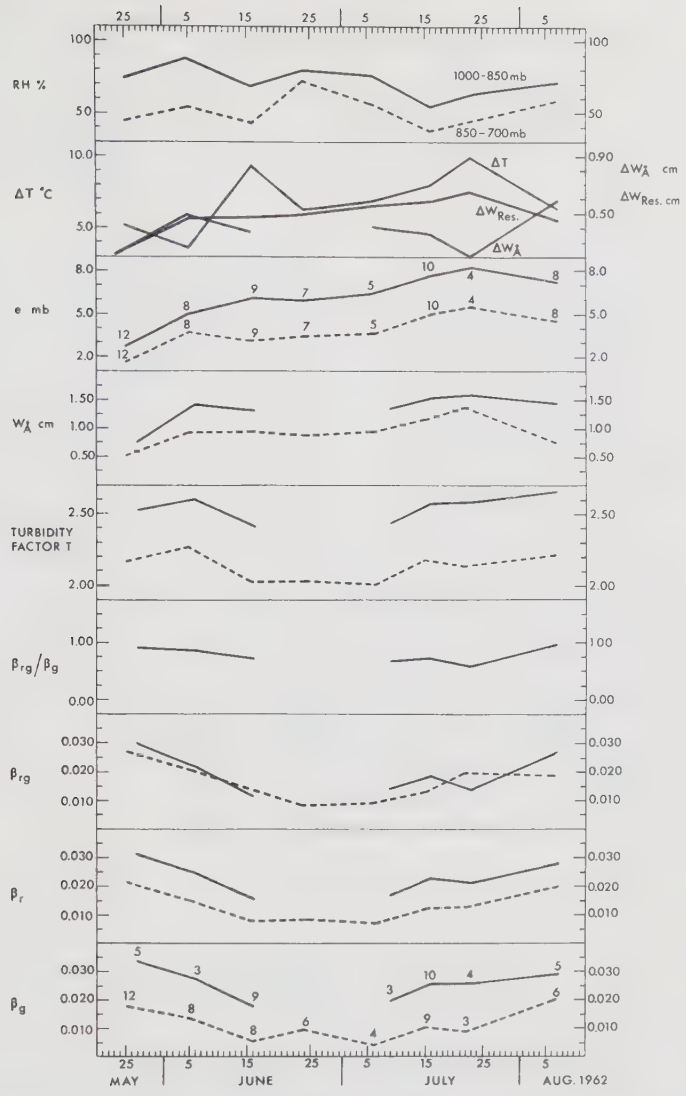

Fig. 6. Variation of the ten-day means of turbidity parameters and selected meteorological parameters at Devon Base Station (full curves) and at Devon Ice Cap Station (dashed curves). The figures at the curves denote the number of days with measurements within each period. The interruption in the curves for the lower station is caused by a period with fog and Stratus.

β_g, β_r and β_{rg} = turbidity coefficients derived from the intensity in the wave-length intervals 0-525 mμ, 0-630 mμ and 525-630 mμ respectively.

$w_Å$ = amount of precipitable water in cm computed with Ångström's formula Eq. (12).

$\Delta w_Å$ and Δw_{Res} = amount of precipitable water in the layer 1000-850 mb computed with Ångström's formula and from radiosoundings at Resolute respectively.

e = water vapor pressure in mb.

ΔT = difference in temperature in ^oC between the two stations.

RH = relative humidity in percent.

tion. Fig. 6 also shows the water vapor content Δw_{Res} in an air column between the levels of the two stations, i.e. approximately between the 1000 mb and 850 mb levels. These values have been calculated from the radiosonde data from Resolute. The mean relative humidity RH in the layers 1000-850 mb and 850-700 mb have been obtained from the same data for days when pyrheliometric measurements were performed.

The variation with time of β_g and β_r is much the same for the two stations with a turbidity difference of about 0.010, while the β_{rg}-curves almost coincide. This β_{rg}-anomaly may depend on improper filter factors. Such errors would cause an appreciable deviation in β_{rg} due to the rather small amount of energy within the wavelength interval 525-630 mμ. The β_{rg}-anomaly could, of course, also be real and would, in that case, be explained by a deviation in α from its normal value 1.3 (Eqs. 4 and 5).

The ratio β_{rg}/β_g which is a useful measure on α (see Section 1.1.1.) is entered in Fig. 6. However, as already mentioned, the accuracy of the measurements does not allow conclusions to be drawn about the absolute value of α. It is evident from Table 6 that, due to the low turbidity, both filter factors and energy integral calculations employed (Eq. 4) strongly affect the outcome of α . Provided that Ångström's relation Eq. (5) is valid, the variation of β_{rg}/β_g might nevertheless be interpreted as a real variation of α in the sense that a high value on β_{rg}/β_g corresponds to a low value on α and vice versa.

An α-value less than 1.3 implies that the β-value (evaluated under the assumption $\alpha = 1.3$) comes out too low, and with $\alpha > 1.3$ β will come out to high (see Ångström, 1963). Also, the calculation of the amount of precipitable water w will be influenced because the absorption value F depends on the turbidity. Thus, a too high turbidity value will give a too small F-value which in its turn will give a too small w-value. Similarly, an underestimation of β recognized by the ratio β_{rg}/β_g being greater than the unity will result in an overrating of w.

Fig. 6 shows the amount of precipitable water in the layer between the sea level and the level of Devon Ice Cap Station. This amount has been determined from pyrheliometric measurements with Ångström's absorption formula Eq. (12) applied, $\Delta w_{\AA}$, and from radiosonde ascents at Resolute, Δw_{Res} . A rather striking inconsistency is that the $\Delta w_{\AA}$-curve shows a minimum during the period 21.7-31.7 while the Δw_{Res}-curve has a maximum at that time. The small number of days with observations, only 4 at the lower and 3 at the higher station, during that period makes the Δw-values uncertain, but, on the

other hand, the same trend also be found during first part of July. The low value of Δw_A in July is also contradicted by the variation of the water vapor pressure e, which indicates a maximum in the water vapor content w in the layer 1000-850 mb at that time. The pyrheliometric method seems to fail in determining the amount of precipitable water in this case.

The temperature difference ΔT between the two stations has an absolute maximum in late July and a secondary maximum in mid June, indicating an increased vertical mixing during those periods. The July maximum certainly coincides with the β_{rg}/β_g-extremes, but a physical explanation of the occurence in terms of aerosol particle sizes appears not to be justified considering the uncertainties involved. Neither does the variation of the relative humidities seem to be simply related to the variation of β_{rg}/β_g, even though it may be noticed that the relative humidity in the layer 1000-850 mb varies roughly in the same way as β_{rg}/β_g for Devon Base Station.

Finally, regarding the variation of the turbidity factor T, it is evident from Fig. 6 that the two curves have the same shape while the difference is increasing towards the end of the season. This divergence is probably due to the increase of water vapor content in the layer between the stations, which is accompanied by a simultaneous increase of water vapor pressure e at both levels. It should also be noted that the amount of precipitable water in the layer 1000-850 mb as calculated from radiosonde data from Resolute, Δw_{Res}, attains its highest value at the end of July.

1.4. The duration of sunshine and the cloudiness

The duration of sunshine offers a possibility to estimate monthly totals of global radiation. For that purpose an empirical relationship between the global radiation and the relative duration of sunshine for each month has been determined (see Section 5.5.). The global radiation can also be computed from the monthly means of cloudiness which is closely related to the relative duration of sunshine.

The duration of bright sunshine was measured with a Campbell-Stokes sunshine recorder specially designed for use in polar regions. When evaluating the recording strips the full length of the burnt trace, no matter how weak, was counted. It is assumed that the instrument, owing to the high transparency of the arctic air, records the sunshine even with the solar altitude = 0, uncorrected for refraction. During winter, early spring and late autumn the

disturbing effect of rime on the glass ball of the instrument may have been of importance, but during the rest of the light season rime or dew was not observed very often.

The possible duration of sunshine S_0 should, according to WMO recommendations, be determined from measurements with the sunshine recorder during days with a completely clear sky. This method, however, requires a measuring period which is long enough to contain a suitable number of clear days. In the present investigation this condition was not fulfilled and therefore the S_0 had to be calculated from Eq. (6).

For that purpose the elevation of the natural horizon at different azimuths should preferably have been determined with a theodolite. That was neglected, but from observations of the exact time of sunset or sunrise the altitude of the visible horizon could be determined. It was found to correspond to a solar elevation, uncorrected for refraction, of about 3° within the sector W - S - E, where the plateau-land ascends abruptly from the coastal plain to a height of 300 m.

During the months of February, March and October sunset and sunrise took place in this sector and during the rest of the light season in the opposite sector occupied by Jones Sound and the distant Ellesmere Island. In this latter sector the visible horizon could be regarded as coinciding with the astronomical horizon.

By putting $h = 0^\circ$ and 3°, respectively, the hour angle of the sun at sunset or sunrise corresponding to the solar altitudes mentioned could be determined from Eq. (6). The double hour angle then gives the possible duration of sunshine S_0 for each day. The relative duration of sunshine S is given by S_a/S_0 where S_a is the actually observed duration of sunshine during a day. In Table 8 is shown the monthly values of S and monthly totals of S_a and S_0. The annual cycle of S can also be studied in Fig. 7. As can be expected, the highest values of relative duration of sunshine S are found in winter and early spring, though it must be stressed that a small deviation in the elevation of the visible horizon from the value accepted here will introduce an appreciable error in the calculated S_0-value for February with its low sun. The annual mean of S, 40 %, is quite equivalent to the highest values found in the Arctic, viz. in Eastern Siberia and in the interior of Alaska (see Gavrilova, 1963, p. 23). On the other hand, not much weight can be given to this comparison because of the short measuring period on Devon Island.

Table 8. Duration of sunshine at Devon Base Station.

S_a = observed duration of sunshine in hours
S = relative duration of sunshine
S_0 = possible duration of sunshine in hours

Month	S_0	1961		1962		Mean of two years observations		Mean duration per day
	hours	S_a hours	S %	S_a hours	S %	S_a hours	S %	hours
Jan.	0							
Feb.*	36	-	-	25	69.8	25	69.8	0.89
Mar.*	289	-	-	187	64.5	187	64.5	6.02
Apr.	545	-	-	322	59.1	322	59.1	10.74
May	744	-	-	291	39.1	291	39.1	9.39
June	720	274	38.1	384	53.3	329	45.7	10.97
July	744	211	28.3	420	56.5	316	42.4	10.18
Aug.	661	148	22.4	187	28.2	168	25.3	5.40
Sept.	405	51	12.7	48	11.9	50	12.3	1.65
Oct.*	123	26	20.1	-	-	25	20.1	0.81
Nov.	0							
Dec.	0							
Year	4267					1713	40.1	

* S_0 for February, March and October with an unobstructed horizon is 90, 341 and 203 hours respectively.

The annual total of S_0 with an unobstructed horizon is 4453 hours.

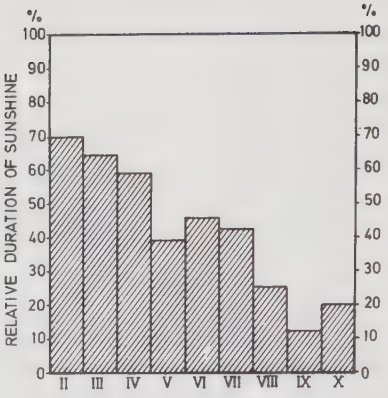

Fig. 7. Annual variation of the relative duration of sunshine at Devon Base Station during the period May 1961-Sept. 1962.

As already mentioned with regard to monthly means, the relative duration of sunshine S is related to the total cloudiness N. This relationship can be written

$$S = 100 - N + K \qquad (20)$$

where K is a correction term which is usually positive in summer and negative during the rest of the year (see Hartmann, 1960). By means of this formula the monthly mean of S can be computed from a known monthly mean cloudiness. With the relationship shown in Section 5.5. monthly totals of global radiation can then be computed from S. However, the applicability of Eq. (20) depends on the constancy of K from one year to another. In order to get an idea of this quality of K monthly means of K-values from Resolute have been analyzed. In doing so average deviation, standard deviation and maximum deviation of K from a ten year period (1960-1969) have been computed. From Table 9 it is evident that Eq. (20) gives the most accurate S-values for the summer months and the least accurate values for winter and early spring. In February and March, ice crystals, which appear as ice haze or thin cirrostratus, are formed also at low levels due to the low temperature. Because of the low sun the ice crystals may cause a reduction of the sunshine without making a corresponding contribution to the observed cloudiness. That might explain the negative K-values and, on account of the difficulty in determining the amount of clouds under such weather conditions, also the larger variability of K. Furthermore, because the cloud amount observed during darkness is included in the monthly mean value, the general tendency to overlook thin cirrus clouds under

Table 9. Mean value and variability of the correction term K at Resolute during a 10 year period (1960-1969).

K is defined by S = 100 - N + K
S = relative duration of sunshine
N = total cloudiness
AD = average deviation of K
s = standard deviation of K

Month	K	AD	s	Maximum deviation
	%	%	%	%
Feb.	- 49	9.7	10.9	17
Mar.	- 22	6.5	8.5	19
Apr.	- 4	5.9	8.5	22
May	+ 7	4.9	5.6	10
June	+ 10	2.5	2.9	4
July	+ 11	2.9	3.4	6
Aug.	+ 7	4.8	5.7	9
Sept.	- 5	4.6	5.2	10
Oct.	- 21	4.6	5.9	12

such conditions may cause an underestimation of N. Especially during the early part of the light season when such clouds are common this may have contributed to the high negative values of K.

Table 10 and Fig. 8 show the annual cycle of cloudiness at Devon Base. Total cloudiness N is defined as the amount in percent of the whole sky that is covered by clouds observed irrespective of height or optical density. Analogously total opacity N_{op} is the amount in percent of the whole sky that is concealed by clouds observed.

Maximum cloudiness is found in September, minimum cloudiness in February, which is in good agreement with the cloud conditions observed at Craig Harbour on the opposite side of Jones Sound on the coast of Ellesmere Island during the period 1935-1940 (see Rae, 1951). In Table 10 is also entered the ratio N/N_{op}, which gives some idea of the optical density of the cloud cover. It will be shown later (Fig. 27) that N/N_{op} shows an annual cycle

Table 10. Monthly means of cloudiness at Devon Base Station.

N = total cloudiness in %

N_{op} = total opacity in %

Month	1961			1962			Mean of two years observations		
	N	N_{op}	N_{op}/N	N	N_{op}	N_{op}/N	N	N_{op}	N_{op}/N
Jan.				41	30	0.73	41	30	0.73
Feb.				25	15	0.60	25	15	0.60
Mar.				43	26	0.61	43	26	0.61
Apr.				55	28	0.51	55	28	0.51
May	56*	41*	0.73*	72	48	0.67	64	45	0.70
June	72	57	0.79	56	45	0.79	64	51	0.79
July	84	72	0.86	51	41	0.81	67	57	0.84
Aug.	81	72	0.89	81	73	0.90	81	72	0.89
Sept.	87	80	0.92	88*	82*	0.93*	88	81	0.93
Oct.	81	71	0.88				81	71	0.88
Nov.	63	54	0.86				63	54	0.86
Dec.	67	59	0.88				67	59	0.88
Year							62	49	0.80

May 1961: 18 days of observation

Sept. 1962: 29 days of observation

* When forming the two year means the May 1961 and September 1962 observations have <u>not</u> been weighted according to the number of observations during these months.

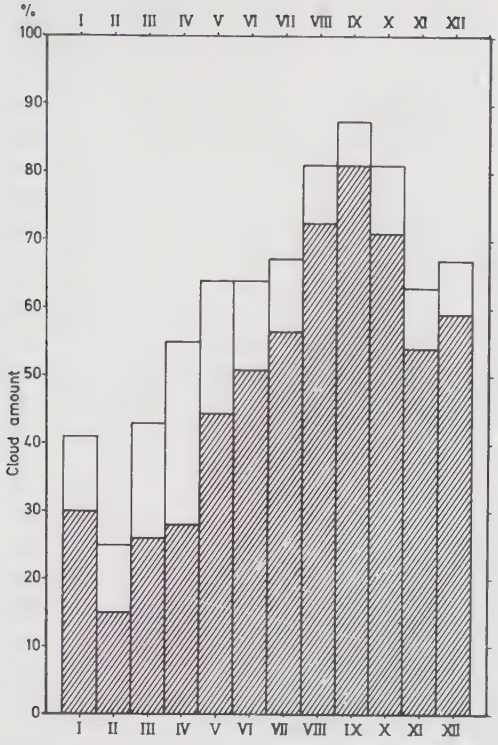

Fig. 8. Annual variation of total cloudiness and of total opacity (shaded areas) during the period May 1961-Sept. 1962.

which is opposite to that of G/G_0 where G denotes daily totals of actual global radiation and G_0 denotes daily totals of the global radiation which would have been measured in the case of a clear sky. The ratio G/G_0 is a useful parameter in climatological work because knowing that ratio together with the normal value of G_0, it is possible to compute G from records of the duration of sunshine by the aid of Savinov-Ångström's formula Eq. (27). However, as is shown in Section 5.5. this formula has deficiencies.

Total cloudiness N, total opacity N_{op}, relative duration of sunshine S and the corresponding K-values at Devon Base Station have been put together in Table 11. The best agreement between S and 100 - N, i.e. the lowest K-values (see Eq. 20), seems to be obtained by using the mean value of N and N_{op}. Compared with the conditions at Resolute, the difference between S and 100 - N is much smaller at Devon Base in winter, early spring and autumn. In March, for instance, K is -22 % at Resolute and +8 % at Devon Base Station. This may be just a coincidence due to the short observation period at Devon Base. It may also be a consequence of certain differences in the maintenance of the two stations, e.g. in the attendance of the sunshine recorders and in the subjective estimation of cloudiness.

Table 11. The relationship between relative duration of sunshine and cloudiness at Devon Base Station

$S = 100 - N + K$ where S = relative duration of sunshine in %

N = total cloudiness in % N_{op} = total opacity in %

K = correction term in % $\bar{K}$ = mean of K and K_{op} in %

	1961						1962						Mean of two years observations					
Month	S	N	K	N_{op}	K_{op}	$\bar{K}$	S	N	K	N_{op}	K_{op}	$\bar{K}$	S	N	K	N_{op}	K_{op}	$\bar{K}$
Jan.							-	41	-	30	-	-	-	41	-	30	-	-
Feb.							70	25	- 6	11	-19	-12.5	70	25	- 6	15	-19	-12.5
Mar.							65	43	+ 8	26	- 9	- 0.5	65	43	+ 8	26	- 9	- 0.5
Apr.							59	55	+14	28	-13	+ 0.5	59	55	+14	28	-13	+ 0.5
May							39	72	+11	48	-13	- 1.0	39	72	+11	48	-13	- 1.0
June	38	72	+10	57	- 5	+ 2.5	53	56	+ 9	45	- 2	+ 3.5	46	64	+10	51	- 3	+ 3.5
July	28	84	+12	72	± 0	+ 6.0	57	51	+ 8	41	- 2	+ 3.0	42	67	+ 9	57	- 1	+ 4.0
Aug.	22	81	+ 3	72	- 6	- 1.5	28	81	+ 9	73	+ 1	+ 5.0	25	81	+ 6	72	- 3	+ 1.5
Sept.	13	87	± 0	80	- 7	- 3.5	12	88	± 0	82	- 6	-3.0	12	88	± 0	81	- 7	- 3.5
Oct.	20	81	+ 1	71	- 9	- 4.0							20	81	+ 1	71	- 9	- 4.0
Nov.	-	63	-	54	-	-							-	63	-	54	-	-
Dec.	-	67	-	59	-	-							-	67	-	59	-	-
Mean of K															+5.9		-8.6	- 1.3

Sept. 1962: 29 days

Feb. 1962: 10 days (sun above the horizon)

The February and September 1962 values are not weighted according to the number of days when calculating the mean of two years.

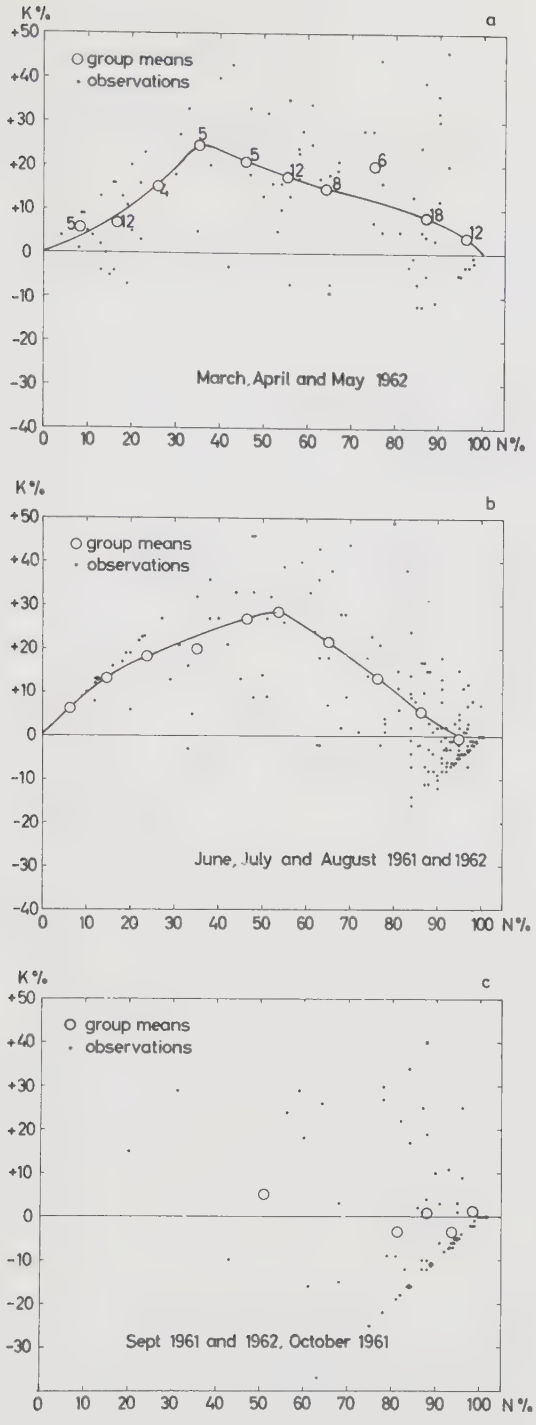

Fig. 9 a–c. The correction term K as a function of total cloudiness N. The relation between relative duration of sunshine S and cloudiness N is given by S = 100 – N + K.

As will be discussed in greater detail in Section 5.5. there is no linear relationship between S and G/G_0 which is presupposed in the Savinov-Ångström formula (Eq. 27). Therefore, the use of this formula may lead to errors in the computation of G or G/G_0. Another way of calculating G/G_0 with known S is to use normal curves showing the relationship between S and G/G_0 for each month (Fig. 31 a-j). To that end it is suitable to separate the S-values observed during a month in a number of groups, as a suggestion five, instead of using one single mean value. If, however, only cloud observations are available for this calculation, it is not advisable to apply the correction term K (Eq. 20) obtained from Table 11 for the month in question to each interval of cloudiness in order to get the corresponding S-value. It is, for example, obvious that K must be equal to zero when N = 0, provided that no other obstructions exist, such as low fog or haze, which are not included in the cloud observations (see above).

In order to investigate the relationship between the last mentioned parameters, K has been plotted versus N in a diagram and group means have been computed for cloudiness - intervals of 10 % (see Fig. 9 a-c). Because of the relatively small number of available observations, months with approximately the same K-values have been referred to the same group. Thus March, April and May form one group (Fig. 9 a), June, July and August one group (Fig. 9 b) and September and October one group (Fig. 9 c). From the curves of Fig. 9 a and b can be seen that K attains a maximum in June-August which is about three times the mean value of K for the same period and a maximum in March-May about twice the mean value of K for the latter period. The maximum of K occurs in the first case at a cloudiness of 50 % and in the second case at a cloudiness of 35 %, i.e. at a cloudiness which is generally less frequent than the extremes of 0 % and 100 %. No characteristic features in the variation of K with cloudiness can be distinguished for the months of September and October (Fig. 9 c).

2. Calibration of the Eppley pyranometer

2.1. Calibration with the Ångström pyrheliometer

During the period May 22 - Aug. 11, 1962 a total of 87 calibrations of the Eppley pyranometer (no. 4255, model 50 junction) were made. Immediately before and after a series of measurements of the direct solar radiation with the Ångström pyrheliometer the pyranometer was shaded with a circular disk occupying the same angle as seen from the sensing surface as the effective opening angle of the pyrheliometer, namely 5°. The voltage output from the pyranometer with and without shading disk was read on a precision potentiometer.

The direct solar radiation intensity as measured with the pyrheliometer was extrapolated to be valid for the time when the output from the Eppley was read. The calibration factor C (ly min^{-1} $millivolt^{-1}$) is given by

$$C = \frac{I \sin h}{V_g - V_d}$$

where I = intensity of direct solar radiation
h = solar altitude
V_g = output in millivolt from the pyranometer when measuring global radiation with a clear sky
V_d = output in millivolt from the shaded pyranometer, i.e. when measuring diffuse clear sky radiation.

With a few exceptions each value of C is the mean obtained from two shadings of the pyranometer, namely one made before and one made after the pyrheliometer measuring series. In order to make sure that no rapid changes in the intensity of the diffuse sky radiation occured during the calibration procedure, no calibrations were performed unless the sky was completely or almost clear.

It became obvious rather soon that there was a pronounced dependence of the calibration factor on the azimuth of the sun. In order to get more information about this azimuth effect, the asymmetry around true noon of the recorded global radiation with a completely clear sky G_o was studied. It is then assumed that there is no real difference between the global radiation energy received before and after noon. This assumption is supported by the

β-determinations. The temperature difference between forenoon and afternoon was so small that the temperature influence on the calibration factor could be neglected (see below). To that end the global radiation energy G_0 (expressed in scale units) received during hourly intervals of true solar time was evaluated from the records.

In the absence of registrations of diffuse clear sky radiation, normal values of the diffuse clear sky radiation D for hourly intervals true solar time were computed from point measurements with a shaded pyranometer. Values obtained in this manner have been used to form a ratio R" where forenoon values on G - D are compared with afternoon values for corresponding hourly interval, i.e. with the same absolute hour angle. A total of 338 values on R" was obtained from clear days in the middle of June and July when the solar altitude could be regarded as much the same for the same hour angle during the whole period. The variation of R" with the hour angle is shown in Fig. 10.

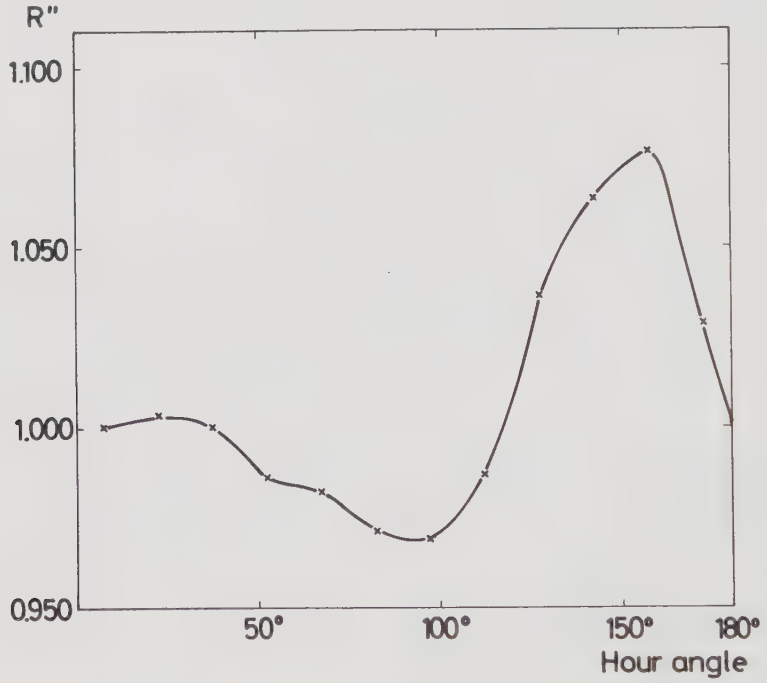

Fig. 10. The ratio R" between forenoon and afternoon recorded values of direct solar radiation on a horizontal surface as a function of the hour angle of the sun.

Group means of the calibration factor C as a function of the hour angle have been computed and are entered in Fig. 11. In this diagram two curves are drawn, one representing forenoon calibrations and one representing afternoon calibrations. By means of the ratio R" it is possible to calculate forenoon calibration factors from known afternoon calibration factors and vice versa.

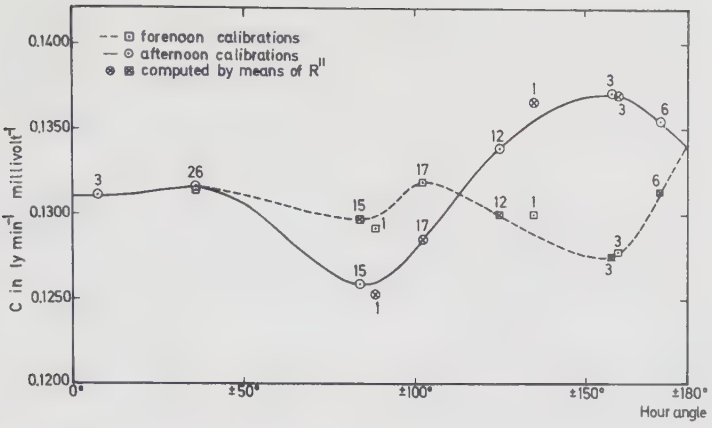

Fig. 11. Calibration factor C as a function of the hour angle of the sun.

In that way the number of points in the diagram has been increased and it can be seen from Fig. 11 that calibration values calculated in the way just outlined are in good agreement with those obtained directly from pyrheliometric measurements.

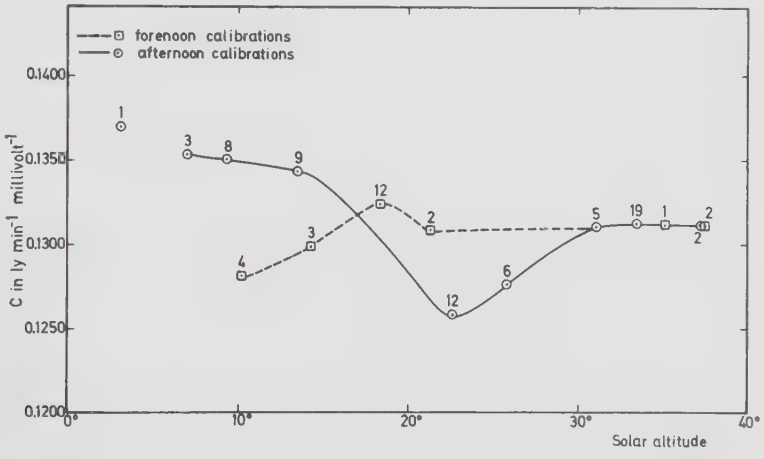

Fig. 12. Calibration factor C as a function of the solar altitude.

Fig. 12 shows the variation of the calibration factor with the solar altitude. Here two sets of group means have been computed with forenoon and afternoon values separated. As can be seen from the diagram, the forenoon calibration factor for a solar altitude of 3.1°, which is based on only one observation indicates a deviation from the cosine law at low solar altitudes. A deviation from the cosine law of the Eppley pyranometer has been reported by several authors, e.g. by Woertz and Hand (1941) who found a pronounced decrease in

the sensitivity of the instrument at solar altitudes lower than 20°. However, the predominant factor influencing the sensitivity of the pyranometer seems to be the azimuth of the sun or, which is approximately equivalent, the hour angle. The hour angle will be used as parameter when determining the calibration factor for hourly intervals with the sun unobscured.

It must then be pointed out that the range of variation of the solar altitude at a certain hour angle was rather small, only 8°, throughout the period of calibration. With a longer calibration season it might have been possible to separate the data in groups according to the hour angle and to determine a possible variation of the calibration factor with the solar altitude within each hour angle group. The cause for the azimuth dependence may have been that the receiver was not parallell to the level fixed to the tripode or that the sensing surface was not flat.

Like all pyranometers, unless they are supplied with a special temperature compensation, the Eppley instrument has a temperature coefficient. During the calibration period, May 23 to Aug. 11, the temperature varied between -9°C and +17°C with a mean of +5.4°C as measured at the times when a calibration was made. Consequently, the calibration curve is valid for the temperature +5.4°C. When evaluating the Eppley readings for the summer months with daily mean temperatures departing no more than 5°C from the reference temperature, the calibration factor C (valid for +5.4°C) could be used directly without introducing any serious error, but for the rest of the year the temperature influence on the sensitivity of the pyranometer should not be neglected (compare below).

Due to the small temperature variation during the calibration period it was not possible to determine a temperature coefficient from the measurements with a satisfying accuracy. Therefore, it was necessary to rely on other investigations of these characteristics of the Eppley even though there may exist differences between different pyranometers in that respect. Thus the Eppley Laboratories have given the value -0.05 to -0.1 % per °C and MacDonald (1951) the value -0.06 to -0.12 %. Flowers and Helfert (1966) could distinguish two separate groups with the values -0.09 % and -0.16 % per °C within the temperature interval -40°C to +5°C. From this information an average temperature correction of -0.1 % per °C was chosen to be applied to the present pyranometer observations. A maximum error of 2.5 % is then introduced for the month of February, which has a mean temperature of -37°C, by this rather arbitrary choice of correction factor. As mentioned earlier, no temperature correction was applied for the summer months.

When evaluating spot readings or records of the pyranometer output in situations with a clear sky the calibration factor was taken from the curves of Fig. 11. For measurements with a dense overcast the calibration factor was calculated from the curves of Fig. 11, i.e. a mean value was derived from values read at every 10^{o} of the hour angle and it was determined to 0.1311 ly min^{-1} per millivolt. As a comparison, it may be mentioned that the calibration factor given by the manufacturer was 0.1282 ly min^{-1} per millivolt. However, as is shown in Section 2.2., certain characteristics of the Eppley pyranometer make this rather good agreement between the two calibration factors only apparent. For measurements in situations with scattered clouds or a broken cloud cover the calibration factor was taken as the mean of that valid for an overcast sky and that valid for a clear sky.

From May 13 to September 7, 1962 the global radiation was registrered with a clockdriven galvanometer recorder, Cambridge no C462611, which was supplied with a voltage divider to fit the output from the pyranometer. At regular 3-hour intervals the pyranometer output was read on a precision potentiometer, while the recorder was temporarily disconnected. In situations giving a smooth curve upon the recording paper, 335 such comparisons distributed over the whole output range were obtained. In this way a calibration curve could be constructed which was now valid for the whole circuit consisting of thermopile, leads, voltage divider and recorder. This curve appeared to deviate from a straight line which would have shown the expected performance of the recorder. This deviation may have been caused by the fact that the band supporting the galvanometer coil was broken during the transport. Because spare parts were not available, the remainder of the broken band had to be used. After the repair the band had become shorter for which reason it lost its original characteristics. In drawing the calibration curve the scale units read on the recording paper were plotted versus the pyranometer output as measured with a potentiometer, i.e. the output without voltage drop in the circuit. This curve was used when evaluating the records of global radiation.

2.2. Investigation of some characteristics of the Eppley pyranometer

During our stay on Devon Island some pecularities in the performance of the Eppley pyranometer were observed in connection with albedo measurements, i.e. when the instrument was inverted. Thus, albedo values above 100 % were encountered over a snow surface on a number of occasions in spite of the careful

calibrations of the instrument by means of an Ångström pyrheliometer at different solar altitudes and azimuths of the sun. The direct solar radiation plus the diffuse sky radiation might have affected the instrument when it was inverted, the result being an increase in the output of the pyranometer. There were also good reasons to suspect that the reflected radiation from the snow surface influenced the reading when the pyranometer pointed upwards.

After our return home an attempt was made to study the error thus introduced. Unfortunately, it was not possible to study the same instrument which was used during the expedition. Instead, Eppley no. 4590, model 50 junction, was used with a mounting arrangement as similar as possible to that used on Devon Island. It is then assumed that differences between individual instruments of the same type are small enough to justify such a procedure. Corrections determined in that way have been applied to the Eppley measurements made on Devon Island.

Some simple experiments were first performed to find out the causes of the error. An inverted Eppley was exposed under a cloudless sky and the voltage output was measured with a precision potentiometer. When a shading disk, just large enough to screen off the direct sunshine from the thermopile mount, i.e. from the back of the receiving plate, was attached to the glass bulb, a considerable decrease in the output was encountered. After the shading it took about 15 min for the reading to stabilize. Most of the bulb was exposed to the solar radiation, thus permitting reflexes in the glass cover to strike the thermopile receiving surface. However, no significant difference in the output was observed when the whole glass bulb was screened from direct solar radiation with the help of a second disk. The experiment was repeated twice with the same result. Obviously, there was no noticeable influence from reflections in the glass cover caused by direct solar radiation. It should be added that this experiment was performed at a solar altitude of 10°.

This finding is not consistent with the results from laboratory tests of the Eppley instrument made by Fuquay and Buettner (1957), who found a marked influence on the sensitivity from glass reflections. At the same angle of incidence as in our experiment, but using an artificial light source, they found that the reflections had a maximum effect on the output. Fuquay and Buettner do not specifically mention if the thermopile mount in their experiment was struck by the beam but the fact that they got both positive and negative outputs from the Eppley at low zenith angles unquestionably supports their opinion that the effect in this particular experiment arose from reflections in the glass cover. We always observed an increase in the output from the Eppley apparently due to the radiation from above striking the ther-

mopile mount. This indicates that the heating of the thermopile mount must be the dominating factor. This heating should lead to a change in the convective pattern within the glass cover (see Holmgren, 1971).

Due to the complicated reactions of the instrument laboratory investigations probably have a limited value when the error is to be determined quantitatively. There is then no other choice than to try to determine the error by experiments under natural conditions. One way is to make comparisons with a pyranometer of different construction and lacking the Eppley characteristics just mentioned, both instruments being very carefully calibrated at different solar altitudes and with the temperature coefficients accurately determined. These requirements are, however, not easily fulfilled. Therefore, a method was used which made calibrations with a pyrheliometer unnecessary. A Moll-Gorczynski pyranometer and an Eppley were run simultaneously and both instruments were connected to the same recording electronic potentiometer. The Eppley was supplied with a cylindrical shield having the same height as the thermopile sensing surface and protecting the thermopile mount, i.e. the back of the receiving plate, from radiation.

The Eppley was mounted on an unpainted, wooden plate which had a diameter of 26 cm and, thereby, approximately the same area and reflectivity as that used on Devon Island. The cylinder, which had a diameter of 20 cm, was painted flat black on the inside. Its lower edge was mounted 1 cm above the base plate in order to permit ventilation through the natural air flow. Every time the cylinder was introduced, a black-painted disk with a diameter 1 cm less than that of the cylinder was fixed on the tripod of the pyranometer in order to prevent radiation reflected by the rather bright base plate from reaching the thermopile mount. It is an open question if the precautions described were sufficient to prevent heated air from being trapped around the glass bulb. It is also unknown to what extent long wave radiation from the heated cylinder may have influenced the temperature of the glass bulb. Certainly a temperature difference between the lower and upper part of the glass cover must influence the convective patterns within the bulb and should consequently have <u>some</u> effect on the voltage output. The cylindrical shield was regularly removed at twelve o'clock on one day and replaced at the same time on the next day.

The average outputs (expressed in scale units) within even hours were determined for both instruments and the ratios E_{sh}/M_{sh} and E/M were computed. Here E_{sh} and M_{sh} refer to measurements with the Eppley and with the Moll-Gorczynski pyranometers during hours when the Eppley was supplied with a shield, E and M to measurements with the Eppley unprotected by a shield. The ratio E_{sh}/M_{sh} ob-

tained with a shielded Eppley during certain hour intervals has been compared with the ratio E/M obtained with an unshielded Eppley during the corresponding hour interval on a second day. Only measurements from days with approximately constant solar altitudes at corresponding times have been employed for the comparisons. In that way the effect of solar altitude and azimuth on the calibration factor has been eliminated. Temperature effects arising from the normal diurnal variation of temperature are also eliminated in that way, while, of course, effects due to great changes in temperature from one day to the next day may add to the error which is to be investigated.

The error in percent of a measurement with an unshielded Eppley is then given by

$$\frac{1}{E}\left(E - M\ \frac{E_{sh}}{M_{sh}}\right) \qquad (22)$$

where the second term in the parenthesis represents the radiation energy which would have been obtained with a shielded Eppley.

$$\frac{M}{E}\left(\frac{E}{M} - \frac{E_{sh}}{M_{sh}}\right) \qquad (23)$$

is equivalent to the preceding expression and has been used for the practical computations.

Only data obtained under clear sky conditions or under overcast conditions have been used. Such a separation is necessary due to the dependence on the solar altitude of the amount of radiation reaching the thermopile mount. The error arising from direct solar radiation striking the back side of the Eppley will vary strongly with the solar altitude especially when the Eppley is used in an inverted position, as will be shown below.

An important question is if the magnitude of the error is only a function of the radiation energy received by the thermopile mount or if it is also a function of the radiation energy striking the thermopile sensing surface. If there is direct proportionality between the error and the radiation which is absorbed by the sensing surface, then the error would be included in the calibration factor which is obtained from comparisons in situ with the Ångström pyrheliometer under actual albedo conditions. Our calibrations indicated no relationship between calibration factor and albedo. It is therefore assumed that the error is mainly a function of the amount of radiation energy received by the thermopile mount, i.e. the back of the circular sensing disk.

2.2.1. The instrument error with the Eppley in an upright position

The errors determined here are valid for an Eppley with the mounting arrangement described above, viz. a circular, unpainted, wooden plate with a diameter of 26 cm. From 32 hours of simultaneous runs of the Moll-Gorczynski and Eppley pyranometers in Uppsala during the period April 1 to May 12 under overcast conditions and with the ground bare of snow it was found that the output of the unshielded Eppley was 1.7 % higher than the output of the shielded Eppley. From 73 hours of run under clear sky conditions during the same period the error came out to 1.5 %. No significant dependence on the solar altitude could be detected. The value 1.5 % will be used, as being the most representative for bare ground with an albedo of 20 % as determined with the Moll-Gorczynski pyranometer.

With the sky overcast and the ground snow-covered the error was determined to 3.7 %. This was obtained from 28 hours of recording and with an albedo of 73 %. From 61 hours of recording global radiation from a clear sky at the same albedo a dependence on the solar altitude could be recognized. Group means of the error plotted versus solar altitude are computed and shown in Fig. 13, where the number of observations in each group is also entered. The value 12.1 % at the lowest solar altitude, 1.7°, is uncertain, being based upon

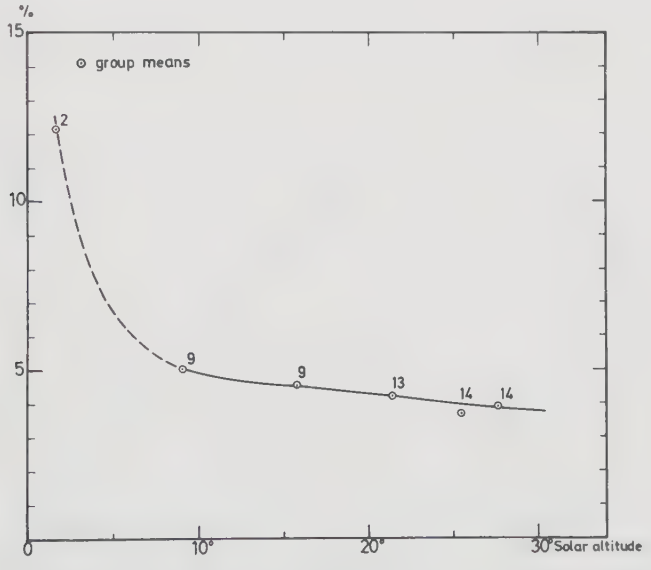

Fig. 13. The instrument error introduced by radiation reflected from the snow surface ground with albedo of 73 %. The Eppley pyranometer no. 4590 faces zenith. The error K, in percent of measured global radiation, is plotted against solar altitude.

only 2 hours of registration. It is, therefore, excluded when computing a weighted mean of the error from all the observations. This mean, which was found to be 4.2 % , has been accepted as the error in percent of the global radiation which is obtained from an unshielded Eppley at an albedo of 73 % during all sorts of sky conditions.

2.2.2. The instrument error with the Eppley in an inverted position

The measurements were performed in Uppsala during the summer at an albedo of 20 %. The error is expressed as a percentage of the reflected radiation from the ground as measured with the unshielded Eppley. The error was determined to 20.9 % of the output from 19 hours of records of the reflected radiation with an unshielded Eppley and from approximately the same number of hours with a shielded instrument during overcast conditions. With a clear sky, as a result of 85 hours of recording, the error in percent of the measured reflected radiation is shown in Fig. 14. The error is given as a function of the solar altitude. No hour intervals with a solar altitude greater than 40°

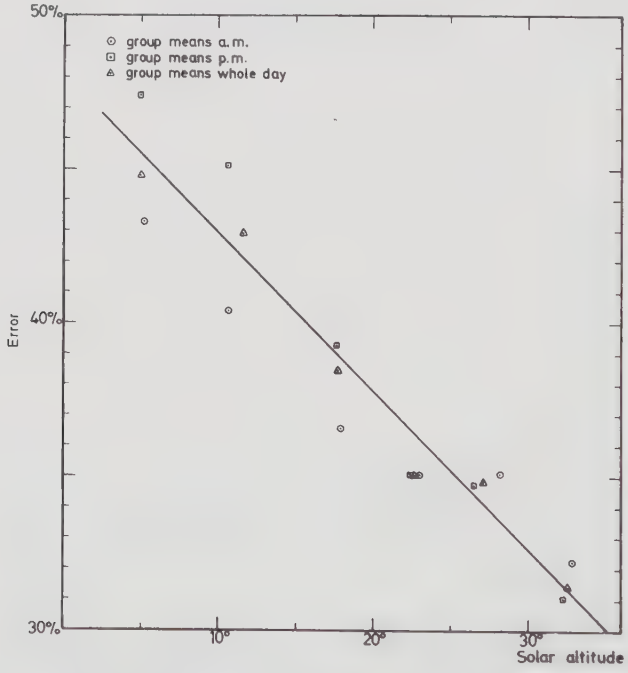

Fig. 14. The instrument error introduced by global radiation from a clear sky on the back of the disk containing the thermopile. The Eppley no. 4590 is in an inverted position over a surface with an albedo of 20 %. The error is given in percent of measured reflected radiation as a function of solar altitude.

were included in the group means because at that altitude the mounting plate, i.e. the wooden disk supporting the pyranometer, started to screen off the thermopile mount from the sun. As can be seen from Fig. 14 the percentage error increases rapidly with decreasing solar altitude. The dependence on the sun's azimuth, as shown by the difference between forenoon and afternoon group mean values, may be explained by an imperfect leveling of the inverted pyranometer. The errors discussed above are all referred to the radiation energy measured with an unshielded Eppley.

2.2.3. The response time of the Eppley as regards the radiation from the back side

From registrations of the output of an Eppley pyranometer it was observed that it took a considerable time for the output to stabilize when the shield was removed or put on. This feature of the instrument was especially pronounced when the pyranometer was inverted under clear sky conditions. When the instrument is used for determining the albedo by making one spot reading with the pyranometer facing zenith and one with the instrument inverted, the thermopile mount will suddenly be exposed to an increased radiation when the instrument is turned over. This increase is particularly great when the albedo of the ground is small. Therefore the time passed between the turning over of the instrument and the reading of the output is of importance.

With the Eppley inverted the response time was determined from records from five clear days. It took about 15 minutes before the final difference in pyranometer output with and without shield had developed. This may be compared with the response for changes in the intensity of the radiation striking the sensing surface of the pyranometer. According to the manufacturer the response time for 98 % signal is approximately 30 seconds. In Fig. 15 the attained part (in percent) of that difference is plotted versus the time that had passed since the shield was removed or put on. The output, which would have been obtained if the shield had not been changed, was calculated from the recorded output of an inverted Moll-Gorczynski pyranometer. The performance of the instrument during the first two minutes was investigated by means of spot readings. It can be seen from Fig. 15 that half the difference between the outputs with and without the shield was attained after 80 seconds.

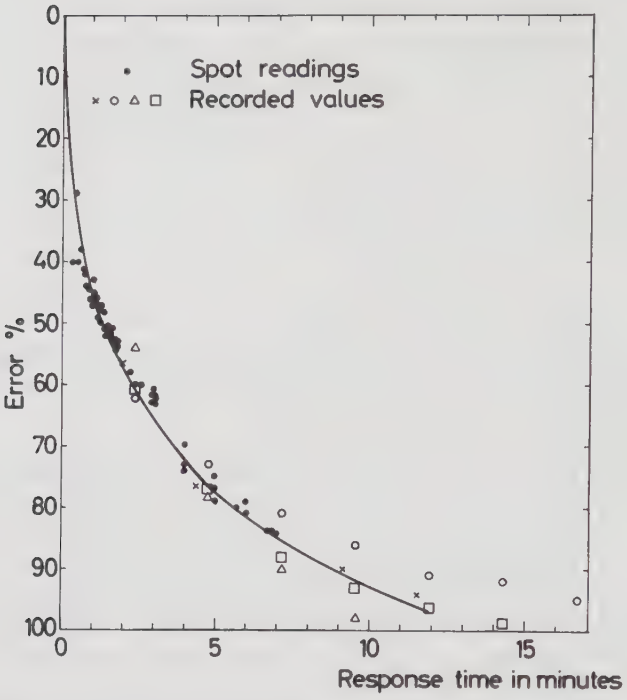

Fig. 15. Response of the inverted Eppley no. 4590 when the back of the disk containing the thermopile is suddenly exposed to the global radiation. Attained part in percent of fully developed difference is plotted against time.

3. Albedo

The albedo measurements were made over a flat area covered with thin, short grass in the summer. The surface, which sloped gently towards NW with an angle of 1° to 2°, was probably in the snow-free season representative for the whole lowland area with the exception of the numerous lakes and ponds. The ice on the larger lakes did not melt away until August. The albedo of the ice was at least twice that of the bare ground. On the other hand, with open water in the lakes the bare ground, which had a mean albedo of 15 %, had a higher reflectivity than the water surfaces except in situations with a clear sky and low solar altitudes. As will be pointed out in Section 4, this inhomogeneity of the surface of the station area influences the diffuse clear sky radiation.

Because only one pyranometer, Eppley, serial number 4255, model 50 junction, was available, the same instrument had to be used for measuring both incoming and reflected shortwave radiation. Thus, a point measurement of the global radiation was made whereupon the pyranometer was turned upside down and the reflected radiation was measured. The time between these two measurements averaged one minute.

As mentioned above, with a snow surface several albedo values turned out to be quite absurd (> 100 %). An investigation of the characteristics of the type of instrument used was therefore carried out (Section 2.2). When the corrections thus obtained were applied to the radiation measurements, the albedo of snow under a clear sky at low solar altitudes was found to exceed that with a dense overcast. At the highest solar altitudes ($h = 35^{\circ}$) the corrected albedo values were equal to or slightly less than those obtained under an overcast sky. This result is not consistent with the generally accepted view on the matter. Thus Liljequist (1956), from measurements on an antarctic shelf-ice, found that the albedo with a clear sky was 3-9 % lower than that with an overcast sky. These latter albedo values valid for clean, frozen snow turned out to be in good agreement with values obtained at comparable places, i.e. the albedo of the snow before the melting had started was found to be around 85 %.

One explanation of the failure of the corrections to give reasonable albedo values during clear sky conditions might be found in the strong dependence of the correction factor on the solar altitude when the pyranometer was inverted (see Fig. 14). At least at low solar altitudes an improper leveling

of the inverted pyranometer will have a great influence on the amount of heat received by the thermopile mount, while the effect from an improper leveling on the amount of reflected radiation received by the sensing surface will be negligible due to the almost isotropic nature of that radiation. Therefore, in our case only albedo measurements with an overcast sky have been accepted.

The following empirical correction formulas were derived by means of the results from the investigation of the characteristics of the Eppley pyranometer. The error with the pyranometer facing the zenith was found to be

$$\Delta P_A = P_A \left[0.015 + 0.051 \ (A - 0.20) \right] \tag{24}$$

where P_A is the measured global radiation at the albedo A.

With the pyranometer in a reversed position the error can be written

$$\Delta RP_A = \frac{0.20 \cdot 0.2}{1 - 0.21} \ (P_A - \Delta P_A) \tag{25}$$

Inserting ΔP_A from Eq. (24) gives

$$\Delta RP_A = 0.0532 \left[0.985 - 0.051 \ (A - 0.20) \right] P_A \tag{26}$$

The reading will not have stabilized until about 15 minutes after the turning due to the great lag of the instrument as regards the radiation towards the thermopile mount. From Fig. 15 it can be seen that 46 % of the maximum error will be attained after one minute, which was the mean time space between the readings of the output during an albedo measurement. Because the error ΔP_A given by Eq. (24) is already attained, the error one minute after the turning over of the pyranometer will be

$$\Delta P_A + 0.46 \ (\Delta RP_A - \Delta P_A)$$

The differences between the measured, uncorrected albedos and the true ones are given in Table 12. The instrument errors are given for two cases, one where one minute has elapsed between the two readings of the pyranometer and

Table 12. Difference between measured and true albedo during overcast conditions when the Eppley pyranometer no. 4590 is mounted on an unpainted disk of red deal with diameter 26 cm.

The difference has to be subtracted from the albedo obtained from uncorrected measurements in order to get the true albedo.

1. One minute between readings with the instrument in upright and reversed position.

2. With fully developed difference.

True albedo	Difference 1	2
0.00	0.027	0.053
0.05	0.028	0.052
0.10	0.029	0.052
0.15	0.029	0.051
0.20	0.029	0.049
0.25	0.029	0.048
0.30	0.029	0.046
0.40	0.027	0.042
0.50	0.025	0.036
0.60	0.021	0.030
0.70	0.017	0.023
0.75	0.014	0.019
0.80	0.011	0.014
0.85	0.008	0.010
0.90	0.005	0.004
0.95	0.001	0.000
1.00	- 0.003	- 0.006

one where the error is fully developed, i.e. after more than 15 minutes. The latter case also corresponds to albedo measurements with two pyranometers which are permanently installed with identical mounting equipments and which have been compared with each other during overcast conditions.

Table 13. Monthly mean values of albedo measured during overcast conditions.

n = number of days with measurements.

	A %	n
March 1962	87	6
April 1962	88	8
May 1962	85	10
September 1961 and 1962 *	15	17

* Only days with no snow on the ground.

The result of the albedo measurements (with corrections applied) are shown in Table 13. Only days with a continuous snow cover or days with the ground bare of snow have been included. During the period with a continuous snow cover the mean albedo with an overcast sky can be taken as 87 %, the albedo of the bare ground as 15 %. In the latter case, however, the albedo value is not representative for a large area around the station, i.e. it is a rather local value. As a comparison it may be mentioned that Liljequist (1956) obtained 88-89 % in overcast weather as a mean for the whole measuring period at Maudheim, Antarctica. Holmgren (1971) found an albedo of 88 % in May 1963 at Devon Ice Cap Station. Gavrilova (1963) reports albedo values of 15-18 % for a bare ground with conditions similar to those at Devon Base Station, i.e. a dry tundra with the remains of the previous season's grass.

4. The diffuse radiation from a clear sky

When the direct solar radiation was measured with the Ångström pyrheliometer, the Eppley pyranometer was shaded from direct solar radiation at the same time with a circular disk. As a calibration generally was made with a more or less cloudless sky, a measurement of the diffuse clear sky radiation was obtained besides. The turbidity of the atmosphere was, in such situations, also determined from filter measurements with the Ångström pyrheliometer. The diffuse clear-sky radiation could, therefore, be studied as a function of the turbidity.

There is, however, an instrumental effect which causes errors which are especially serious when the diffuse sky radiation is to be measured. As mentioned before (Section 2.2), the Eppley pyranometer is sensitive to the reflected radiation which strikes the back of the receiving plate containing the thermo-junctions. This error is proportional to the radiation energy which is reflected by the ground surface and by the support of the pyranometer. Its absolute value does not change when the pyranometer is shaded from direct solar radiation. When the ground is covered by snow the error thus introduced may reach 30 % of the real diffuse sky radiation.

The mean albedo at Devon Base Station with the ground completely covered by dry snow was 87 %, with bare ground 15 %. These values had been obtained in situations with a dense overcast. Assuming the error to be a linear function of the albedo, Eq. (24) will give the error 4.9 % of the read pyranometer output with albedo 87 % and 1.3 % with albedo 15 %. The shading disk which was used occupied a solid angle approximately equal to the effective opening angle of the Ångström pyrheliometer. The disk was big enough to shade the receiving plate, but too small to protect the whole glass bulb from the direct solar radiation. Accordingly, the possibility of multiple reflexions within the glass bulb cannot be excluded, but there are reasons to believe that this effect was small compared with that mentioned above, viz. the influence from solar radiation reflected from the ground and reaching the back of the receiving plate.

All measurements have been corrected by -1.3 % of the read pyranometer output when the ground was bare of snow and by -4.9 % when the ground was covered by non-melting snow and by a percentage obtained from interpolation between these values according to the actual albedo during the period of melting snow.

The whole material consists of 400 spot-measurements of the diffuse clear sky radiation. In most cases the sky was completely cloudless, but up to one eighth of cloudiness was tolerated provided the clouds were close to the horizon and not too near the sun. Every case with even a trace of clouds obscuring the sun was rejected.

About 300 measurements, out of a total number of 400, were made simultaneously with a turbidity measurement or within a few hours from that time. About 80 measurements were made when the ground was covered by snow, but out of those only 20 were made in connection with turbidity measurements. Only measurements with the ground bare of snow were made in sufficient number to permit a study of the relationship between the diffuse sky radiation intensity and the turbidity. All radiation values have been reduced to mean solar distance.

One part of the scattered solar radiation reaches the ground, a small fraction is absorbed in the air and the rest vanishes into space. The solar radiation which is reflected from the earth's surface contributes also to the scattering processes of the air thus increasing the intensity of the diffuse sky radiation. It is, of course, the mean albedo of the whole region which is relevant in this case. The expression "region" here refers to an area having a diameter with an order of magnitude of 10 km.

In winter and spring when the ground and the adjacent sea- and lake-ice are covered by snow the albedo conditions are homogeneous in the area and the measured albedo may be considered as representative also for the region. In

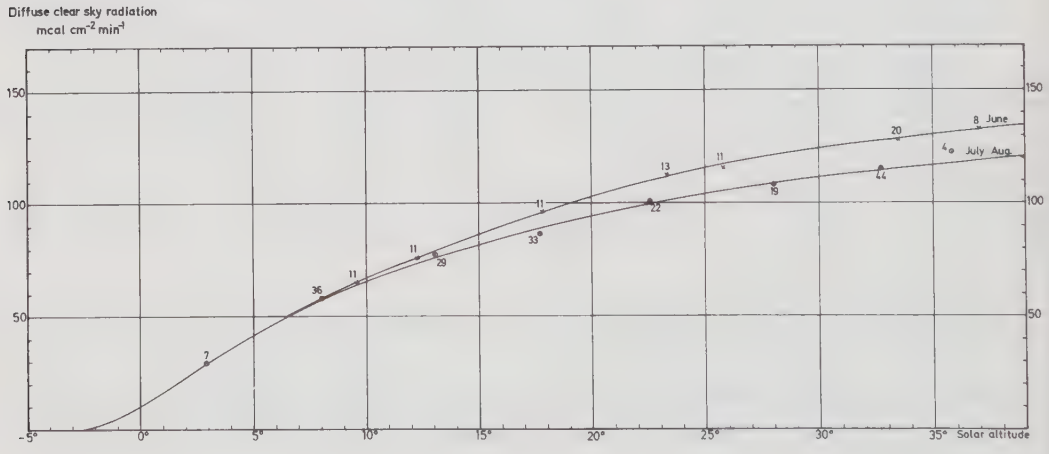

Fig. 16. Diffuse clear sky radiation in June, July and August as a function of the solar altitude. Intensities are reduced to mean solar distance and turbidity $\beta = 0.025$.

summer, at a time when the ground is bare but the lakes and the sea are still covered by ice, the regional albedo is likely to be considerably higher than the 15 % measured at Devon Base Station.

During summer the sea- and lake-ice melts gradually and accordingly the regional albedo should decrease towards the end of the summer. This is also reflected in Fig. 16 and Table 14 which show the diffuse clear sky radiation in June (after the melting of the snow, but with the lakes and the sea still ice-covered) and in July and August. The intensities of both periods are reduced to the same turbidity ($\beta = 0.025$). At a solar altitude of 35° the intensity of the diffuse clear sky radiation is 10 % higher in June than in July and August.

Table 14. Group means of diffuse clear sky radiation data reduced to mean solar distance and turbidity $\beta = 0.025$.

Computed solar altitudes are corrected for refraction.

h = solar altitude in degrees
d = diffuse clear sky radiation in mcal $cm^{-2}min^{-1}$
n = number of observations

Bare ground, June 1962

h	9.6	12.2	17.8	23.3	25.8	33.5	36.7
d	65	76	96	113	116	128	133
n	11	11	16	13	4	20	8

Bare ground, July and August 1962

h	2.9	8.4	12.9	17.7	22.9	27.6	32.9	36.6
d	30	60	77	89	105	109	119	129
n	7	47	40	49	35	23	64	12

From Fig. 17 it can be seen that the diffuse sky radiation intensities at high albedo values measured on Devon Island are generally considerably higher than those taken from Robinson (1966) and those measured by Liljequist in the Antarctic. Considering, however, the altitude of Devon Ice Cap Station, about the 850-mb level, the radiation intensities obtained there are in rather good agreement with those from Devon Base Station.

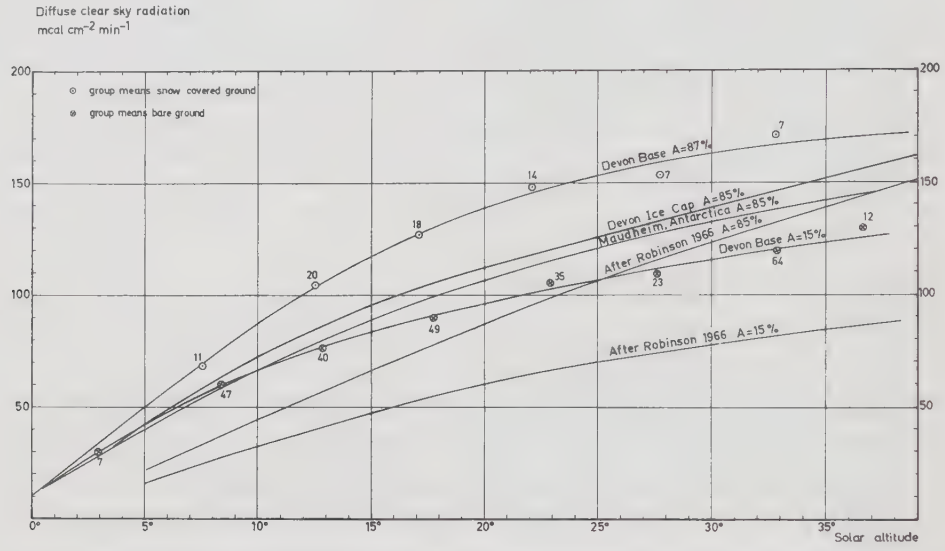

Fig. 17. Comparison between measurements from different places of diffuse clear sky radiation as a function of the solar altitude. Also radiation values computed from Robinson (1966) are entered. Intensities are valid for mean solar distance and turbidity $\beta = 0.025$. Figures denote number of observations belonging to each group mean.

Regarding a bare ground with a measured albedo of 15 %, at least part of the difference between the curve obtained from Devon Base Station and that computed from Robinson may be explained by the higher regional albedo on Devon Island. But when it comes to radiation conditions with the ground covered by snow, the difference between the curve valid for Devon Base Station and that valid for Maudheim remains to be explained. The mean turbidity coefficient during the period 23.5.62 - 10.6.62 was 0.030, but during that time only one fourth of a total number of 80 measurements with snow on the ground were made. During the period 5.3.62 - 7.5.62, when the remaining 60 measurements were made, nothing is known about the turbidity of the atmosphere. Certainly the pyrheliometer measurements indicate a pronounced turbidity maximum during spring, but it is doubtful whether the turbidity was great enough to produce such a high diffuse sky radiation intensity provided for example that the values given by Liljequist (1956, p. 57) are assumed to be valid also

for the Devon Island area. That would require a turbidity coefficient of 0.060 - 0.070.

Then the question inevitably arises whether the high intensities are real or caused by some instrumental error. As to the accuracy of the measurements it must be said that the calibration factor was based upon a fairly large number of comparisons with the Ångström pyrheliometer.

The summer measurements ought to have a satisfactory precision, whereas the accuracy of the measurements made during the spring is more uncertain because of the temperature influence on the sensitivity of the pyranometer. A maximum error of 3 % may be introduced in the diffuse sky radiation values.

However, as mentioned before, the calibration factor obtained by this method does not include the effect of the reflected radiation which is absorbed by the back of the receiving plate of the Eppley pyranometer. It cannot be quite excluded that the correction applied (see Section 2.2.1) is too small, but the intensities obtained from the measurements will nevertheless be accepted here.

The material was divided into three periods, viz. March-beginning of June, June and July-August depending on the value of the regional albedo. The following corrections and reductions were applied:

1. Since the sensitivity of the Eppley pyranometer increases when temperature decreases a temperature correction of -0.1 % per 1°C was applied. The reference temperature was $+5.4^{\circ}$C (see Section 2.1).
2. The effect of the reflected radiation was eliminated by applying the correction -4.9 % with the ground covered by snow and by -1.3 % with bare ground.
3. All values were reduced to mean solar distance by the reduction factor R^2/R_m^2 where R is the actual solar distance and R_m is the mean distance (see IGY Manual, Appendix, Table 3).
4. Computed solar altitudes were corrected for refraction.

No measurements of the diffuse clear sky radiation with a solar altitude less than 1° were made. Radiation values with the sun below that altitude and down to -4° have been taken from Liljequist (1956, p. 60). He measured the diffuse clear sky radiation at low solar altitudes with a selenium photoelectric cell at Maudheim, Antarctica. Even though the albedo at that place is very high, the diffuse sky radiation with these small intensities should differ by a negligible amount from that with a bare ground in the Canadian Arctic Archipelago.

All measurements made when the ground was bare of snow, regardless of the turbidity of the air, have been plotted in Fig. 18. In doing so the gradual change in regional albedo caused by the melting away of the ice on the adjacent lakes and on Jones Sound has been neglected. Group means within solar altitude intervals of 5^{o} have been computed and the result can be seen in Table 15 and Fig. 18.

Table 15. Group means of diffuse clear sky radiation data reduced to mean solar distance at actual turbidity conditions.

h = computed solar altitude in degrees corrected for refraction
d = diffuse clear sky radiation in mcal $cm^{-2} min^{-1}$
n = number of observations

Bare ground 1961 and 1962

h	2.8	8.4	12.8	17.7	22.8	27.5	32.9	36.7
d	28	58	75	87	100	108	115	122
n	12	53	47	52	42	26	72	14

Snow-covered ground 1962. All observations

h	7.6	12.5	17.1	22.1	27.7	32.8	36.2
d	69	104	126	148	153	171	150
n	11	20	18	14	7	7	3

Snow-covered ground March - mid. May. Turbidity unknown

h	6.9	12.6	17.1	21.9	27.4	30.7
d	69	109	135	151	174	198
n	6	15	12	10	3	1

Snow-covered ground end of May - beginning of June. $\bar{\beta} = 0.030$

h	8.5	12.3	17.2	22.5	27.9	33.1	36.2
d	68	90	110	140	138	166	150
n	5	5	6	4	4	6	3

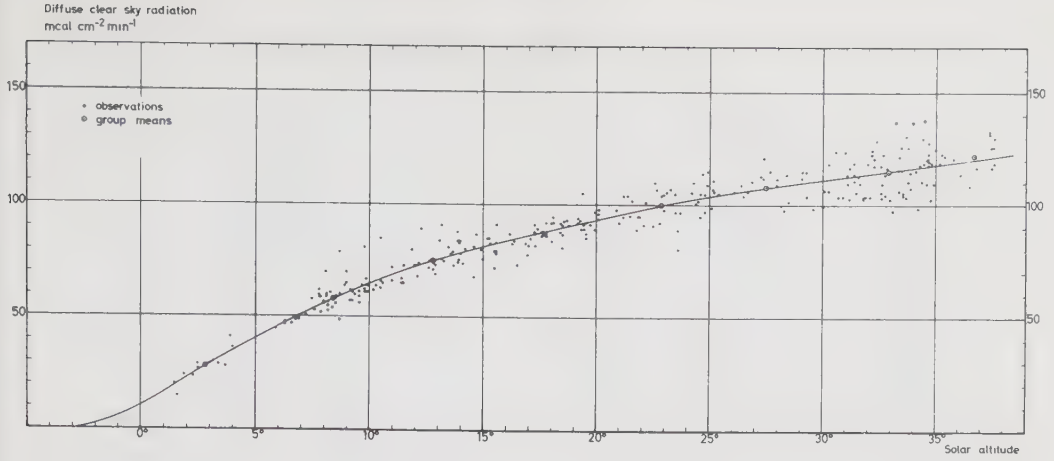

Fig. 18. Diffuse clear sky radiation as a function of solar altitude during the period with the ground bare of snow. Actual turbidity conditions.

The intensity of the diffuse clear sky radiation with the ground covered by snow is shown in Fig. 19. The data are divided into two groups. One comprises intensities from the latter part of May and the earlier part of June, i.e. the time with known air turbidity (β = 0.030). The other group consists of the rest of the data, i.e. those from the beginning of March to the middle of May. The turbidity during that period was not measured. Group means are computed and shown in Table 15 and Fig. 19. The considerably higher values during the early period may depend on a higher albedo; the snow started to melt towards the end of May. Group means for all data, collected when the

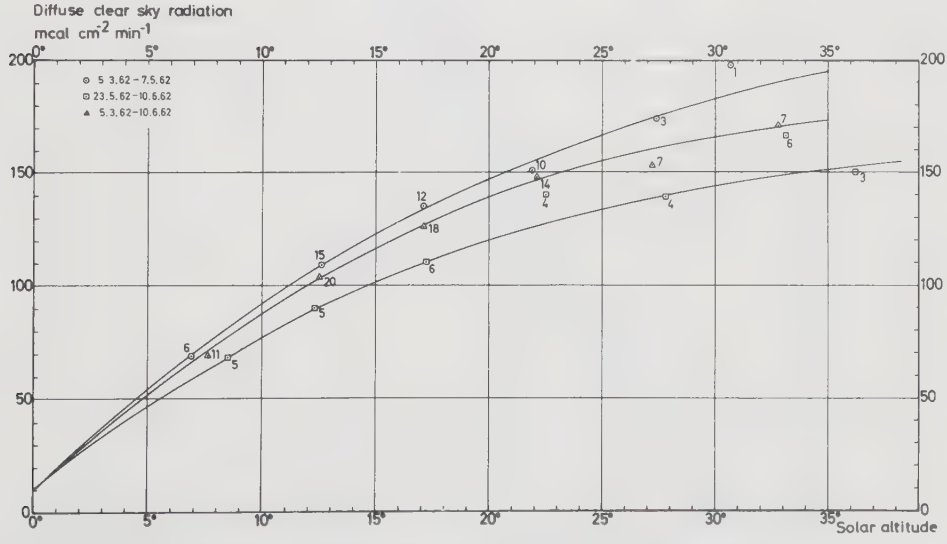

Fig. 19. Diffuse clear sky radiation as a function of solar altitude with the ground covered by snow during the whole period 5.3.62 - 10.6.62 and also during the periods 5.3.62 - 7.5.62 and 23.5.62 - 10.6.62.

ground was covered by snow, have also been computed (Table 15 and Fig. 19). In the following sections these data will be taken as valid for the entire period with snow on the ground.

In order to get the functional relationship between the diffuse clear sky radiation d and the turbidity β the method of least squares was used within solar altitude intervals of 5°. Because of the small β-range a linear relationship was assumed within each interval. Due to the changing regional albedo conditions during the earlier part of the summer, only data from July and August were used for that computation. The coefficient b of the regression equation $d = a + b\beta$ was then plotted in a diagram with the solar altitude as the abscissa (see Fig. 20). Probably because of the rather small number of observations in each interval, the bulk amounting to about 200, the points are fairly scattered. The accuracy of the determinations of b is small due to the low intensity of the radiation, particularly for the lowest solar height interval. For that reason the b-value for the interval $0-5^{\circ}$ has been rejected. Nevertheless it seems to be possible to draw a curve which in conformity with Liljequist's findings brings about a smaller increase of d with β at low solar altitudes than at high ones. In this way curves can be drawn which show the diffuse clear sky radiation as a function of the solar altitude with the turbidity as a parameter (Fig. 21 b). The same values on the coefficient b of the regression equation may, probably without any serious error, be applied to the d-curves for the part of June when the ground was bare of snow (see Fig. 21 a).

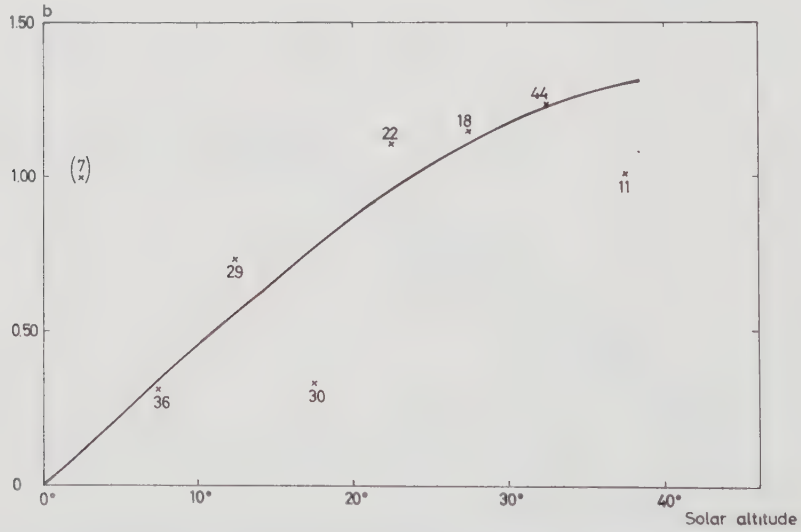

Fig. 20. The dependence of the diffuse clear sky radiation d on the turbidity β at different solar altitudes. The coefficient b is defined by the regression equation $d = a + b\beta$ and computed for solar altitude intervals of 5°. Figures denote number of observations within each interval.

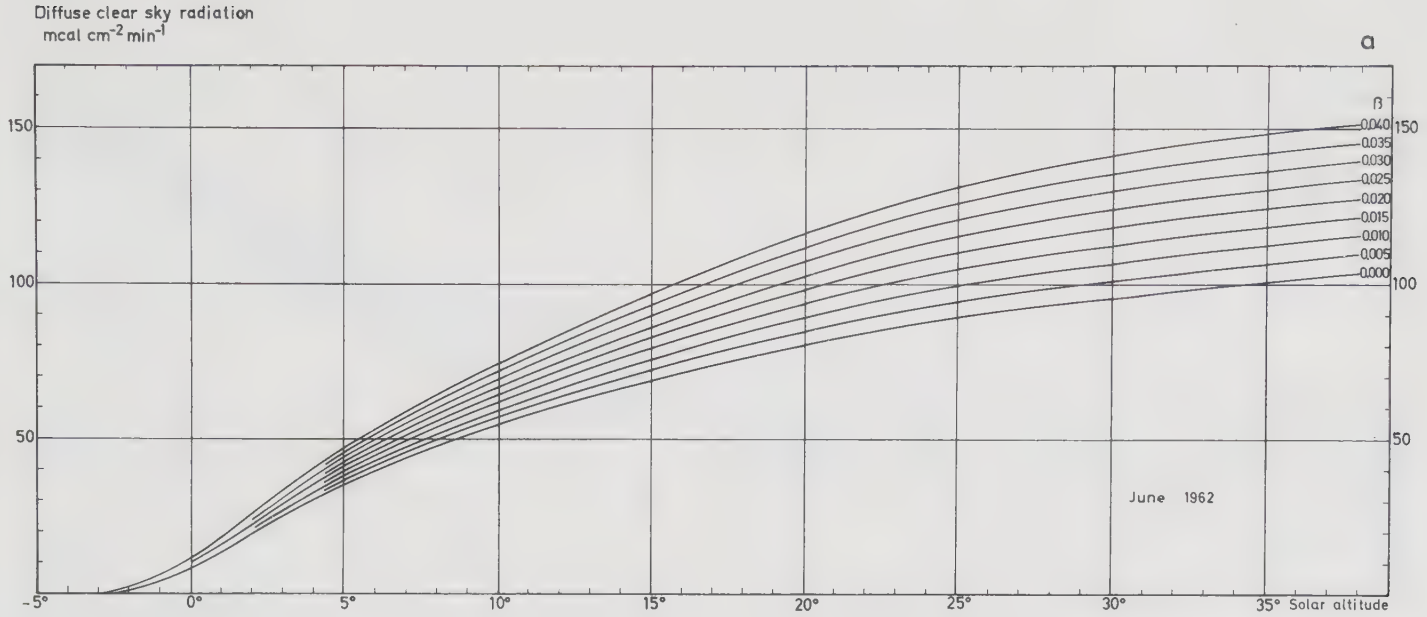

Fig. 21 a and b. Diffuse clear sky radiation as a function of solar altitude and turbidity β with the ground bare of snow in June (a) and in July and August (b). In June the regional albedo and consequently the intensity of the diffuse clear sky radiation is larger than in July and August.

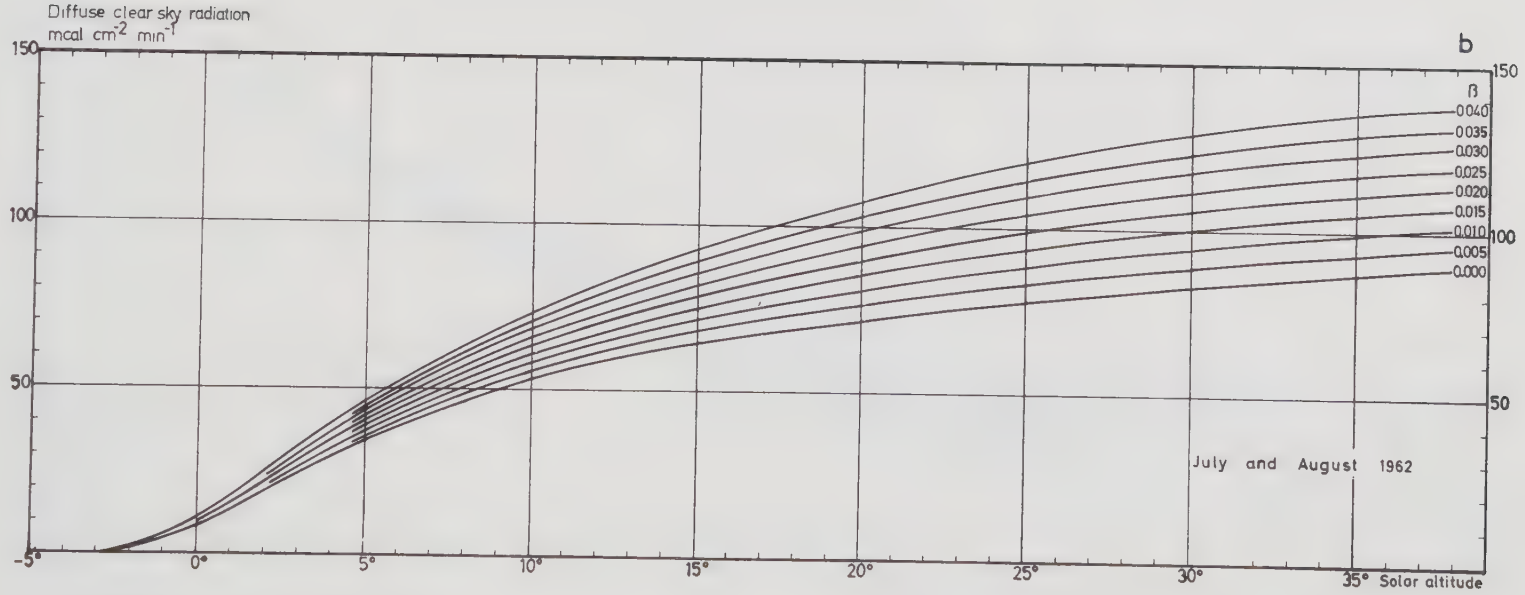
Diffuse clear sky radiation
mcal cm-2 min-1
b
150
100
50
ß
0.040
0.035
0.030
0.025
0.020
0.015
0.010
0.005
0.000
July and August 1962
-5°
0°
5°
10°
15°
20°
25°
30°
35°
Solar altitude

Fig. 21 b

5. Global radiation

5.1. Global radiation with a clear sky as a function of the solar altitude

In a climatological investigation on the radiation conditions the relationship between the measured global radiation at actual cloud conditions or at overcast conditions and the estimated normal global radiation with a completely clear sky has a great significance. By means of such relationships established for the area in question and for a period of suitable length, e.g. one month, it is possible to estimate the global radiation from observed mean values of cloudiness. For that purpose, with known mean values of turbidity and amount of precipitable water, monthly means of the global radiation g_0 as a function of the solar altitude have been computed by means of the relationships established in the previous sections. The daily sums of the global clear sky radiation G_0 can be computed from the curves showing the global radiation g_0 at different solar altitudes.

Spot readings of the global radiation were made regularly. Such readings have also been used to construct curves showing monthly means of the global clear sky radiation g_0 as a function of the solar altitude. Especially for months with no measurements of turbidity and amount of precipitable water these direct observations are valuable.

The curves of Fig. 22 a-h show the global radiation as a function of the solar altitude. The full curves are based upon monthly means of turbidity and amount of precipitable water. The construction was made as follows:

1. The intensity I of the direct solar radiation for every two degrees of the sun's altitude h during the months May - August was obtained from Table 1 of the Appendix and from Fig. 2. These data were obtained using known monthly means of the turbidity and the amount of precipitable water. Table 1 of the Appendix which is computed from Hoelper's data, (Hoelper, 1939) reduced to the International Pyrheliometric Scale 1956, gives the energy of the direct solar radiation in a dry and turbid atmosphere. The curves of Fig. 2, which are constructed from Houghton's absorption values, give the extinction F due to water vapor absorption when the simultaneous effect of scattering by dust is taken into account. The direct solar radiation on a horizontal surface is given by I sin h. For $h < 10^{\circ}$ this method could not be used because Table 1 of the Appendix is not computed for air mass values greater than 6 corresponding to $h = 9^{\circ}3$. Thus the intensity at

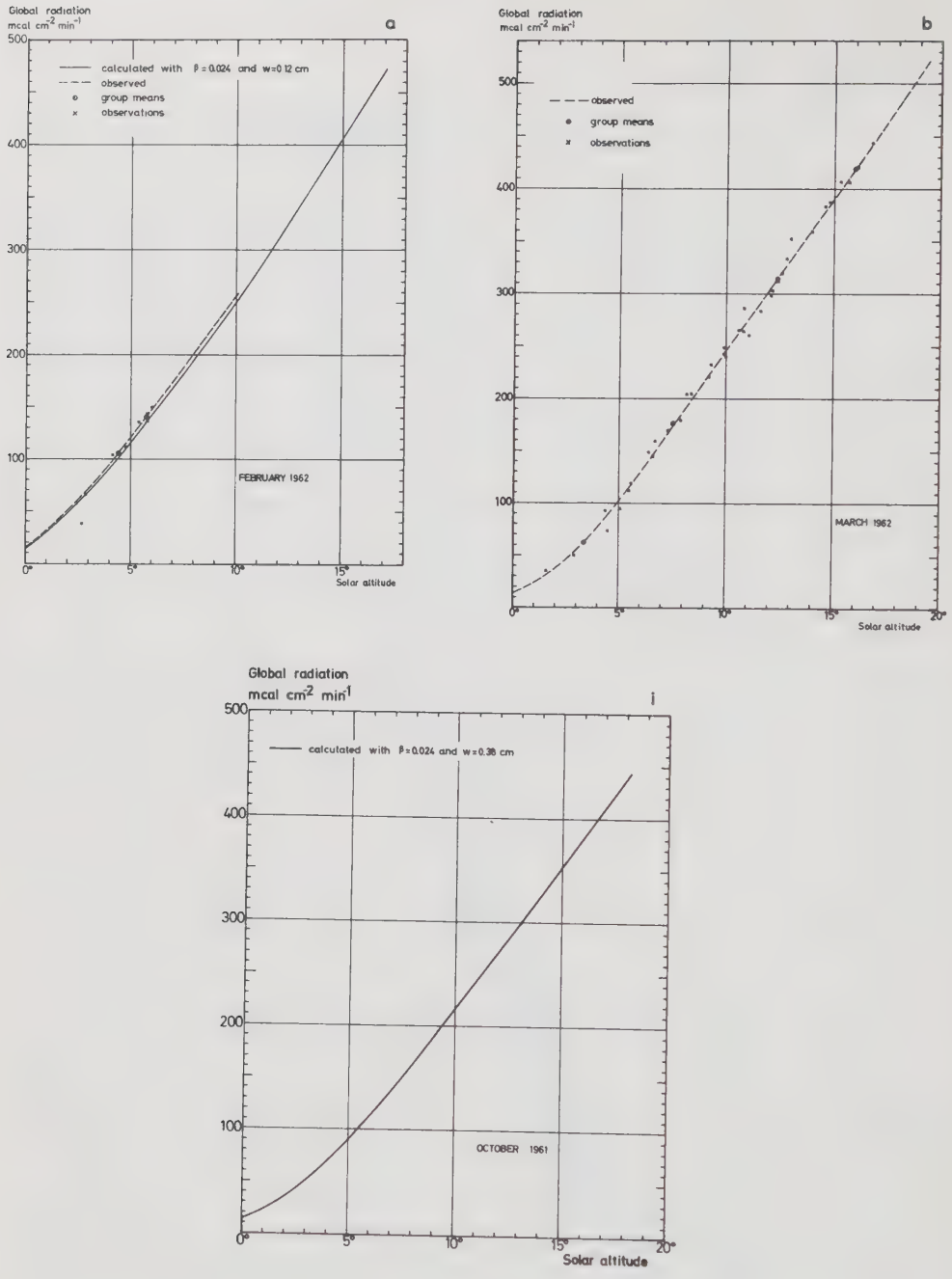

Fig. 22 a-i. Global radiation with a clear sky g_0 as a function of solar altitude. The data are reduced to mean solar distance. Dashed lines denote observed values and full lines values calculated from observed monthly means of turbidity and amount of precipitable water or - for months with no pyrheliometer measurements - from estimated values on β and w. (see text).

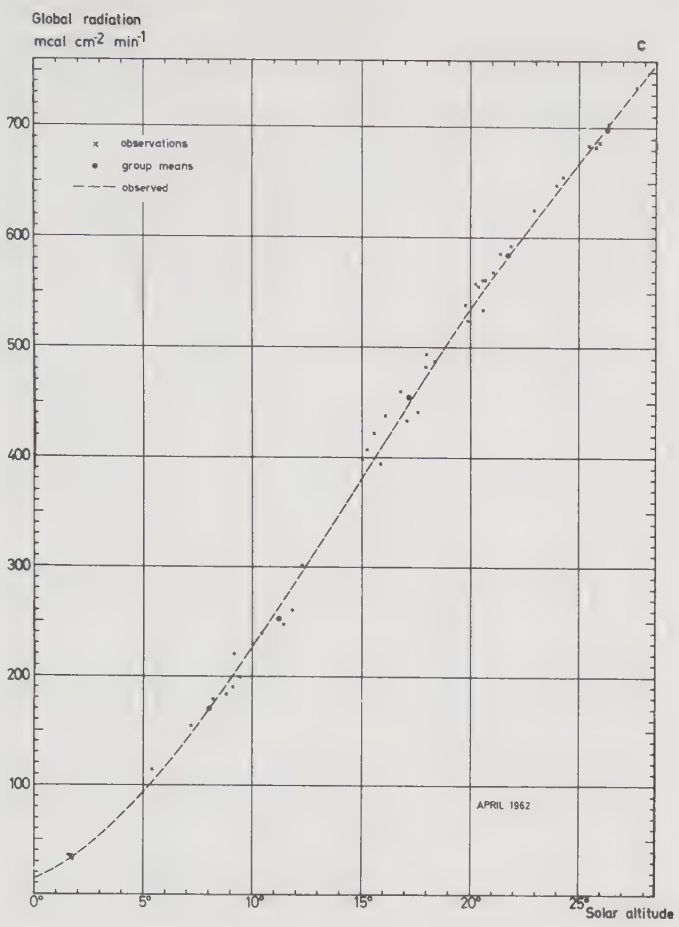
Global radiation
mcal cm-2 min-1
c
x observations
• group means
observed
APRIL 1962
Solar altitude

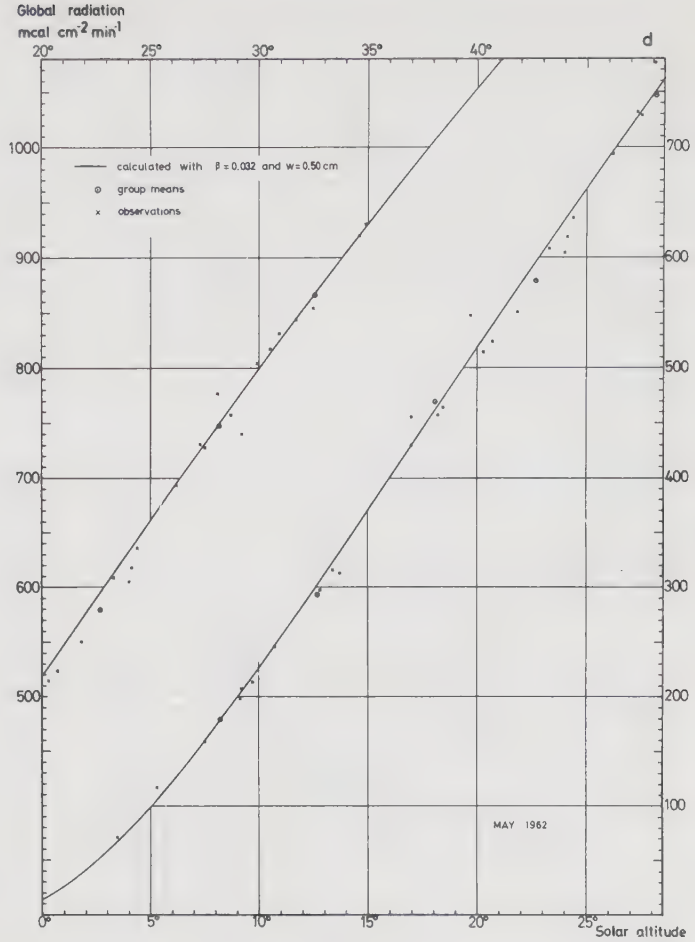
Global radiation
mcal cm-2 min-1
d
calculated with β = 0.032 and w = 0.50 cm
group means
observations
MAY 1962
Solar altitude

Fig. 22 c,d

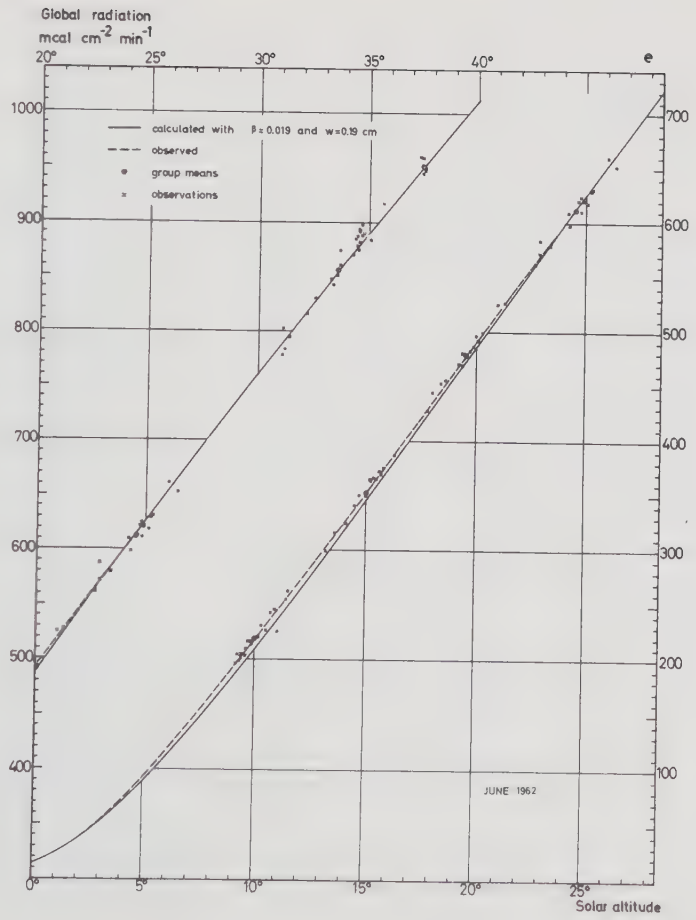
Global radiation
mcal cm^{-2} min^{-1}
e
calculated with β = 0.019 and w = 0.19 cm
observed
group means
observations
JUNE 1962
Solar altitude

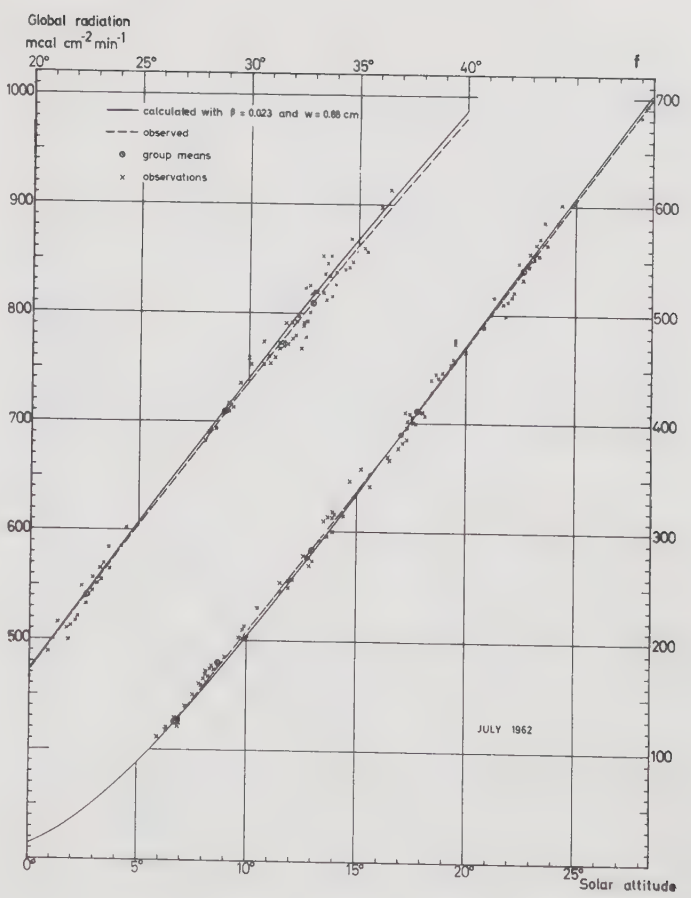
Global radiation
mcal cm^{-2} min^{-1}
f
calculated with β = 0.023 and w = 0.88 cm
observed
group means
observations
JULY 1962
Solar attitude

Fig. 22 e,f

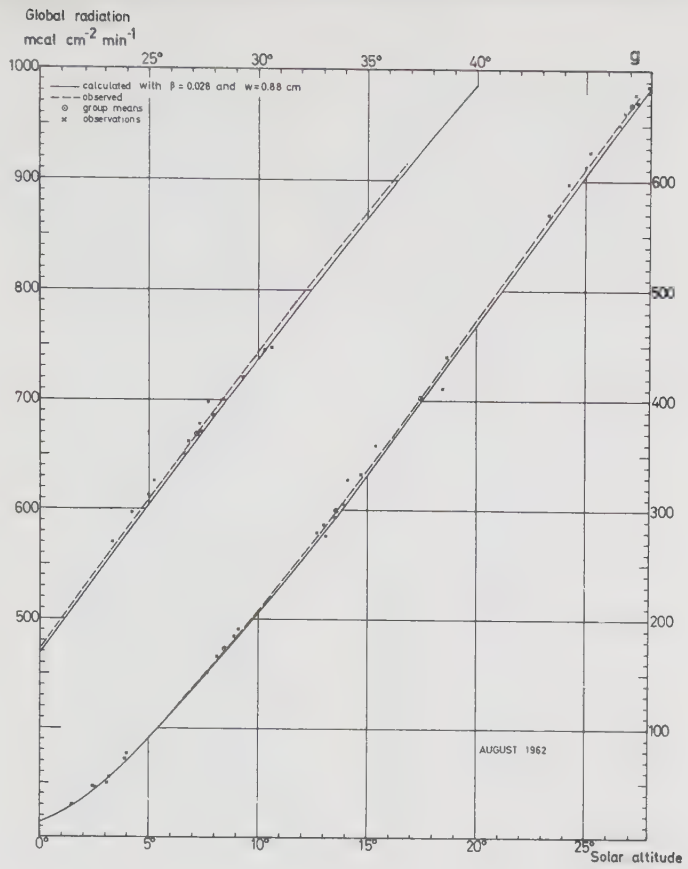
Global radiation
mcal cm-2 min-1
g
calculated with β = 0.028 and w = 0.88 cm
observed
group means
observations
AUGUST 1962
Solar altitude

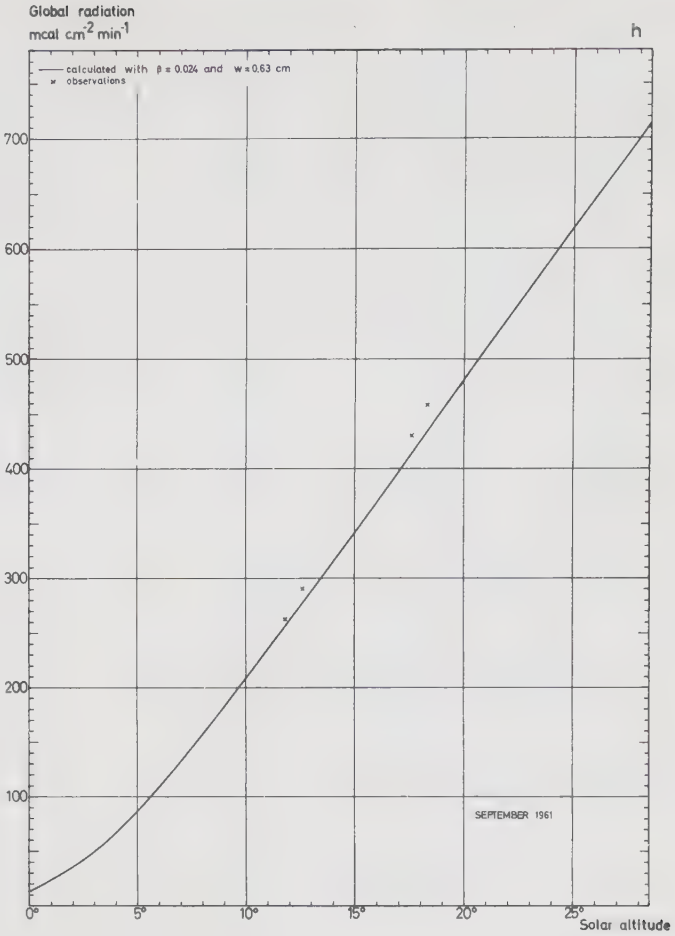
Global radiation
mcal cm-2 min-1
h
calculated with β = 0.024 and w = 0.63 cm
observations
SEPTEMBER 1961
Solar altitude

Fig. 22 g,h

lower solar altitudes has been obtained from Fig. 4, which shows the curve for the mean of all our observations of the direct solar radiation with the Ångström pyrheliometer during the months May-August 1962.

The global radiation with a clear sky and with a low sun was obtained from direct observations during the period March and April, which had low temperatures and consequently low water vapor content of the atmosphere.

2. The diffuse clear sky radiation d was obtained from Fig. 21 a and b for months with a known mean value of the turbidity β. For the period with snow on the ground the curve in Fig. 19, giving the average d for this period, was used.

3. All radiation values obtained from Table 1 of the Appendix and from Figs. 2 and 21 a and b are referred to mean solar distance. A reduction to actual solar distance is performed at a later stage of the calculations which in the first place aim at a computation of the daily totals of the normal global radiation from a clear sky for every day during the whole measuring period.

4. The effect of the pressure variations on the air mass was disregarded because of its small influence on the global radiation. The global radiation, $g_0 = I \sin h + d$, as a function of the solar altitude is calculated for some of the months June 1961 - September 1962 and is given by the full curves in Fig. 22 a-i.

As a total during the period May 1961 - September 1962 470 spot readings of the global clear sky radiation were made. The readings corrected for temperature and reduced to mean solar distance have been plotted against the solar altitude for each month separately and corrected for refraction. Group means within altitude intervals of approximately 5° have been computed and curves showing g_0 as a function of h are drawn for each month and are shown in Fig. 22 a-i (dashed curves). In doing so curves based upon computations sometimes served as models within altitude intervals with none or few spot readings.

As can be seen from Fig. 22 e, f and g the radiation values for June and August 1962 computed from measured monthly means of turbidity and amount of precipitable water (full curve) show a slight underestimate compared to those obtained from direct observations (dashed curve). On the other hand, the computed values are generally higher for July 1962 than for those from direct observations. The difference between the two curves, at maximum amounting to

9 mcal $cm^{-2}min^{-1}$, may be explained by errors in the calibration of the pyranometer or perhaps by errors in the determination of the water vapor absorption.

For subsequent calculations of climatological parameters, such as g_{10}/g_0 or G_{10}/G_0, the curves based on direct readings of the global clear sky radiation have been used, as probably being the most reliable ones. Here g_{10} and g_0 denote instantaneous values of global radiation with an overcast sky and a clear sky, respectively. Analogously, G_{10} and G_0 denote daily totals of global radiation. The computed g_0-values based on estimated values of β and w have been used for two months, September and October 1961, with none or very few clear days (Fig. 22 h and i). For June 1961, when a clear sky was never observed in connection with a spot reading of g, the 1962 curve for the same month was used. The same applies to July and August 1961 with rather few g_0 - readings as a consequence of the cloudy weather during that summer.

5.2. Daily insolation with a clear sky G_0

The daily insolation G_0 was calculated for the 1^{st}, 5^{th}, 10^{th}, 15^{th}, 20^{th} and 25^{th} day of every month. The following steps were made in the computation:

1. The calculated solar altitude h, corrected for refraction, has been computed for even hours true solar time or, which is equivalent, for even hours before and after local noon.

2. With h as the argument the normal global radiation g_0 for each month has been obtained from Fig. 22 a-i. Whenever possible the curves based upon direct observations were used.

3. The radiation values are reduced to actual solar distance valid for the day in question.

4. The g_0-values are plotted in diagrams with abscissa = true solar time - 12^h (numerical value) and curves are drawn. The g_0-values for the 1^{st} of a month are obtained by interpolation between the curves of Fig. 22 a-i for the present and the previous month.

5. The daily insolation is computed by graphic integration of the curves and the results can be seen in Table 16. G_0 for any day can be found by interpolation.

Table 16. Global radiation with a clear sky at actual solar distance.

g_0 = global radiation (mcal/cm^{2}min) with a clear sky

G_0 = daily insolation (ly/day) with a clear sky (daily total of global radiation)

D = daily insolation (ly/day) from a clear sky (daily total of diffuse radiation)

Hour angle = True solar time −12^h	g_0 mcal/cm^2 min													Sun on horizon	g_0 = 0	Daily insolation G_0	D	D/G_0
	00	01	02	03	04	05	06	07	08	09	10	11	12	h m	h m	ly/day	ly/day	%
Jan 28	0														0 00	0	0	-
Feb 8	14	8	2											0 00	2 46	2.0	2.0	100
10	25	17	5											1 12	2 59	4.1	4.0	98
15	49	43	20	4										2 16	3 36	10.7	7.7	72
20	86	77	49	14	1									3 01	4 10	22.0	12.8	58
25	137	122	86	43	7									3 40	4 40	38.9	19.2	49
Mar 1	166	152	115	64	18	1								4 08	5 06	51.9	25.2	49
5	203	188	146	88	31	5								4 35	5 31	66.9	31.2	47
10	261	246	203	137	64	16								5 07	6 01	95.9	39.5	41
15	316	301	258	192	111	36	7							5 38	6 32	127.5	49.0	38
20	373	358	314	251	163	73	18							6 09	7 04	163.9	58.8	36
25	427	415	371	305	218	121	39	8						6 40	7 37	202.8	68.5	34
Apr 1	506	489	443	376	284	184	88	26	4					7 24	8 28	257.0	83.0	32
5	546	532	487	412	321	219	116	45	11					7 52	8 59	289.6	91.4	31
10	595	583	541	471	380	272	165	78	26	6				8 28	9 46	338.2	101.9	30
15	639	628	588	522	430	326	214	113	50	17	5			9 06	10 57	385.5	112.6	29
20	683	669	630	567	480	374	261	153	77	32	12	5	2	9 52		432.6	123.7	29
25	722	709	671	610	529	422	312	204	114	54	26	14	8	11 02		484.5	134.8	28
May 1	769	754	715	652	570	470	358	255	161	93	53	32	28			542.1	147.1	27
5	800	788	746	682	595	494	391	285	192	124	77	51	43			581.5	154.0	27
10	836	821	782	717	629	532	425	323	231	158	107	76	67			630.8	163.6	26
15	865	850	811	746	622	563	460	358	264	187	133	105	94			674.8	170.4	25
20	893	876	839	774	691	591	491	386	291	215	160	128	118			713.9	176.5	25
25	915	900	860	799	713	618	514	412	319	242	186	150	139			748.5	181.8	24
Jun 1	910	896	859	798	722	625	526	427	339	259	205	169	160			763.3	160.8	21
5	919	907	869	809	731	637	538	440	350	273	218	184	172			780.4	162.8	21
10	918	905	867	806	726	634	535	439	355	281	227	191	180			784.5	136.6	17
15	924	911	873	812	733	638	543	447	360	288	234	198	188			796.0	137.3	17
21	925	913	875	814	736	643	547	451	366	291	236	203	192			798.6	137.3	17
25	923	911	873	812	734	642	545	450	365	290	235	202	190			797.4	137.3	17

Table 16. (continued)

Hour angle = True solar time −12h	00	01	02	03	04	05	06	07	08	09	10	11	12	Sun on horizon h m	$g_0 = 0$ h m	Daily insolation G_0 ly/day	D ly/day	D/G_0 %
Jul 1	903	894	853	793	714	624	527	431	349	277	224	190	179			769.4	133.3	17
5	882	868	834	774	694	605	509	415	335	264	212	180	168			745.5	129.0	17
10	868	855	820	759	680	588	495	401	319	249	197	162	153			723.8	127.0	18
15	854	840	802	741	665	572	476	382	299	229	178	146	135			698.6	125.2	18
20	835	822	783	723	645	552	456	363	282	212	161	127	116			671.6	122.2	18
25	812	797	759	699	621	528	431	340	258	188	136	107	98			638.1	119.8	19
Aug 1	777	764	724	663	583	488	390	300	218	148	102	74	66			584.8	116.5	20
5	756	742	704	638	560	463	365	274	192	128	82	54	51			552.4	116.0	21
10	722	706	666	602	520	426	333	239	161	97	54	33	29			505.0	109.0	22
15	684	669	630	566	487	389	298	207	129	68	33	20	16			461.2	102.1	22
20	641	628	589	525	444	350	255	168	96	42	19	7	5	10 24		413.5	94.0	23
25	600	584	544	480	399	309	216	132	61	23	5	1	0	9 30		366.0	85.8	23
Sep 1	540	526	489	420	343	250	158	78	27	7				8 32	9 54	307.5	73.6	24
5	505	491	450	388	305	216	124	51	17	2				8 06	9 15	275.2	66.1	24
10	456	442	402	342	259	171	87	30	6					7 31	8 34	235.8	60.1	26
15	403	390	354	293	213	125	51	13						6 59	7 58	197.3	52.9	27
20	355	344	301	242	164	85	30	4						6 28	7 24	161.8	46.7	29
25	301	288	250	190	118	51	12							5 57	7 03	127.5	40.4	32
Oct 1	244	234	194	138	73	25	3							5 23	6 16	94.6	33.4	35
5	211	197	158	106	48	12								4 56	5 50	75.1	28.4	38
10	156	143	110	63	25	4								4 24	5 20	50.7	22.3	44
15	111	102	71	35	11									3 50	4 50	33.0	16.9	51
20	74	64	42	19	2									3 14	4 15	19.7	12.4	63
25	44	38	23	7										2 32	3 47	10.6	8.4	79
30	24	20	9	1										1 36	3 12	4.9	4.6	94
Nov 3	14	8	2											0 00	2 46	2.0	2.0	100
14	0														0 00	0	0	-

The global clear sky radiation g_0 at even hours is given in Table 16. The same table also shows the time-difference between local noon and the time when the sun is on the horizon. It is assumed that this occurs when the uncorrected solar altitude $h_0 = -0^\circ.7$ (see Liljequist, 1956, p. 17). Further, the time-difference between local noon and the time of the day when the diffuse sky radiation is negligible, which occurs approximately when $h_0 = -4^\circ$, is computed and shown in the same table (see Liljequist, 1956, p. 58). The computations are valid for a horizon with no obstructions.

During the months of October, February and March sunrise and sunset took place within a sector of the horizon with obstructions reaching a mean altitude of 3°. Therefore, when the relative insolation G/G_0 was computed, the loss of direct solar radiation must be considered for solar altitudes less than 3°. Thus, the direct solar radiation reaching a horizontal surface at solar altitudes less than 3° was subtracted from the calculated values of daily insolation G_0. This was done in order to make G_0 comparable to the actually measured daily insolation G. The corrections amounted to 0.6, 3.0, 3.4 and 2.2 ly/day for February 10, 15, 20 and 25, respectively, and to about 1 ly/day during March. For October 1, 5, 10, 15, 20, 25 and 30 the corrections were 1.0, 1.2, 1.6, 2.0, 2.8 and 0.4 ly/day, respectively. Especially with a small cloudiness, this loss of direct solar radiation must influence the actually measured global radiation values. But in overcast conditions with the top of the cloud layer at a higher level than the obstructing mountains this influence must be quite small. Consequently, the horizon was considered as unobstructed when the ratio G_{10}/G_0 was computed (see below). During months other than October, February and March no correction had to be applied to G_0 because sunset and sunrise took place in directions with no obstructions on the horizon.

The daily insolation on the top of the atmosphere B_0 has been calculated and the ratio G_0/B_0 for the 1^{st} and the 15^{th} of every month is shown in Table 17. The annual variation of G_0/B_0 can also be studied in Fig. 24 together with the same ratio for two selected stations. G_0 refers here to a horizon with no obstructions. The fact that G_0 is greater than B_0 on February 15 is explained by the effect of the atmospheric refraction at very low solar altitudes and to contributions to G_0 from the diffuse clear sky radiation when the sun is below the horizon. It can be seen that G_0/B_0 increases from March to May when it reaches a maximum. This may be due to the decrease in the extinction of the direct solar radiation as a result of scattering when the solar hwights gradually increase during spring. In June G_0/B_0 decreases in spite of greater solar altitudes and smaller tur-

Table 17. Normal daily insolation with a clear sky G_0 and without atmosphere B_0.

The values are referred to actual solar distance.

	G_0 ly/day	B_0 ly/day	G_0/B_0 %
Feb. 15	11	9	-
Mar. 1	52	73	71.2
" 15	128	178	71.9
Apr. 1	257	345	74.5
" 15	385	505	76.2
May 1	543	708	76.7
" 15	675	875	77.1
June 1	763	1009	75.6
" 15	796	1059	75.2
July 1	769	1049	73.3
" 15	699	981	71.3
Aug. 1	585	829	70.6
" 15	461	654	70.5
Sept. 1	308	450	68.4
" 15	197	298	66.1
Oct. 1	95	152	62.5
" 15	33	57	57.9

bidity than in the previous months. This may partly be due to a reduction of the diffuse clear sky radiation as a consequence of the reduced albedo of the ground, it may partly be due to an increased absorption of solar radiation by water vapor in summer.

Most characteristic is, however, the different values of G_0/B_0 during spring and autumn with equal solar altitudes. The lower values in autumn are a consequense of the much lower albedo and the higher water vapor content of the atmosphere as compared with spring. Differences in turbidity may also have contributed. This question cannot, however, be settled here as we lack data on the turbidity. The annual mean of G_0/B_0 is 75.1 % obtained by dividing the annual totals of G_0 and B_0. This value should be

compared with the annual mean of G_0/B_0, 82.5 %, observed by Liljequist at Maudheim in the Antarctic (see Liljequist, 1956, p. 57). This latter station has a high albedo during the whole light season and a lower turbidity and a lower water vapor content in the atmosphere than Devon Base Station.

5.3. Global radiation with a dense overcast

The global radiation in the presence of a dense overcast depends to a very high degree on the albedo of the ground and the thickness and density of the clouds. A high albedo will thus increase the global radiation as a consequence of multiple reflection of the radiation between the ground surface and the cloud base.

In order to study the annual variation of the global radiation with a dense overcast the relations G_{10}/G_0 and g_{10}/g_0 have been used. Here G_{10} and G_0 denote daily totals of global radiation with a dense overcast and with a clear sky, respectively, and g_{10} and g_0 denote corresponding instantaneous values of global radiation. As for the calculations of G_{10} the cloud cover has been regarded as a dense overcast when the relative duration of bright sunshine S = 0. In order to also increase the number of days with a dense overcast those cases have been considered in which there has been no trace burnt on the sunshine recorder strip during half the day, i.e. 00^h - 12^h or 12^h - 24^h true solar time. Then the amount of global radiation from half that day has been doubled to be valid for the whole day.

Spot readings of global radiation g and cloud observations were made simultaneously. If the whole sky was then covered by clouds which were heavy enough to conceal the sun completely the overcast was considered as dense. The global radiation then consisted only of diffuse radiation. On the other hand, on days used for calculation of G_{10} part of the incoming radiation may have consisted of direct solar radiation in spite of S = 0. Monthly means of the relative insolation with a dense overcast, i.e. the ratio between the daily totals of global radiation G_{10} and G_0, are shown in Table 18 and Table 19. As a comparison data from a few other high-latitude station are also given in the latter table. The values are plotted in Fig. 23. It can be seen that G_{10}/G_0 has a maximum = 0.67 in April and a minimum = 0.31 in July. This should be compared with the relative insolation found at Abisko, northern Sweden (Ångström and Tryselius, 1934), a place with snow cover during more than six months of the year. G_{10}/G_0 generally has a lower value, especially in winter, possibly due to a lower regional albedo caused by the forests in

Table 18. Relative insolation G_{10}/G_0 with a dense overcast at Devon Base Station.

Month	1961 Number of days	1961 G_{10}/G_0	1962 Number of days	1962 G_{10}/G_0	Mean Number of days	Mean G_{10}/G_0
Febr. March			9	0.651	9	0.651
April			3	0.667	3	0.667
May			5	0.637	5	0.637
June	9	0.490	6	0.457	15	0.477
July	11	0.264	9	0.360	20	0.307
August	15	0.299	21	0.349	36	0.330
September	14	0.365	7	0.349	21	0.360
October	14	0.506			14	0.506

the Abisko area. Also thicker clouds at the latter place may have contributed to a lower relative insolation, though it must be stressed that the albedo is probably the most important factor. In July the difference between the two places with respect to G_{10}/G_0 is small. At Maudheim, Antarctica, the annual variation is much smaller with a spring maximum equal to that at Devon Base, but with a much higher summer minimum = 0.52 (see Liljequist, 1956, p. 69).

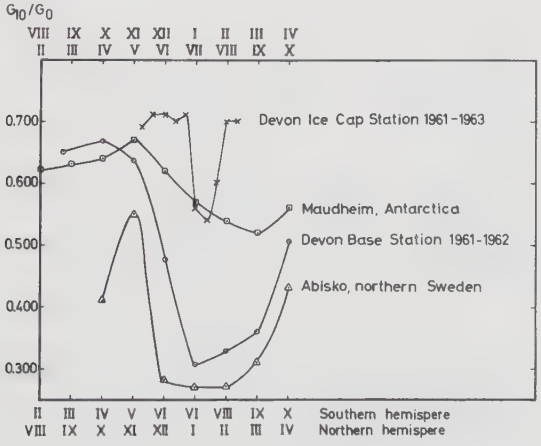
G_{10}/G_0
VIII IX X XI XII I II III IV
II III IV V VI VII VIII IX X
0.700
0.600
0.500
0.400
0.300
Devon Ice Cap Station 1961-1963
Maudheim, Antarctica
Devon Base Station 1961-1962
Abisko, northern Sweden
II III IV V VI VII VIII IX X Southern hemispere
VIII IX X XI XII I II III IV Northern hemispere

Fig. 23. Annual variation of relative insolation G_{10}/G_0 at Devon Base Station and at three selected stations. G_{10} and G_0 denote the daily insolation with a dense overcast and with a clear sky respectively.

Table 19. Relative insolation G_{10}/G_0 with a dense overcast at some stations.

Northern hemisph. Southern hemisph.	Feb. Aug.	Mar. Sept.	Apr. Oct.	May Nov.	June Dec.	July Jan.	Aug. Feb.	Sept. Mar.	Oct. Apr.	Feb.-Mar.	Feb.-Apr.	June-Oct.
Devon Base Station 1961, 1962 G_{10}/G_0			0.67	0.64	0.48	0.31	0.33	0.36	0.51	0.65		0.38
Devon Base Station 1961, 1962 g_{10}/g_0				0.58	0.46	0.29	0.29	0.36	0.49	0.59	0.62	0.34
Maudheim, Antarctica G_{10}/G_0	0.62	0.63	0.64	0.67	0.62	0.57	0.54	0.52	0.56			
Abisko, Northern Sweden G_{10}/G_0			0.41	0.55	0.28	0.27	0.27	0.31	0.43			
Devon Ice Cap Station 1961-1963 G_{10}/G_0				0.69	0.71	0.62	0.67					

This is, of course, due to the high albedo of the shelf-ice the year round. The annual variation of G_{10}/G_0 at Devon Ice Cap Station shows a pronounced minimum during the ablation season when the albedo of the snow decreases to about 60 %. According to Holmgren (1971) the high values during the rest of the measuring period may be caused by the altitude of the latter station (1320 m). Generally, clouds at a high level station should be less dense than clouds at a low level station in the same area.

The normal daily radiation G_{10} with a dense overcast on the 1st and 15th of every month have been computed (Table 20) by multiplying the normal values of G_0 (Table 17) with G_{10}/G_0 obtained from the curve in Fig. 23. In the same table the daily insolation B_0 without atmosphere and the ratio G_{10}/B_0 have also been entered. G_{10}/B_0 is plotted in Fig. 24. This curve has, as can be expected, the same general shape as the G_{10}/G_0-curve.

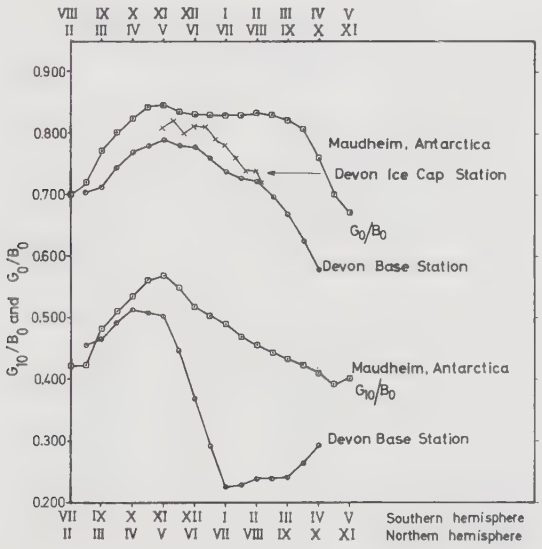

Fig. 24. Annual variation of G_0/B_0 and G_{10}/B_0 at Devon Base Station and at two selected stations. G_{10} and G_0 denote the daily insolation with a dense overcast and with a clear sky respectively. B_0 denote the daily total of solar radiation on a horizontal surface at the top of the atmosphere.

The spot readings of the global radiation with a dense overcast g_{10}, a total number of 811, have been arranged in groups according to the cloud type. Within these groups monthly means of g_{10}/g_0 have been computed (Table 21). Galperin, quoted by Gavrilova (1963), has found that no clear dependence of the diffuse radiation on the cloud type at arctic stations exists. This he ascribes to the fact that in polar regions low-level and medium-level

Table 20. Normal global radiation G_{10} with a dense overcast.

G_0 = normal daily insolation with a clear sky
B_0 = daily insolation without atmosphere.
Solar constant 1.98 cal $cm^{-2}min^{-1}$.
Actual solar distance.

	G_{10}/G_0	G_0	G_{10}	B_0	G_{10}/B_0
Febr. 15 appr.	0.650	11	7	9	(0.778)
March 1 appr.	0.650	52	33	73	0.452
" 15	0.655	128	84	178	0.472
April 1	0.660	257	170	345	0.493
" 15	0.667	386	257	505	0.509
May 1	0.655	542	355	708	0.501
" 15	0.637	675	430	875	0.491
" 20	0.620	714	443	922	0.480
" 25	0.600	749	449	963	0.466
June 1	0.575	763	439	1009	0.435
" 15	0.477	796	380	1059	0.359
July 1	0.385	769	296	1049	0.282
" 15	0.307	699	215	981	0.219
Aug. 1	0.315	585	184	829	0.222
" 15	0.330	461	152	654	0.232
Sept. 1	0.343	308	106	450	0.236
" 15	0.360	197	71	298	0.238
Oct. 1	0.425	95	40	152	0.263
" 15	0.506	33	17	57	0.298

clouds have more or less the same water content and thickness. However, from the mean values valid for a dense overcast for the whole measuring period June 1961 - September 1962 at Devon Base Station it appears that Ns has the lowest transmission and St and As has the highest. It may also be noticed that similar cloud types, though situated at different levels, give the same relative insolation. Thus g_{10}/g_0 for St and As is 0.391 and 0.397, respectively, and for Sc and Ac 0.365 and 0.368.

Table 21. Monthly means of relative insolation g_{10}/g_0 with a dense overcast (from spot readings) for different cloud types.

n = number of observations

Month	St		Sc		Ns		Ac		As		All cloud types	
	n	g_{10}/g_0	n	g_{10}/g_0	n	g_{10}/g_0	n	g_{10}/g_0	n	g_{10}/g_0	n	g_{10}/g_0
June 1961	20	0.376	15	0.550	26	0.451	16	0.483	12	0.480	90	0.459
July 1961	36	0.326	70	0.301	45	0.207	21	0.378	9	0.404	181	0.297
Aug. 1961	21	0.316	50	0.300	25	0.209	28	0.257	15	0.290	139	0.277
Sept. 1961	21	0.357	40	0.353	7	0.446	7	0.358	1	0.795	76	0.369
Oct. 1961	2	0.408	15	0.495	2	0.544	1	0.643	2	0.397	22	0.489
Febr.-Apr. 1962	1	0.512	1	0.797	2	0.681	4	0.580	6	0.607	14	0.617
May 1962	27	0.629	9	0.620	27	0.540	2	0.610	3	0.405	68	0.582
June 1962	11	0.466	19	0.463	4	0.428	1	0.463	1	0.349	36	0.456
July 1962	22	0.370	19	0.288	16	0.253	3	0.121	4	0.093	64	0.287
Aug. 1962	26	0.322	16	0.363	46	0.289	8	0.374	3	0.375	99	0.319
Sept. 1962	3	0.302	3	0.320	12	0.305	2	0.443	2	0.310	22	0.320
June 1961-Sept. 1962	191	0.391	257	0.365	212	0.326	93	0.368	58	0.397	811	0.363
June 1961, 1962	32	0.407	34	0.501	30	0.447	17	0.481	13	0.470	126	0.458
July 1961, 1962	58	0.343	89	0.298	61	0.219	24	0.346	13	0.308	245	0.294
Aug. 1961, 1962	47	0.320	66	0.316	71	0.261	36	0.283	18	0.304	238	0.294
Sept. 1961, 1962	24	0.350	43	0.351	19	0.357	9	0.377	3	0.471	98	0.358
Febr.-May 1962*	28	0.624	10	0.638	29	0.550	6	0.590	9	0.540	82	0.588
June-Sept. 1961, 1962**	161	0.350	231	0.344	181	0.288	86	0.350	46	0.370	705	0.333

* Snow-covered ground

** Bare ground

The annual variation of g_{10}/g_0 is shown in Fig. 25. Due to the small number of occasions with a dense overcast in the spring the g_{10}/g_0 values from February-May have been brought together into one single group for every cloud type which has been referred to April. When g_{10}/g_0 is studied for all cloud types together, the February-April values are numerous enough to be arranged in one group centered in the first half of March. Ns shows the greatest annual range of variation in g_{10}/g_0, 0.36, while St and As shows the smallest range, 0.30 and 0.24, respectively. For all types of clouds taken together g_{10}/g_0 has a maximum in spring, 0.59, a minimum in July and August, 0.29.

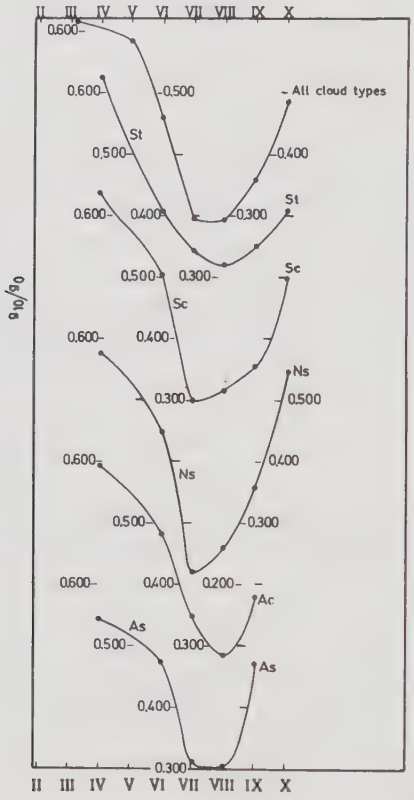

Fig. 25. Annual variation of g_{10}/g_0 for different types of cloud. The g_{10}/g_0-values have been calculated from spot readings of g_{10}.

A comparison between the annual variation of the relative insolation with a dense overcast obtained with the two methods used here (Fig. 26) shows that G_{10}/G_0 indicates a higher transmission by clouds than g_{10}/g_0, especially in the spring when the difference amounts to 0.06. The reason for this must be a higher frequency in spring of clouds which are dense enough

to keep the sun from burning a trace on the strip of the sunshine recorder but not sufficiently thick to conceal the sun. In such a case the cloud cover would not be classified as an overcast according to the visual observation in connection with the spot reading of g. On the other hand, according to the sunshine recorder, the daily total of global radiation would belong to the G_{10}-group.

The annual variation of the ratio between the daily totals of global radiation with a dense overcast G_{10} and the daily totals of radiation falling on

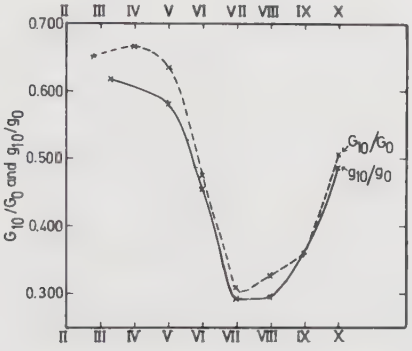

Fig. 26. Comparison between annual variation of relative insolation with a dense overcast obtained from daily totals of global radiation (G_{10}/G_0) and from spot readings of (g_{10}/g_0).

a horizontal surface on the top of the atmosphere B_0 are shown in Table 20 and Fig. 24. As a comparison the same ratio for Maudheim, Antarctica, is given in the same figure. The considerably lower values for Devon Base Station in summer and autumn are mainly due to the low albedo in the area during this time of the year.

Moreover, the thickness, drop size and water vapor content of a cloud must have an influence on the reflectivity and energy absorption of the cloud. Some idea of the density of the clouds is given by the ratio between the monthly means of total opacity and total cloudiness N_{op}/N. Total opacity is here defined as the fraction of the sky which is concealed by all cloud layers observed.

The curves of Fig. 27 show that the annual variation of the ratio N_{op}/N is more or less a reflected image of the variation of G_{10}/G_0, or better of G/G_0, where G stands for the actual daily insolation regardless of the character of the cloud cover, overcast or broken. In other words, thin clouds through which the sky is visible are most frequent in spring when the relative insolation is high, less frequent in summer when the relative insola-

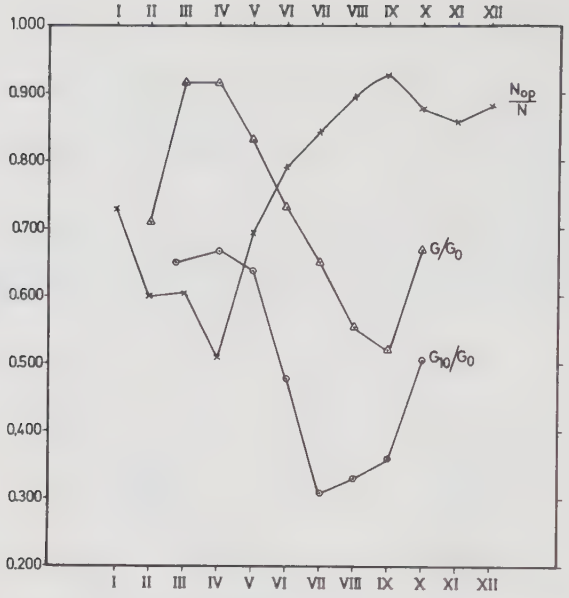

Fig. 27. Annual variation of relative insolation G/G_0 and G_{10}/G_0 and of the ratio of total opacity to total cloudiness N_{op}/N.

tion is low. Still, the albedo of the ground should be the most important factor influencing G_{10}/G_0, as is indicated by the curves in Fig. 25.

Knowing the annual variation of G_{10}/G_0 (Table 20) it is possible to obtain normal values of G_{10} simply by multiplying the data of the table with G_0 (Table 16). In Fig. 28 curves are constructed which show G_{10} obtained from

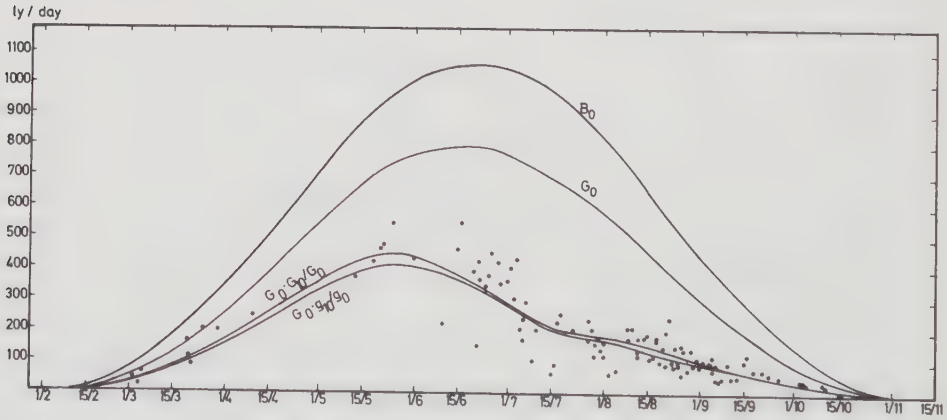

Fig. 28. Annual variation of daily totals of B_0, G_0 and G_0 . The two curves marked G_{10} have been obtained by multiplying G_0 with G_{10}/G_0 or g_{10}/g_0. Dots denote measured values of daily insolation.

monthly means of G_{10}/G_0 as well as from g_{10}/g_0. The annual variation of G_{10}, as computed from the relative insolation g_{10}/g_0 obtained from spot readings, can also be studied in Table 22. In that latter calculation a possible diurnal variation of g_{10}/g_0 and consequently different weights of the three-hourly observations of g_{10}/g_0 depending on the solar altitude has been disregarded. While the G_0-curve of Fig. 28 only exhibits a slight deviation from the quite symmetric form of the B_0-curve around the maximum at the summer solstice, the G_{10}-curves attain their highest values in

Table 22. Normal global radiation G_{10} with a dense overcast obtained from g_{10}/g_0.

G_0 = normal daily insolation with a clear sky
B_0 = daily insolation without atmosphere
g_{10}/g_0 from spot readings
Actual solar distance.

	g_{10}/g_0	G_0	G_{10}	B_0	G_{10}/B_0
Febr. 15 appr.	0.62	11	7	9	(0.778)
March 1 appr.	0.62	52	32	73	0.438
" 15	0.62	128	79	178	0.444
April 1	0.61	257	157	345	0.455
" 15	0.61	386	235	505	0.465
May 1	0.60	542	325	708	0.459
" 15	0.58	675	392	875	0.448
" 20	0.57	714	407	922	0.442
" 25	0.55	749	412	963	0.428
June 1	0.53	763	404	1009	0.400
" 15	0.46	796	366	1059	0.346
July 1	0.37	769	285	1049	0.273
" 15	0.29	699	203	981	0.207
Aug. 1	0.29	585	170	829	0.205
" 15	0.29	461	134	654	0.205
Sept. 1	0.32	308	99	450	0.220
" 15	0.36	197	71	298	0.238
Oct. 1	0.42	95	40	152	0.263
" 15	0.49	33	16	57	0.280

late May. This variation of G_{10} is due mainly to the fact that the albedo is much higher in spring than in autumn. The difference between the two G_{10}-curves is greatest in spring by about 10 %.

The daily insolation with a dense overcast as obtained from measurements is entered in the diagram of Fig. 28. The scattering of these points around the normal curve gives some idea of the variability of thickness and density of a dense overcast. A comparison with the conditions at a place like Maudheim, Antarctica (see Liljequist, 1956, p. 65) shows that the dispersion of the measured G_{10}-values there is noticeably smaller. This may be due to the generally higher albedo and to the lower mean temperature which latter restricts the thickness and density of the clouds in the Antarctic.

It might be expected that a similar difference would occur between the season with snow-covered ground and the season with bare ground on Devon Island. From Table 23 it is evident that the average deviation and the standard deviation of G_{10}/G_0 are much the same for both seasons while the coefficient of variation (the standard deviation expressed as a percentage of the arithmetic mean) is 12 % higher in June-September than in February-May. This may indicate a greater range of thickness and density of the clouds in the warm season. On the other hand, albedo variations may again be the main factor in which case no definite conclusions can be drawn from the values of Table 23.

Table 23. Average and standard deviation and coefficient of variation of G_{10}/G_0.

AD = average deviation
s = standard deviation
CV = coefficient of variation

Period		AD	s	CV %
June-Sept. 1961 and 1962	Bare ground	0.085	0.108	29
Febr.-May 1962	Snow-covered ground	0.082	0.109	17
June 1961-Sept. 1962	Whole measuring period	0.089	0.114	30

5.4. The relation between solar altitude h and g_{10}/g_0 with different cloud types

Spot readings of the global radiation and simultaneous cloud observations were made every 2 hours in the summer of 1961 and every 3 hours during the rest of the measuring period. Only those cases have been selected where the sun was completely concealed by a 10/10 cloud cover, i.e. by clouds forming a dense overcast. The g_{10}/g_0-values were grouped in 5°-intervals of solar altitude. The following cloud types were distinguished: St, Sc, Ns, Ac and As. In this connection it is worth mentioning that it is often difficult to identify a cloud type when the cloud cover is very dense and the whole sky is covered. The opinions of observers will differ. In an investigation of the relation between solar radiation and cloud type in the Arctic made by Vowinckel and Orvig (1962) Ns and St were taken into the same group owing to difficulties in distinguishing between them.

Monthly means of g_{10}/g_0 within 5°-intervals of solar altitude was calculated for the different cloud types. There were too few observations to make possible an analysis of the variation of g_{10}/g_0 with the solar altitude for each month separately. Therefore only the whole measuring period has been studied.

The variation of g_{10}/g_0 with the solar altitude is shown in Fig. 29. Generally, as can be seen from the curve "all cloud types", the relative insolation g_{10}/g_0 increases with the solar elevation which is in agreement with results from other investigations (see, for instance, Vowinckel and Orvig, 1962). The relative insolation with different cloud types given by these two authors for seven stations along the arctic coast is shown in Fig. 30. The stations were Aklavik, Resolute, Tiksi Bay, Calm Bay, Lonely Island and Cape Zhlenaiya. The number of observations amounted to 3500, which should be compared to 811 observations in the present investigation. It is noteworthy that the curves of Fig. 30 indicate a greater increase of g_{10}/g_0 with solar altitude for the arctic coast stations than for Devon Base Station. However, Vowinckel's and Orvig's data refer to cloud amounts of 10/10 irrespective of the cloud thickness, whereas our data refer to dense cloud covers only.

A marked undulatory shape is discernible in some of our curves, see Fig. 29. The low cloud types Sc and St exhibit relative maxima and minima in g_{10}/g_0 at approximately the same solar altitudes while the medium height cloud types Ac and As seem to cause a variation in g_{10}/g_0, which is similar for these two types of clouds but different from that of the low clouds.

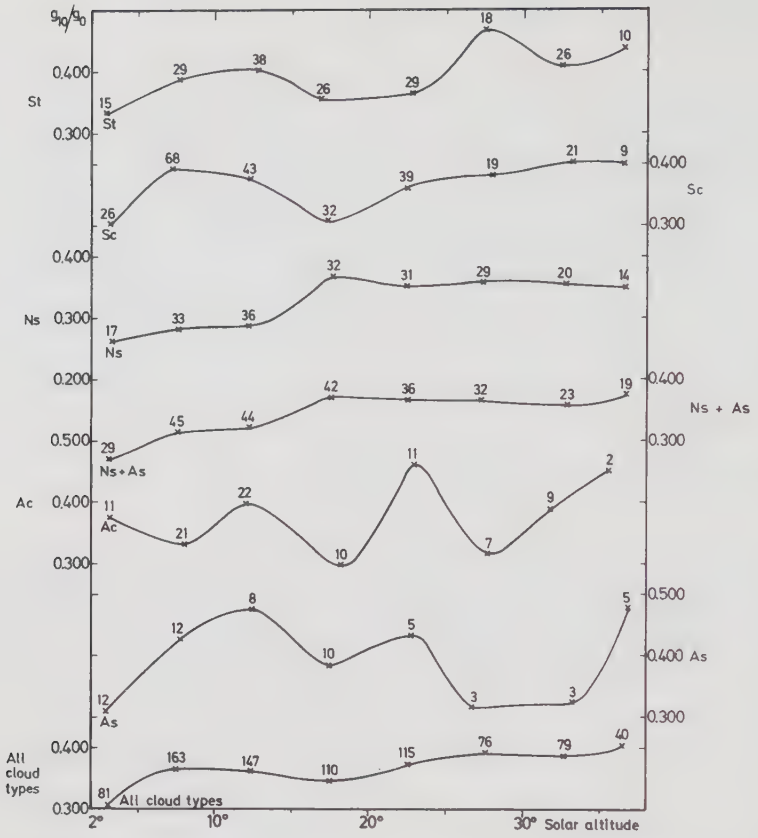

Fig. 29. Variation of g_{10}/g_0 with solar altitude for different types of cloud. The figures in connection with the curves denote number of data.

These features may, however, be of local origin and thus lack general applicability. Devon Island is high, 1885 m above m.s.l., and the undulations which are set up in the air flow by the orography can give rise to lenticular clouds above the observed overcast. Variations in the thickness of the continuous cloud cover may also be created. The consequence of such standing waves would be a variation in g_{10}/g_0, like that described above, with the solar elevation and also with the azimuth of the sun. An investigation of the existence of such effects would perhaps require a grouping of the data according to the wind direction in relation to the general direction of the mountain slopes and possibly also to the azimuth of the sun. Available data are, however, not sufficient to permit such a separation.

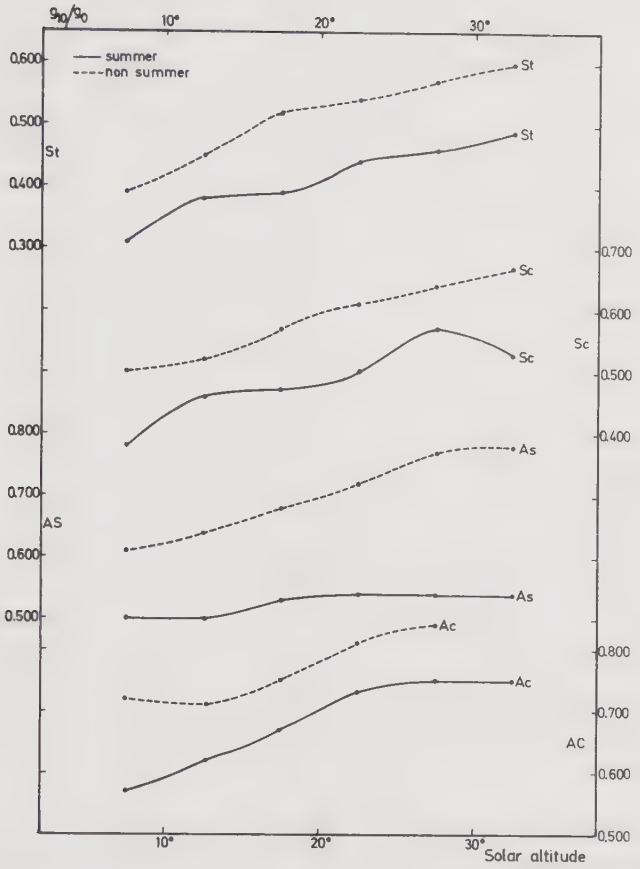

Fig. 30. Variation of g_{10}/g_0 with solar altitude for different cloud types from observations at seven stations along the Canadian and Siberian arctic coast. After Vowinckel and Orvig (1962).

5.5. Relative insolation G/G_0 with actual cloud cover

When calculating the insolation for periods of several days, commonly a month, the Savinov-Ångström formula is frequently used:

$$G = G_0 \left[k + (1 - k)\, S \right] \tag{27}$$

where k is the monthly mean of G_{10}/G_0 and S is the monthly mean of the relative duration of sunshine expressed as a fraction of a unit.

Measurements of S are not always available. In that case it is possible to substitute S with the expression 100 - N + K. Here N is the monthly mean cloudiness in %, K is a correction term which varies over the light season in a rather regular manner (see Section 1.4.). As can be seen from Table 9, showing the conditions at Resolute Bay (300 km from Devon Base Station), the applicability of the relation S = 100 - N + K is better for the summer months than for the winter and early spring months.

Eq. (27) presupposes a linear relationship between the relative insolation G/G_0 and the relative duration of sunshine S. The validity of this assumption has been tested by plotting G/G_0 versus S for each month. Group means within S-intervals of about 20 % have been computed and are shown in Fig. 31 a-j. Also group means for periods consisting of months with the same type of relationship between G/G_0 and S are entered there. It is evident that the assumption of linearity is not fulfilled. For the months with snow-covered ground, i.e. February, March, April and May (see Fig. 31 i) the relationship is best described by a straight line which cuts G/G_0 = 100 % at approximately S = 80 %. This is in agreement with Liljequist's result with a snow surface at Maudheim, Antarctica. For the months with bare ground, i.e. June, July, August and September (see Fig. 31 j), a curve convex towards the G/G_0-axis fits the mean values best. Monthly means of the relative insolation G/G_0 are shown in Table 24.

The Savinov-Ångström formula has the obvious advantage of making possible quick calculations of monthly totals of G from observed monthly means of S or N. It may though be of interest to make a comparison with other methods of obtaining G or G/G_0 from simple observations of S or N. Some other methods have been tested with the present data and the result can be seen in Table 25 where the first five columns show actually observed values. A practical way might be to use group means of S within intervals of - as a suggestion - 20 % to get G/G_0 from Fig. 31 a-h. The sum of the weighted grouped means of G/G_0 (weighted according to the number of days within each interval of S) will then give the monthly mean of G/G_0 (Table 25, column 6).

A method of using the observed total cloudiness N to get G/G_0 from the curves of Fig. 31 a-h has been tested on the present data. The observed daily means of cloudiness during a month have been collected in five groups, and the S-values corresponding to respective group means of cloudiness have been calculated from the relation S = 100 - N + K, where the correction term K was obtained from Fig. 9 a-c. As described above a weighted mean of G/G_0 has then been derived. These mean values are also entered in Table 25, column 8. They show a satisfactory agreement with the observed values. In Table 25, column 7

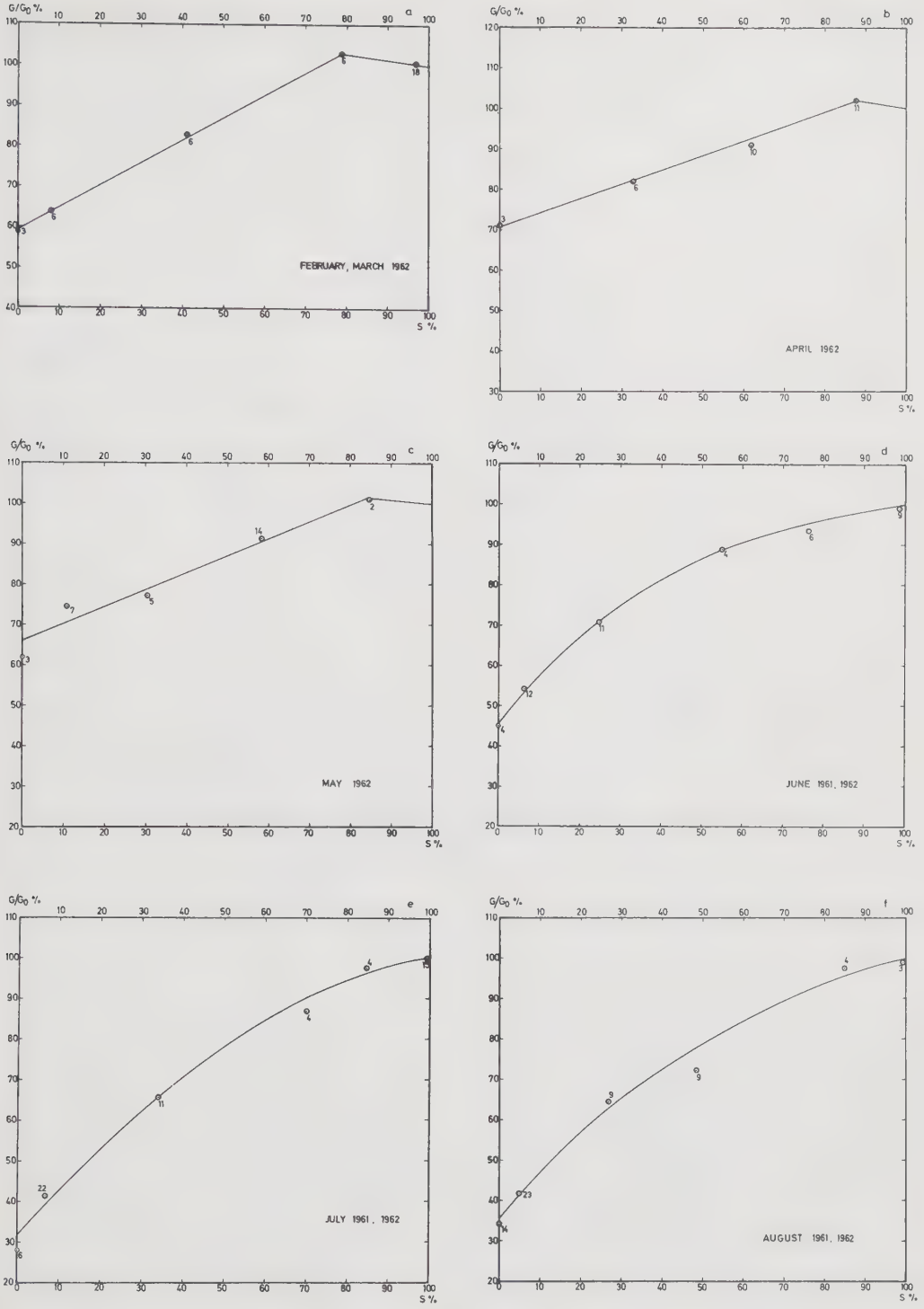

Fig. 31 a-j. The relative insolation G/G_0 as a function of the relative duration of sunshine S. The period February-May with snow on the ground (i) is compared with the period June-September with the ground bare of snow (j).

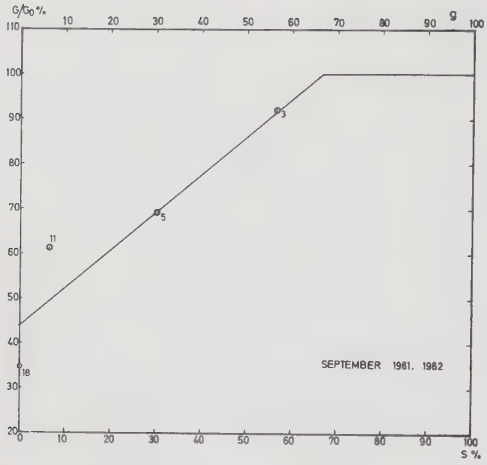
G/G0 %
S %
SEPTEMBER 1961, 1962

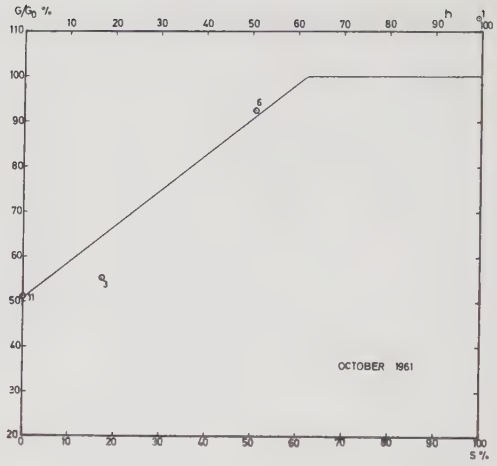
G/G0 %
S %
OCTOBER 1961

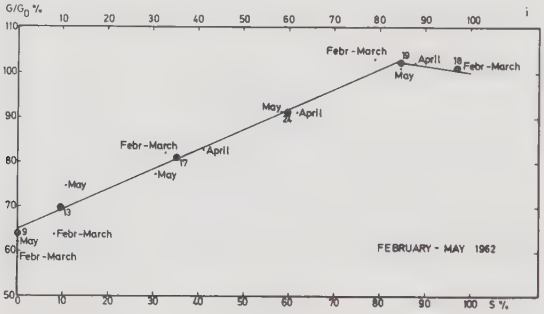
G/G0 %
S %
FEBRUARY - MAY 1962
Febr - March
April
May

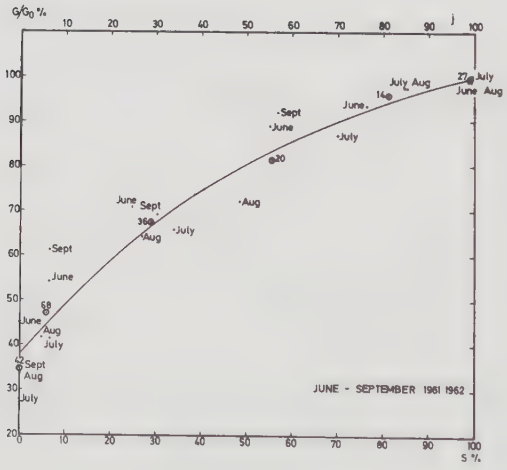
G/G0 %
S %
JUNE - SEPTEMBER 1961 1962
June
July
Aug
Sept

Fig. 31 g-j

Table 24. Monthly means of relative insolation G/G_0.

G = daily insolation at actual cloudiness

G_0 = daily insolation with a clear sky

Month	1961 G/G_0	1962 G/G_0	Mean G/G_0
Febr.		0.708	0.708
Mar.		0.916	0.916
Apr.		0.913	0.913
May		0.830	0.830
June	0.651	0.792	0.743
July	0.552	0.751	0.651
Aug.	0.556	0.542	0.549
Sept.	0.548	0.403	0.521
Oct.	0.667		0.667
Year			0.722

June 1961: 16 days of observation
Sept. 1962: 7 days of observation
Means of two years for June and September have been weighted according to the number of days with observation.

are also entered monthly means of G/G_0 as obtained from Savinov-Ångström's formula. Here we find the greatest deviations from the observed values. Monthly means of G/G_0 obtained from the curves of Fig. 31 a-h by applying monthly means of S show a smaller deviation than those obtained from Savinov-Ångström's formula. The insolation for the whole year computed with Savinov-Ångström's formula (Table 25, column 9) deviates from the observed value by 6.5 %.

These considerations only deal with the best way of obtaining G or G/G_0 from observed relationships between S and G/G_0 or between G_{10} and G_0 by means of simple observations of S and N. Decisive of the accuracy of estimated global radiation values is the variability of the applied relationships, such as G/G_0, G_{10}/G_0 and $S = 100 - N + K$, and their applicability at other places

Table 25. Relative insolation and monthly insolation (in ly) over the year.

S = relative duration of sunshine

G = monthly insolation in ly, actual cloud conditions

G_0 = monthly insolation in ly with a clear sky

G_{10} = monthly insolation in ly with a dense overcast.

	1	2	3	4	5	6	7	8	9	10
	S	G_{10}/G_0	G/G_0	G_0 ly	G ly	G/G_0	G/G_0	G/G_0	G ly	G ly
	obs.	obs.	obs.	obs.	obs.	calc.	calc.	calc.	calc.	calc.
Febr.	0.698	0.651	0.708	376	302	0.803	0.90	0.96	338	361
March	0.645	0.651	0.916	4300	3951	0.919	0.88	0.92	3784	3956
April	0.591	0.667	0.913	11744	10769	0.917	0.86	0.89	10100	10452
May	0.391	0.637	0.830	20876	17243	0.826	0.78	0.82	16283	17118
June	0.457	0.477	0.746	23639	17658	0.747	0.72	0.78	17020	18438
July	0.424	0.307	0.651	21343	13980	0.655	0.60	0.65	12806	13873
Aug.	0.253	0.330	0.541	13981	7926	0.567	0.50	0.59	6991	8249
Sept.	0.123	0.360	0.521	5905	2923	0.495	0.44	0.53	2598	3130
Oct.	0.201	0.506	0.667	1111	739	0.665	0.61	0.66	678	733
Year				103275	75491				70598	76310

Values in columns 7 and 9 are calculated by the aid of Savinov-Ångström's formula Eq. (27) using observed values S and G_{10}/G_0. Values in columns 8 and 10 are calculated by the aid of the relationship between S and G/G_0 as shown in Fig. 31 a-h and with S obtained from observed daily means of cloudiness by the aid of the relation S = 100 - N + K. G_0-values are referred to the visible horizon. Annual total of G_0 with an astronomical horizon = 103420 ly.

in the region. No conclusions about that can be drawn from the present data because of the relatively short observation period. But the data from a ten year period at Resolute (see Table 9) suggest that the variability of K is small enough, at least during the summer months, to permit a calculation of G from observed N, variations in other relevant relationships being disregard.

Acknowledgements

The field work was performed during the Arctic Institute of North America Devon Island Expedition 1961-1962. The Arctic Institute supported the reduction and writing up of the data. Professor G.H. Liljequist, a pioneer in polar meteorology, gave encouraging support at all stages in the work. He also read the manuscript and made valuable suggestions. I had interesting discussions with B. Holmgren, who also read the manuscript. S. Apollonio, field leader of the expedition, made every effort to support the work at Devon Base Station. J.W. Fellows, A. Gill, C.W. Nicol and C. Shackleton were skilful and interested field-assistants. Miss Marianne Björklund did the typewriting and Mrs Ulla Lindqvist and Miss Gun Engström drew the figures. To all these persons and to the Arctic Institute of North America I express my sincere thanks.

Lars Dahlgren
Meteorologiska institutionen
Uppsala universitet

References

Ambach, W., 1963: Untersuchungen zum Energieumsatz in der Ablationszone des Grönländischen Inlandeises. Meddelelser om Grønland, Kommissionen for videnskabelige undersøgelser i Grønland. Bd. 174, Nr. 4. København.

Ångström, A., 1929: On the atmospheric transmission of sun radiation and on dust in the air. Geogr. Ann., Bd. 11.

Ångström, A., 1961: Techniques of determining the turbidity of the atmosphere. Tellus, Vol. 13, No. 2.

Ångström, A., 1961: Absorption of solar radiation by atmospheric water vapor. Arkiv för Geofysik, Kungl. Sv. Vetenskapsakademin, Bd. 3, No. 23.

Ångström, A., 1964: The parameters of atmospheric turbidity. Tellus, Vol. 16, No. 1.

Ångström, A., 1964: On the absorption of solar radiation by atmospheric water vapor. Arkiv för Geofysik, Kungl. Sv. Vetenskapsakademin, Bd. 4, No. 24.

Ångström, A. and Drummond, A.J., 1959: Transmission of "cutoff" glass filters employed in solar radiation research. Journ. of Opt. Soc. of Am., Vol. 49, No. 11.

Ångström, A. and Drummond, A.J., 1960: Transmission of "cutoff" glass filters employed in solar radiation research II. Journ. of Opt. Soc. of Am., Vol. 50, No. 10.

Ångström, A. and Drummond, A.J., 1961: Basic concepts concerning cutoff glass filters used in radiation measurements. Journ. of Met., Vol. 18, No. 3.

Ångström, A. and Rodhe, B., 1966: Pyrheliometric measurements with special regard to the circumsolar sky radiation. Tellus, Vol. 18, No. 1.

Ångström, A. and Tryselius, O., 1934: Total radiation from sun and sky at Abisko. Geogr. Ann., Bd. 16.

Feussner, K. and Dubois, P., 1930: Trübungsfaktor, precipitable water, Staub. Gerlands Beitr. z. Geophys., Bd. 27.

Flowers, E.C. and Helfert, N.F., 1966: Laboratory and field investigations of Eppley radiation sensors. Mon. Wea. Rev., Vol. 94, No. 4.

Foitzik, L. and Hinzpeter, H., 1958: Sonnenstrahlung und Lufttrübung. Akad. Verlagsges., Leipzig.

Fowle, F.E., 1912: The spectroscopic determination of aqueous vapor. Astrophys. Journ., Vol. 35.

Fowle, F.E., 1915: The transparency of aqueous vapor. Astrophys. Journ., Vol. 42.

Fritz, S. and McDonald, T.H., 1960: Some normal-incidence solar radiation observations during I.G.Y., U.G.G.I. Monographie 4, Symposium on radiation. Oxford 20-25. July 1959, 4, 1960.

Fuquay, D. and Buettner, K., 1957: Laboratory investigation of some characteristics of the Eppley Pyrheliometer. Transact. Am. Geoph. Union., Vol. 38, No. 1.

Gavrilova, M.K., 1963: Radiation climate of the Arctic. Israel Progr. for Scient. Transl. Jerusalem, 1966.

Hartmann, W., 1960: Sonnenscheindauer und Bewölkung. Meteorol. Raundschau, 13. Jahrg. Heft 2.

Hoelper, O., 1939: Atmosphärische Trübungs- und Wasserdampfbestimmungen nach Filtermessungen der Sonnenstrahlung. Reichsamt. f. Wetterdienst, Viss. Abh. 5(10).

Hoinkes, H., 1960: Studies of solar radiation and albedo in the Antarctic (Little America V and South Pole, 1957/58). Arch. Met. Geoph. Biokl., Bd. 10.

Holmgren, B., 1971: Climate and energy exchange on a sub-polar ice cap in summer. Part E. Radiation climate. Meteorologiska institutionen, Uppsala universitet, Meddelande Nr. 111.

IGY Instruction Manual, Part VI. Radiation instruments and measurements. London, Pergamon Press, 1958, Radiation Commission of the IAMAP.

Kondratyev, K. Ya., 1969: Radiation in the atmosphere. International Geophys. Ser., Vol. 12, Academic Press, New York and London.

Liljequist, G.H., 1956: Energy exchange of an Antarctic snow field. Part I A: Short-wave radiation. Norwegian-British-Swedish Antarctic Expedition, 1949-52. Scientific Res., Vol. II, Oslo.

List, R.J., 1951: Smithsonian meteorological tables. 6 th rev. ed. Smithsonian Inst. Washington.

MacDonald, T.H., 1951: Some characteristics of the Eppley pyrheliometer. Mon. Wea. Rev., Vol. 79, No. 7.

McDonald, J.E., 1960: Absorption of solar radiation by atmospheric water vapor. Journ. of Met., Vol. 17, No. 3.

Rae, R.W., 1951: Climate of the Canadian Arctic Archipelago. Dept. of Transport, Met. Div. Toronto.

Robinson, N., 1966: Solar radiation. Elsevier Publishing Company, Amsterdam, 1966.

Sivkov, S.I., 1968: Computation of solar radiation characteristics. Israel progr. for Scient. Transl. Jerusalem, 1971.

Woertz, B.B. and Hand, I.F., 1941: The characteristics of the Eppley pyrheliometer. Mon. Wea. Rev., Vol. 69, No. 5.

Vowinckel, E. and Orvig, S., 1962: Relation between solar radiation income and cloud type in the Arctic. Arctic, Met. Res. Group Mc Gill Univ. Montreal. Publ. in Met., No. 48.

A P P E N D I X

Appendix 1. The intensity of the direct solar radiation in a dry atmosphere as a function of the air mass m and the turbidity β according to Hoelper (1939).

The values which are given in mcal $cm^{-2}min^{-1}$ are reduced to the International Pyrheliometric Scale 1956 and are valid for mean solar distance.

m	1.0	1.5	2.0	2.5	3.0	3.5	4.0	4.5	5.0	5.5	6.0
β											
0.000	1720	1651	1591	1539	1490	1445	1402	1364	1330	1299	1272
005	1705	1632	1566	1509	1456	1408	1363	1321	1286	1253	1226
010	1691	1613	1542	1482	1425	1374	1326	1282	1245	1210	1181
015	1678	1595	1519	1454	1395	1342	1291	1246	1206	1170	1138
020	1664	1576	1497	1428	1365	1310	1257	1211	1169	1131	1098
025	1650	1558	1476	1402	1337	1280	1226	1177	1134	1094	1060
030	1637	1541	1455	1378	1309	1251	1195	1145	1100	1059	1024
035	1624	1523	1435	1354	1283	1222	1165	1113	1067	1025	990
040	1611	1506	1414	1331	1257	1195	1137	1083	1036	993	956
045	1598	1490	1394	1308	1233	1168	1109	1054	1006	961	923
050	1586	1473	1374	1286	1208	1143	1081	1026	976	931	892

Appendix 2. The intensity of the direct solar radiation within the wavelength interval 0 - 525 mμ as a function of the air mass m and the turbidity β according to Hoelper (1939).

The values which are given in mcal $cm^{-2}min^{-1}$ are reduced to the International Pyrheliometric Scale 1956 and are valid for mean solar distance.

m	1.0	1.5	2.0	2.5	3.0	3.5	4.0	4.5	5.0	5.5	6.0
β											
0.000	367	321	281	249	220	196	175	157	140	126	114
005	360	314	273	240	210	186	166	147	131	117	104
010	354	307	266	231	201	177	157	138	123	109	96
015	349	300	258	223	192	168	149	130	115	101	88
020	344	294	250	214	183	159	140	123	107	93	81
025	339	288	242	206	175	152	132	115	99	86	75
030	334	282	235	199	168	145	125	108	93	80	69
035	329	276	229	192	161	138	118	101	87	75	64
040	324	270	223	185	155	131	111	95	81	70	59
045	319	264	216	178	149	125	105	90	76	65	55
050	314	259	209	172	142	119	99	84	71	60	51

Appendix 3. The intensity of the direct solar radiation within the wavelength interval 525 - 630 $m\mu$ as a function of the air mass m and the turbidity β.

The table is based on calculations by Hoelper (1939) for the intervals 0 - 525 $m\mu$ and 0 - 625 $m\mu$. The values which are given in mcal $cm^{-2}min^{-1}$ are reduced to International Pyrheliometric Scale 1956 and are valid for mean solar distance.

m	1.0	1.5	2.0	2.5	3.0	3.5	4.0	4.5	5.0	5.5	6.0
β											
0.000	239	226	214	200	188	178	169	159	151	143	135
005	238	223	209	195	183	171	162	152	143	137	129
010	236	220	205	190	177	165	155	145	136	130	120
015	233	217	201	186	172	160	148	138	129	122	114
020	230	213	197	182	168	155	143	132	122	115	107
025	228	209	193	178	164	150	138	126	117	108	101
030	225	206	189	174	160	145	133	121	111	101	95
035	222	203	185	170	154	139	128	116	105	94	89
040	221	200	180	166	149	134	123	111	100	89	83
045	219	197	177	162	144	130	118	106	95	84	78
050	217	192	174	158	140	126	114	101	91	80	74

Appendix 4. The intensity of the direct solar radiation within the wavelength interval 0 - 630 $m\mu$ as a function of the air mass m and the turbidity β.

The table is based on the intensity in the interval 0 - 625 $m\mu$ given by Hoelper (1939) and corrected to be valid for the interval 0 - 630 $m\mu$. The values which are given in mcal $cm^{-2}min^{-1}$ are reduced to the International Pyrheliometric Scale 1956 and are valid for mean solar distance.

m	1.0	1.5	2.0	2.5	3.0	3.5	4.0	4.5	5.0	5.5	6.0
β											
0.000	606	548	495	449	407	374	344	316	291	270	249
005	598	537	482	435	392	358	328	299	274	254	233
010	590	527	470	422	278	343	312	283	258	238	217
015	582	517	458	409	364	329	297	268	243	223	202
020	574	507	446	396	351	315	283	254	229	208	188
025	567	497	435	384	339	302	270	241	216	194	175
030	559	488	424	373	327	290	258	229	204	181	164
035	551	479	414	362	315	278	246	217	192	169	152
040	544	470	404	351	303	266	234	206	181	159	142
045	537	461	393	340	292	255	223	196	171	149	133
050	530	451	383	329	282	245	212	186	162	140	125

Appendix 5. The intensity of the direct solar radiation in a dry atmosphere as a function of the air mass m and the turbidity β.

The table is based on the intensity in an ideal atmosphere given by Sivkov (1968). The values which are given in mcal $cm^{-2}min^{-1}$ are referred to the International Pyrheliometric Scale 1956 and are valid for mean solar distance.

m	1.0	1.5	2.0	2.5	3.0	3.5	4.0	4.5	5.0	5.5	6.0
β											
0.000	1753	1677	1617	1560	1512	1467	1428	1392	1358	1327	1298
005	1739	1659	1593	1533	1481	1434	1391	1351	1315	1282	1251
010	1726	1641	1570	1507	1451	1401	1355	1312	1275	1239	1206
015	1713	1623	1548	1481	1422	1368	1320	1276	1236	1198	1164
020	1699	1605	1526	1456	1393	1337	1287	1241	1199	1159	1123
025	1686	1587	1504	1432	1366	1307	1254	1207	1163	1122	1084
030	1673	1570	1483	1408	1339	1278	1223	1173	1128	1086	1047
035	1661	1553	1462	1384	1312	1250	1193	1141	1094	1051	1012
040	1648	1536	1442	1361	1286	1222	1163	1110	1063	1018	978
045	1636	1521	1422	1338	1261	1195	1135	1081	1032	987	946
050	1623	1505	1402	1315	1237	1169	1108	1053	1002	957	915

Appendix 6. The intensity of the direct solar radiation within the wavelength interval 0 - 525 mμ as a function of the air mass m and the turbidity β.

The table is based on the intensity in an ideal atmosphere given by Sivkov (1968). The values which are given in mcal $cm^{-2}min^{-1}$ are referred to the International Pyrheliometric Scale 1956 and are valid for mean solar distance.

m	1.0	1.5	2.0	2.5	3.0	3.5	4.0	4.5	5.0	5.5	6.0
β											
0.000	367	316	278	244	217	192	172	154	138	124	112
005	361	309	270	236	208	183	163	145	129	115	103
010	356	302	262	228	199	174	154	136	120	107	95
015	351	296	255	220	191	166	146	128	113	99	88
020	345	290	248	212	183	158	138	120	105	92	81
025	340	284	241	205	176	151	131	113	98	86	75
030	335	278	234	198	168	144	124	106	92	79	69
035	331	272	227	191	161	137	117	100	86	74	64
040	326	267	221	184	155	131	111	94	80	69	59
045	321	262	215	178	148	124	105	88	75	64	54
050	316	256	209	172	142	118	99	82	70	59	50

Appendix 7. The intensity of the direct solar radiation within the wavelength interval 525 - 630 mμ as a function of the air mass m and the turbidity β.

The table is based on the intensity in an ideal atmosphere given by Sivkov (1968). The values which are given in mcal $cm^{-2}min^{-1}$ are referred to the International Pyrheliometric Scale 1956 and are valid for mean solar distance.

m	1.0	1.5	2.0	2.5	3.0	3.5	4.0	4.5	5.0	5.5	6.0
β											
0.000	247	233	220	208	197	186	176	166	157	149	140
005	244	229	216	203	191	180	169	159	149	141	132
010	242	226	212	198	185	173	162	152	142	133	124
015	239	222	207	193	179	167	156	145	135	125	117
020	237	219	203	188	174	161	149	138	128	119	110
025	234	216	199	183	169	155	143	132	122	112	103
030	232	212	195	179	164	150	138	126	116	106	97
035	230	209	191	174	159	145	132	120	110	100	91
040	227	206	187	170	154	140	127	115	104	95	86
045	225	203	183	166	149	135	122	110	99	90	81
050	223	200	180	162	145	130	117	105	94	85	76

Appendix 8. The intensity of the direct solar radiation within the wavelength interval 0 - 630 mμ as a function of the air mass m and the turbidity β.

The table is based on the intensity in an ideal atmosphere given by Sivkov (1968). The values which are given in mcal $cm^{-2}min^{-1}$ are referred to the International Pyrheliometric Scale 1956 and are valid for mean solar distance.

m	1.0	1.5	2.0	2.5	3.0	3.5	4.0	4.5	5.0	5.5	6.0
β											
0.000	613	550	498	453	413	379	348	320	295	273	252
005	605	540	486	439	399	363	332	303	278	256	235
010	598	530	474	426	384	348	316	287	262	240	219
015	590	520	462	413	370	334	301	272	247	225	205
020	582	510	451	400	357	320	287	258	233	211	191
025	575	500	440	388	344	306	274	244	220	198	178
030	567	491	429	376	332	294	261	232	207	186	166
035	560	482	418	365	320	282	249	220	196	174	155
040	553	473	408	354	309	271	238	208	185	163	145
045	546	464	398	342	298	260	227	198	174	153	135
050	539	455	388	332	287	249	216	188	164	144	126

Appendix 9. Water vapor absorption in mcal $cm^{-2}min^{-1}$ as a function of $m \cdot \beta$ and $m \cdot w$ calculated from Eq. (18).

Absorptivities are given by Fowle (List, 1951) and the extraterrestrial solar energy within the absorption bands by McDonald (1960). The absorption values are valid for mean solar distance.

m · w	0.5	1.0	2.0	3.0	4.0	5.0	6.0	7.0	8.0
m · β									
0.000	122.2	149.5	184.7	209.0	228.3	244.4	258.3	270.1	280.7
010	121.4	148.4	183.3	207.4	226.5	242.5	256.2	267.9	278.3
020	120.5	147.4	181.9	205.8	224.7	240.5	254.2	265.2	276.0
030	119.7	146.3	180.5	204.2	222.9	238.9	252.1	263.5	273.8
040	118.9	145.2	179.2	202.6	221.2	236.7	250.1	261.4	271.5
050	118.0	144.2	177.8	201.0	219.3	234.8	248.1	259.2	269.3
060	117.2	143.2	176.5	199.5	217.7	233.0	246.1	257.1	267.0
070	116.4	142.1	175.1	198.0	216.0	231.1	244.1	255.0	264.8
080	115.6	141.1	173.8	196.5	214.4	229.3	242.1	253.0	262.7
090	114.8	140.1	172.5	194.9	212.7	227.5	240.2	250.9	260.5
100	114.0	139.1	171.2	193.5	211.0	225.7	238.3	248.9	258.4
110	113.2	138.1	170.0	192.0	209.4	223.9	236.4	246.9	256.3
120	112.4	137.1	168.7	190.5	207.7	222.1	234.5	244.9	254.2
130	111.7	136.1	167.4	189.0	206.1	220.4	232.6	242.6	252.1
140	111.0	135.2	166.3	187.8	204.7	218.8	230.9	241.1	250.2
150	110.1	134.1	164.9	186.2	202.9	216.9	228.9	239.0	248.0
160	109.4	133.2	163.7	184.8	201.4	215.2	227.1	237.1	246.0
170	108.6	132.2	162.4	183.3	199.7	213.4	225.2	235.0	243.8
180	107.9	131.3	161.3	182.0	198.3	211.8	223.5	233.3	242.0
190	107.2	130.4	160.1	180.6	196.8	210.2	221.7	231.4	240.1
200	106.4	129.4	158.9	179.2	195.2	208.5	220.0	229.5	238.1

Appendix 10. The ratio (Eq. 19) between the water vapor absorption in a turbid atmosphere and the absorption in a clean atmosphere as a function of $\beta \cdot m$ and $w \cdot m$.

Absorptivities given by Fowle (List, 1951) and extraterrestrial energy within the absorption bands given by McDonald (1960) has been employed.

m · β \ m · w	0.5	1.0	2.0	3.0	4.0	5.0	6.0	7.0	8.0
0.010	0.9931	0.9928	0.9925	0.9922	0.9921	0.9920	0.9919	0.9918	0.9917
020	0.9862	0.9856	0.9850	0.9846	0.9843	0.9841	0.9839	0.9837	0.9835
030	0.9793	0.9784	0.9775	0.9770	0.9766	0.9762	0.9759	0.9756	0.9754
040	0.9725	0.9713	0.9702	0.9695	0.9689	0.9685	0.9681	0.9677	0.9674
050	0.9658	0.9643	0.9629	0.9620	0.9613	0.9608	0.9603	0.9598	0.9594
060	0.9592	0.9574	0.9557	0.9546	0.9538	0.9532	0.9526	0.9521	0.9515
070	0.9525	0.9505	0.9485	0.9473	0.9463	0.9456	0.9449	0.9443	0.9437
080	0.9460	0.9436	0.9414	0.9401	0.9390	0.9381	0.9374	0.9367	0.9359
090	0.9394	0.9368	0.9343	0.9329	0.9316	0.9307	0.9299	0.9291	0.9283
100	0.9330	0.9301	0.9274	0.9258	0.9244	0.9234	0.9225	0.9216	0.9207
110	0.9267	0.9235	0.9205	0.9187	0.9173	0.9161	0.9151	0.9142	0.9132
120	0.9201	0.9168	0.9135	0.9116	0.9100	0.9088	0.9077	0.9067	0.9056
130	0.9138	0.9102	0.9067	0.9046	0.9029	0.9016	0.9004	0.8993	0.8982
140	0.9075	0.9036	0.8999	0.8977	0.8959	0.8945	0.8932	0.8921	0.8908
150	0.9013	0.8972	0.8932	0.8909	0.8890	0.8875	0.8861	0.8849	0.8836
160	0.8951	0.8908	0.8866	0.8841	0.8820	0.8805	0.8791	0.8778	0.8765
170	0.8889	0.8842	0.8799	0.8774	0.8750	0.8735	0.8721	0.8707	0.8693
180	0.8829	0.8781	0.8734	0.8707	0.8684	0.8667	0.8652	0.8637	0.8623
190	0.8769	0.8719	0.8671	0.8642	0.8619	0.8700	0.8584	0.8569	0.8554
200	0.8708	0.8656	0.8605	0.8575	0.8551	0.8532	0.8515	0.8499	0.8483

Appendix 11. Water vapor absorption in mcal $cm^{-2}min^{-1}$ as a function of $\beta \cdot m$ and $w \cdot m$ obtained by multiplying Houghton's absorption values with the ratios of Table 10 of the Appendix.

The absorption values are valid for mean solar distance.

m · β \ m · w	0.5	1.0	2.0	3.0	4.0	5.0	6.0	7.0	8.0
0.000	143.9	186.0	240.4	279.3	310.7	337.4	361.0	382.1	401.5
010	142.9	184.7	238.6	277.1	308.2	334.7	358.1	379.0	398.2
020	141.9	183.3	236.8	275.0	305.8	332.0	355.2	375.9	394.9
030	140.9	182.0	235.0	272.9	303.4	329.4	352.3	372.8	391.6
040	139.9	180.7	233.2	270.8	301.0	326.8	349.5	369.8	388.4
050	139.0	179.4	231.5	268.7	298.7	324.2	346.7	366.7	385.2
060	138.0	178.1	229.8	266.6	296.3	321.6	343.9	363.8	382.0
070	137.1	176.8	228.0	264.6	294.0	319.0	341.1	360.8	378.9
080	136.1	175.5	226.3	262.6	291.7	316.5	338.4	357.9	375.8
090	135.2	174.2	224.6	260.6	289.4	314.0	335.7	355.0	372.7
100	134.3	173.0	222.9	258.6	287.2	311.6	333.0	352.1	369.7
110	133.4	171.8	221.3	256.6	285.0	309.1	330.4	349.3	366.6
120	132.4	170.5	219.6	254.6	282.7	306.6	327.7	346.5	363.6
130	131.5	169.3	218.0	252.7	280.5	304.2	325.0	343.6	360.6
140	130.6	168.1	216.3	250.7	278.4	301.8	322.4	340.9	357.7
150	129.7	166.9	214.7	248.8	276.2	299.4	319.9	338.1	354.8
160	128.8	165.7	213.1	246.9	274.0	297.1	317.4	335.4	351.9
170	127.9	164.5	211.5	245.1	271.9	294.7	314.8	332.7	349.0
180	127.0	163.3	210.0	243.2	269.8	292.4	312.3	330.0	346.2
190	126.2	162.2	208.5	241.4	267.8	290.2	309.9	327.4	343.4
200	125.3	161.0	206.9	239.5	265.7	287.9	307.4	324.7	340.6

Appendix 12.

Various parameters obtained from each series of pyheliometric measurement at Devon Base Station in 1962.

Daily means are also entered in the table. In the columns the following parameters are listed:

1. Mean time for each pyrheliometric series.
2. Optical air mass m.
3. Ångström's turbidity coefficient $\beta_H \cdot 10^3$ calculated from Hoelper's tables as a mean of β_g and β_r (Appendix 2 and 4).
4. Linke's turbidity factor T.
5. Linke's turbidity factor $T_{m=2}$ reduced to m=2.
6. Extinction F_H calculated from Hoelper's tables (Appendix 1).
7. The product $\beta_H \cdot m$.
8. Amount of precipitable water $w_{Å,H}$ calculated according to Ångström (Eq. 12) and Hoelper (Appendix 1).
9. Amount of precipitable water $w_{H,H}$ calculated according to Houghton (Fig. 2) and Hoelper (Appendix 1).
10. Extinction F calculated from Appendix 5 based on Sivkov's calculations.
11. Amount of precipitable water $w_{H,S}$ calculated according to Houghton (Fig. 2) and Sivkov (Appendix 5).
12. Amount of precipitable water w_{Res} calculated from radiosoundings at Resolute.

	1	2	3	4	5	6	7	8	9	10	11	12
Date	Time	m	$10^3 \cdot \beta_H$	T	$T_{m=2}$	F_H	$\beta_H \cdot m$	$w_{Å,H}$	$w_{H,H}$	F_S	$w_{H,S}$	w_{Re}
23.5	1639	2.55	38.0	2.34	2.44	140	0.097	0.25	0.22	168	0.36	0.4
26.5	1149	1.76	37.3	2.50	2.44	143	0.065	0.39	0.33	174	0.54	
	1430	1.97	32.0	2.40	2.39	156	0.063	0.46	0.36	181	0.54	
	1709	2.70	32.5	2.30	2.42	165	0.088	0.41	0.32	193	0.49	
Day			34.5	2.40	2.42			0.42	0.34		0.52	0.3
27.5	1640	2.52	30.0	2.37	2.46	186	0.076	0.65	0.46	211	0.65	
	2015	4.88	30.3	2.20	2.50	194	0.148	0.41	0.31	219	0.43	
Day			30.1	2.23	2.48			0.53	0.38		0.55	0.5
28.5	1715	2.73	29.8	2.40	2.52	205	0.081	0.84	0.56	230	0.77	0.6
31.5	1815	3.13	28.3	2.54	2.72	265	0.089	1.72	1.00	287	1.26	0.7
5.6	1139	1.69	33.3	2.72	2.65	199	0.056	1.20	0.79	229	1.17	0.8

cont.

	1	2	3	4	5	6	7	8	9	10	11	12
Date	Time	m	$10^3 \cdot \beta_H$	T	$T_{m=2}$	F_H	$\beta_H \cdot m$	$w_{\AA,H}$	$w_{H,H}$	F_S	$w_{H,S}$	w_{Res}
6.6	0046	6.29	20.5	2.18	2.51	277	0.129	1.02	0.61	287	2.18	0.89
8.6	1717	2.58	23.5	2.54	2.64	264	0.061	2.02	1.14	292	1.50	1.47
12.6	0454	2.96	17.5	2.27	2.43	246	0.052	1.39	0.80	271	1.05	0.81
13.6	1432	1.84	17.5	2.48	2.45	226	0.032	1.65	0.98	244	1.22	
	1744	2.67	14.0	2.32	2.44	264	0.037	1.91	1.04	290	1.35	
	2016	4.17	15.0	2.12	2.40	261	0.063	1.20	0.69	290	0.91	
Day			15.5	2.31	2.43			1.59	0.90		1.16	0.90
14.6	0057	5.77	16.5	2.15	2.47	284	0.095	1.18	0.67	312	0.86	
	0530	2.67	19.0	2.30	2.42	234	0.051	1.30	0.78	256	0.99	
	1424	1.82	22.0	2.43	2.40	194	0.040	1.01	0.67	224	0.98	
	1719	2.50	17.0	2.28	2.37	228	0.043	1.26	0.76	259	1.06	
Day			18.5	2.29	2.41			1.19	0.72		0.97	0.74
15.6	0442	3.08	12.0	2.19	2.36	263	0.037	1.63	0.89	287	1.14	
	2213	5.68	15.0	2.04	2.36	260	0.085	0.89	0.52	288	0.69	
Day			13.5	2.12	2.36			1.26	0.70		0.91	0.72
16.6	0110	5.55	15.0	2.05	2.37	263	0.083	0.94	0.55	287	0.83	
	0443	3.07	15.5	2.17	2.34	233	0.048	1.11	0.66	253	1.04	
	1350	1.76	18.5	2.41	2.35	197	0.033	1.09	0.71	227	0.91	
	1656	2.37	15.5	2.21	2.28	210	0.037	1.00	0.61	240	0.84	
	2207	5.59	13.5	2.07	2.39	280	0.075	1.14	0.63	310	0.84	
Day			15.5	2.18	2.45			1.06	0.63		0.89	0.89
17.6	0505	2.87	14.0	2.19	2.34	243	0.040	1.36	0.78	266	1.00	
	1418	1.81	15.5	2.38	2.35	210	0.028	1.31	0.82	238	1.14	
	1710	2.45	14.5	2.26	2.34	232	0.036	1.36	0.80	259	1.07	
	2011	4.08	17.0	2.16	2.43	257	0.069	1.17	0.68	287	0.92	
Day			15.0	2.25	2.36			1.30	0.77		1.03	0.75
18.6	0430	3.17	14.0	2.18	2.37	251	0.060	1.39	0.80	276	1.01	
	1410	1.79	16.5	2.44	2.39	213	0.030	1.39	0.86	246	1.26	
	2003	3.95	14.0	2.15	2.41	268	0.055	1.38	0.76	296	1.00	
	2315	6.09	14.0	2.09	2.42	294	0.085	1.25	0.68	321	0.86	
Day			14.5	2.21	2.40			1.35	0.76		1.03	0.70
19.6	1418	1.80	22.0	2.47	2.43	202	0.040	1.17	0.76	231	1.08	
	1656	2.35	17.0	2.32	2.38	230	0.040	1.38	0.82	258	1.12	
Day			19.5	2.40	2.40			1.28	0.79		1.10	1.28
20.6	1158	1.64	24.5	2.61	2.53	205	0.040	1.35	0.86	234	1.23	1.00

cont.

	1	2	3	4	5	6	7	8	9	10	11	12
Date	Time	m	$10^3 \cdot \beta_H$	T	$T_{m=2}$	F_H	$\beta_H \cdot m$	$w_{Å,H}$	$w_{H,H}$	F_S	$w_{H,S}$	w_{Res}
8.7	1356	1.81	16.5	2.39	2.35	207	0.034	1.25	0.80	235	1.11	0.96
9.7	0241	4.81	15.0	2.13	2.44	280	0.072	1.32	0.73	302	0.91	
	1416	1.85	14.0	2.34	2.31	211	0.026	1.30	0.81	239	1.12	
	1713	2.55	14.0	2.22	2.33	236	0.033	1.37	0.80	267	1.11	
	2304	6.77		2.13	2.46							
Day			14.0	2.20	2.38			1.33	0.78		1.05	1.45
10.7	1415	1.85	23.5	2.54	2.51	213	0.043	1.36	0.85	244	1.23	
	1713	2.56	25.0	2.49	2.58	244	0.064	1.57	0.93	270	1.23	
Day			24.5	2.52	2.55			1.46	0.89		1.23	0.90
11.7	2003	4.25	19.5	2.17	2.45	245	0.083	0.97	0.59	273	0.80	1.10
12.7	0454	3.22	21.5	2.31	2.50	247	0.069	1.30	0.77	275	1.06	
	1726	2.69	30.0	2.47	2.59	219	0.081	1.05	0.68	245	0.93	
	2304	7.13		2.18	2.51							
Day			26.0	2.32	2.53			1.17	0.72		1.00	1.17
13.7	0453	3.25	22.0	2.31	2.51	247	0.072	1.29	0.77	272	1.00	
	1330	1.82	20.5	2.46	2.42	205	0.037	1.21	0.77	240	1.18	
	1726	2.70	16.5	2.29	2.41	245	0.045	1.49	0.86	270	1.11	
Day			19.5	2.35	2.44			1.33	0.80		1.10	1.05
14.7	0451	3.32	15.0	2.19	2.39	253	0.050	1.35	0.77	274	0.96	
	1420	1.91	18.0	2.39	2.38	207	0.034	1.19	0.75	239	1.10	
Day			16.5	2.29	2.38			1.27	0.76		1.03	1.00
15.7	0445	3.40	24.0	2.48	2.69	283	0.082	1.96	1.09	310	1.40	
	1347	1.85	33.5	2.78	2.75	225	0.062	1.65	1.03	255	1.45	
	2017	4.70	35.0	2.53	2.83	258	0.165	1.11	0.59	286	0.97	
Day			31.0	2.60	2.76			1.57	0.90		1.27	0.98
16.7	1431	1.95	35.0	2.82	2.80	235	0.068	1.83	1.11	261	1.48	
	2210	6.88		2.29	2.63							
Day			35.0	2.55	2.71			1.83	1.11		1.48	1.31
17.7	1347	1.85	23.5	2.64	2.61	234	0.043	1.86	1.10	261	1.48	0.71
18.7	0508	3.22	19.5	2.41	2.60	284	0.063	2.07	1.11	310	1.42	
	1356	1.88	24.0	2.62	2.60	234	0.045	1.83	1.09	290	1.52	
	2000	4.56	23.5	2.34	2.64	276	0.107	1.37	0.80	305	1.05	
	2322	8.15		2.37	2.70							
Day			22.3	2.44	2.63			1.76	1.00		1.33	1.34
19.7	0452	3.44	24.5	2.41	2.62	263	0.084	1.52	0.89	285	1.11	
	1720	2.76	23.5	2.45	2.58	252	0.065	1.60	0.94	281	1.27	
Day			24.0	2.43	2.60			1.56	0.92		1.19	1.35

cont.

	1	2	3	4	5	6	7	8	9	10	11	12
Date	Time	m	$10^3 \cdot \beta_H$	T	$T_{m=2}$	F_H	$\beta_H \cdot m$	$w_{Å,H}$	$w_{H,H}$	F_S	$w_{H,S}$	w_{Res}
20.7	0518	3.17	22.0	2.46	2.64	284	0.070	2.11	1.15	305	1.41	
	1418	1.95	25.0	2.65	2.64	239	0.049	1.90	1.12	265	1.49	
	1953	4.60	20.5	2.32	2.62	290	0.094	1.58	0.88	321	1.17	
Day			22.5	2.44	2.63			1.86	1.05		1.36	1.19
21.7	1403	1.90	21.5	2.60	2.58	240	0.041	1.96	1.14	269	1.55	
	1727	2.83	22.5	2.41	2.56	252	0.064	1.56	0.92	274	1.17	
	2306	8.53		2.24	2.58							
Day			22.0	2.42	2.57			1.76	1.03		1.36	1.24
22.7	0450	3.55	21.0	2.36	2.59	275	0.075	1.70	0.95	300	1.21	
	1354	1.90	25.5	2.62	2.60	224	0.048	1.57	0.96	251	1.31	
Day			23.0	2.49	2.59			1.63	0.96		1.26	1.20
23.7	1345	1.89	28.5	2.60	2.58	210	0.054	1.29	0.82	240	1.17	
	1922	4.22	17.5	2.26	2.54	285	0.074	1.61	0.88	316	1.17	
Day			23.0	2.43	2.56			1.45	0.85		1.17	1.05
24.7	0455	3.54	24.0	2.36	2.59	255	0.085	1.33	0.79	285	1.06	
	1400	1.92	24.5	2.59	2.58	226	0.045	1.59	0.96	255	1.35	
Day			24.5	2.48	2.58			1.46	0.71		1.20	1.83
4.8	1500	4.11	28.0	2.44	2.71	269	0.115	1.40	0.84	293	1.07	1.49
5.8	0513	3.94	25.0	2.24	2.50	224	0.099	0.78	0.51	253	0.72	
	1353	2.10	28.0	2.55	2.57	215	0.059	1.25	0.81	243	1.11	
	2010	6.87		2.28	2.61							
Day			26.5	2.36	2.56			1.02	0.66		0.92	0.93
6.8	2005	6.83		2.43	2.75							
7.8	1416	2.16	29.0	2.61	2.64	251	0.052	2.02	1.16	257	1.27	0.97
8.8	0515	4.06	28.0	2.36	2.63	243	0.114	1.01	0.64	272	0.88	
	1410	2.16	30.0	2.62	2.65	227	0.065	1.46	0.90	254	1.23	
	1950	6.61		2.39	2.39							
Day			29.0	2.46	2.66			1.23	0.77		1.06	1.42
11.8	1426	2.31	28.5	2.60	2.65	238	0.066	1.60	0.97	267	1.32	1.10

Recent publications in

Meddelanden från

Uppsala Universitets Meteorologiska
Institution

93. Bergeron, T., 1966: Der vollständige Wetterdienst. Archiv für Meteorologie, Geophysik und Bioklimatologie, Supplementum 1/1966.
94. Högström, U., 1967: A new sensitive eddy flux instrumentation. Tellus, Vol. 19, No. 2.
95. Högström, U., 1968: Studies of the natural evaporation and energy balance. Tellus, Vol. 20, No. 1.
96. Högström, U., 1967: Turbulent transfer at different stability conditions. The Physics of Fluids. Vol. 10, No. 9, Part II.
97. Andersson, T., 1968: Om nederbördens dygnsvariation. Svensk Naturvetenskap 1968.
98. Högström, U., 1968: A statistical approach to the air pollution problem of chimney emission. Atmospheric Environment, Vol. 2.
99. Högström, U. and Larsson, I., 1968: Studies on the water balance of a natural catchment area in southern Sweden. Tellus, Vol. 20, No. 4.
100. Andersson, T., 1969: On the diurnal variation of precipitation in Sweden. Geografiska Annaler, Vol. 51, No. 3.
101. Andersson, T., 1969: Small-scale variations of the contamination of rain caused by washout from the low layers of the atmosphere. Tellus, Vol. 21, No. 5.
102. Andersson, T., 1969: Annual and diurnal variation of fog.
103. Andersson, T., 1969: Some characteristics of temperature and precipitation in Sweden.
104. Dahlström, B., 1971: A general classification of error sources at raingauging, and some applications.
105. Dahlström, B., 1971: Automatic error checking and correction of rainfall data.
106. Dahlström, B., 1971: Calculation of rain values in grid points on the basis of irregularly spaced rainfall observations attained by dense network.
107–112. Holmgren, B., 1971: Climate and energy exchange on a sub-polar ice cap in summer. Arctic Institute of North America Devon Island Expedition 1961–1963.
113. Högström, U., 1972: A method for predicting odour frequencies from a point source. Atmospheric Environment, Vol. 6, No. 2.
114. Bergeron, T., 1972: L'origine de la théorie des noyaux de glace comme déclencheurs de précipitation un cinquantenaire. Journal de Recherches Atmosphériques, Vol. VI, no. 1–3.
115. Högström, U., 1974: Wet fallout of sulfurous pollutants emitted from a city during rain or snow.
116. Högström, U., 1974: A critical examination of the turbulence instrument used in the Marsta micro-meteorological field project.
117. Högström, U., 1974: In situ calibration of ground heat flux plates.
118. Högström, U., 1974: A field study of the turbulent fluxes of heat, water vapour and momentum at a 'typical' agricultural site. Quart. J. Roy. Met. Soc.
119. Högström, U. and Smedman-Högström, A-S., 1974: Turbulence mechanisms at an agricultural site. Boundary-Layer Meteorology.
120. Smedman-Högström, A-S. and Högström, U., 1974: Spectral gap in surface layer measurements. J. of Atm. Sciences.
121. Dahlgren, L., 1974: Solar radiation climate near sea level in the Canadian Arctic Archipelago. Arctic Institute of North America Devon Island Expedition 1961–1962.

Distributer: Department of Meteorology, Uppsala University
Box 516
751 20 UPPSALA 1
Sweden

ISBN 91-506-0001-X

LiberTryck Stockholm 1974